9-23-2024

Effects of Microplastic Biofilms on an Anthropogenically Impacted Suburban Lake

Paris M. Velsaquez

Effects of Microplastic Biofilms on an Anthropogenically Impacted Suburban Lake

Paris M. Velasquez

A Thesis Submitted to the Graduate Faculty of

GRAND VALLEY STATE UNIVERSITY

In

Partial Fulfillment of the Requirements

For the Degree of

Master of Science

Department of Biology

August 2024

Thesis Approval Form

GRAND VALLEY STATE UNIVERSITY

The signatories of the committee members below indicate that they have read and approved the Thesis of Paris M. Velasquez in partial fulfillment of the requirements for the degree of. Master of Science in Biology- Aquatic Sciences Emphasis.

9/20/24
Dr. Alan Steinman, Theses committee chair Date

9/18/24
Dr. Charlyn Partridge, Committee member Date

18 Sept 2024
Dr. Sarah Hamsher, Committee member Date

9/20/24
Dr. Alan Steinman, Committee member Date

Accepted and approved on behalf of the Department of Biolgy

Dean of the College

9/23/2024

Date

Accepted and approved on behalf of the Graduate Faculty

Erica K. Hamilton

Dean of The Graduate School

9/23/2024

Date

Dedication

To Lillia Trillo whose perseverance inspires me every day.

Que descanse en paz sabiendo que somos fuertes gracisas a ti.

Acknowledgments

I would like to express my deepest appreciation to my graduate advisor, Dr. Al Steinman, for his guidance, support, and encouragement. I would also like to express my gratitude to members of my graduate committee, Drs. Sarah Hamsher and Charlyn Partridge, for their input and support to my thesis project. Additionally, special thanks to the staff at Annis Water Resources Institute, Allison Passejna, Mike Hassett, Brian Skull, Roxana Taylor, Heidi Feldpausch, Tonya Brown, Travis Ellens, as well as my fellow graduate students, who have encouraged and helped me both in the field and the lab. Funding for my project was provided by the Allen and Helen Hunting Research and Innovation Fund, Grand Valley State University Presidential Research Grant, and the Steinman Environmental Education Fund at the Community Foundation for Muskegon County. I also acknowledge and thank the Gardner family for permission to access the property where the field work for my thesis was performed. Finally, I would like to thank my loved ones Jeannette and Phil Laura, Jasper Bailey and Alejandro Ramirez for their tremendous love and support in all aspects of my life.

Abstract

Plastics have been observed in every location on the planet, and their prevalence in the environment is due in part to their strong resistance to degradation. Inland lakes are susceptible to plastic pollution by highway runoff, which contains plastic fragments of brake pads, car tires, litter, and road paint. These plastics eventually enter freshwater environments and degrade into microplastics (<5mm). Once these microplastics enter lakes, they become coated with a biofilm (plastisphere), whose ecological role has received little attention. My thesis examines the ecology of two polymer types commonly found in stormwater drains from urban areas: polypropylene (PP) and polyethylene terephthalate (PET). I incubated unweathered microplastics (i.e., previously unused) for two weeks in salt-impacted Church Lake, located in Grand Rapids, MI. After the incubation period, microplastics were retrieved, returned to the lab, and placed in beakers housed in growth chambers mimicking natural conditions. The experimental design consisted of two treatments: 1) microplastics incubated in the low phosphorus, low salinity, high light epilimnion of Church Lake were retrieved and then in the lab, grown in either its ambient water or placed in water from the hypolimnion, which is high phosphorus, high salinity, and low light; and 2) the reverse treatment using microplastics incubated in the hypolimnion of Church Lake, and placed in either ambient conditions or epilimnetic water. The experiment had two goals: 1) test the role of lake salinity and phosphorus content on P uptake by the plastisphere; and 2) investigate whether polymer substrates exert a strong enough selection to drive species sorting by evaluating species composition on different polymers following the salinity/P concentration experiment.

Table of Contents

List of Tables

List of Figures

Abbreviations

MPs, Microplastics; PE, Polyethylene; PP, Polypropylene; PVC, Polyvinyl chloride; PS, Polystyrene; PET, Polyethylene terephthalate; NPs, Nano-plastics; Cl^-, Chloride; Ca, calcium; P, phosphorus; NH_3, ammonia; N, nitrogen; MDOT, Michigan Department of Transportation; AADT, Annual average daily traffic; EPS, Extracellular polymeric substances; BPA, Bisphenol A; DO, Dissolved oxygen; Sp. Cond, Specific conductivity; TDS, Total dissolved solids; YSI, Yellow Springs Instruments; TP, Total phosphorus; SRP, Soluble reactive phosphorus ; AFDM, Ash-free dry mass; POP, Particulate organic phosphorus; DOP, Dissolved organic phosphorus; KPA, atmospheric pressure; ISTC, Illinois Sustainable Technology Center; KI, Potassium iodide; IR, Thermo Infrared; T-1, Treatment group 1; T-2, Treatment group 2; T-3, Treatment group 3; T-4, Treatment group 4; C-1, Control group 1; C-2, Control group 2; ANOVA, Analysis of variance; ASVs, Amplicon sequence variants; PCoA, Principal Coordinate Analysis; DESeq, Differential Expression Analysis for Sequence; NMDS, Nonmetric multidimensional scaling; N, Nitrogen; m, Meters.

Chapter I: Plastic Pollution

Introduction

Plastics are widely used because of their light weight, durability, and resistance to degradation. The rising production and low rates of plastic recovery have contributed to waste and pollution in our environment. After long-term exposures to ultraviolet radiation, which causes photo- and thermal oxidation, as well as mechanical weathering and biodegradation, plastics eventually fragment into smaller pieces defined as microplastics (MPs) (≤ 5mm) or nano-plastics (NPs) (1 to 1000nm) (Driedger et al., 2015). Many studies have found plastics of various sizes in oceans, lakes, rivers, and groundwater in every known biome on Earth (He et al., 2021). Plastics come in numerous forms based on their sources, monomers, polarities, and intended applications (Amaneesh et al., 2022). The most common polymers found in products are polypropylene (PP), polyethylene (PE), polyethylene terephthalate (PET), polystyrene (PS), and polyvinyl chloride (PVC) (Amaneesh et al., 2022). After production, plastic debris exists in the environment as primary or secondary MP. Primary plastics refer to plastics manufactured for industrial or domestic applications, for example, toothpaste, bottle caps, cigarette butts, and resin pellets (Driedger et al., 2015). Secondary plastics originate from the breakdown of primary plastics due to environmental conditions (He et al., 2021). Complete plastic mineralization takes longer than a human lifetime.

MP accumulation in the environment has caused a range of ecological and economic impacts on freshwater environments (Driedger et al., 2015). Aquatic organisms are at risk of becoming entangled by plastic debris and ingesting plastic fragments. As a consequence of their small size, MPs easily transfer through trophic food webs (Guasch et al., 2022). MP

consumption leads to tearing, clogging, displacement of accumulated particles, and plastic-absorbed toxins (Verla et al., 2019). During plastic manufacturing, toxic chemicals such as phthalates, nonylphenols, bisphenol A (BPA), heavy metals, and polybrominated diphenyl ethers are incorporated into plastic compounds (Driedger et al., 2015). As plastics degrade, these chemicals can be released into the environment. These chemical compositions are known to disrupt endocrine functions leading to cancerous tumors and causing birth and developmental defects in aquatic animals (Driedger et al., 2015).

MPs can be transported from riverine outflows, tributaries, highway runoff, landfills, stormwater drains, textile laundering facilities, and wastewater treatment plants into larger water bodies (Driedger et al., 2015). Depending on the density of MPs in the water column, MPs can settle to the bottom and wash to shore from wave action. Plastic debris accumulation on freshwater shorelines is an eyesore for beachgoers. In turn, litter on beaches has become an economic liability to the tourism industry (English, 2019). These plastic fragments can cause cuts and abrasions to swimmers and beachgoers. The indirect cost to the tourism industry could affect homeowners in coastal communities by depreciating coastal property values and reducing shoreline business revenue. Driedger et al. (2015) have estimated that it would cost the Great Lakes region $468,000,000 annually to combat plastic pollution from land-based activities. MP transport through the environment is a cause of concern.

Transport of Plastic Debris

Urban, agricultural, and wastewater treatment plant runoff are primary sources of MPs (Guasch et al., 2022). The most common polymer types found in urban and agricultural areas that may end up in stormwater drains or direct surface runoff, such as PE, PP, PVC, PET, and PS,

including those associated with synthetic textiles or domestic products (Lutz et al., 2021). Urban lakes are particularly vulnerable to MPs due to their proximity to the highway and urban runoff (He et al., 2021). MP commonly accumulates in street dust from road surfaces, brake pads, car tires, and road paint (Alimi et al., 2018). Rain and storm events transport a range of non-point source pollutants such as sediment, road salt, nutrients, pathogens, and MPs (Eadie et al., 2002; Hitchcock, 2020; Johnson et al., 2011; Kaushal et al., 2022). MPs enter larger bodies of surface water during storm or rain events through streams and estuaries. The temporal and spatial variability of MPs transport from terrestrial to aquatic ecosystems may not be unidirectional (Guasch et al., 2022). Once MPs are in the stormwater drainage system, the size, shape, and density of MPs impact particle movement and/or settling rates (Kowalski et al., 2016). During storms, the energy of streams increases and resuspends MPs that accumulate in benthic regions. In drier months, MP is likely to accumulate and create MP plumes that get washed downstream during storm events (Hitchcock, 2020). The plastic polymer type determines the density of debris. Plastics with a lower density than water are likely to remain afloat in the water column for extended periods (Driedger et al., 2015). Subsequently, once plastics enter the aquatic environment they can be influenced by microbial communities, influencing their density, chemistry, and toxicity.

The Plastisphere

The introduction of plastics to the environment has created a unique ecological niche called the plastisphere (Zettler et al., 2013). Once MPs enter aquatic environments, their surface area becomes colonized by microbial communities. The plastisphere is composed of bacteria, fungi, algae, and protozoans (He et al., 2021). Biofilms are complex, with

taxonomically diverse communities influenced by the biogeochemical properties present in water (Hoellein et al., 2014). The abiotic characteristics that influence biofilm growth include water currents, nutrients, temperature, light, salinity, and pH (Dong et al., 2021; He et al., 2021). Biofilm colonization can serve as an initial biological interaction as primary producers or microbial decomposers in aquatic food webs. Other interactions include small predators feeding on the microorganism within biofilms. Biofilms play important roles in nutrient cycling and are a source of food for higher trophic levels. Hence, their interactions in aquatic ecosystems can be ecologically significant (Hoellein et al., 2014).

Substrate selection can influence how and where the biofilm moves within the water body, nutrient dynamics, metabolism, and community structure (Uzun et al., 2021). MPs are suitable substrates for microbial communities because of their high hydrophobicity (He et al., 2021). Shortly after entering the water, MP adsorbs organic and inorganic substances to form a conditioning surface. Secretion of extracellular polymeric substances by the microbial community facilitates adhesion, allowing the community to proliferate and colonize substrates (Uzun et al., 2021). One concern with MPs being present in aquatic ecosystems is their ability to adsorb hazardous compounds and/or pathogenic microorganisms. These pollutants concentrate at the water and air interface (Uzun et al., 2021). When MP floats on the water's surface, its strong hydrophobicity attracts pollutants. Various studies have found persistent organic pollutants, heavy metals, and antibiotic-resistant bacteria on MP (Oberbeckmann et al., 2018; Steinman et al., 2020; He et al., 2021; Scott et al. 2021). Thus, MP can serve as vectors for the movement of pollutants in the environment. Over time, these potentially contaminated biofilms on MPs may be consumed by aquatic organisms or the MPs themselves may break

down by physical, chemical, and biological mechanisms (Uzun et al., 2021). It is not fully understood how this degradation of plastics, and their associated contaminants, affects aquatic ecosystems currently or in the future but given their abundance, it is clear they deserve more attention.

The Plastisphere Influence in the Water Column

Most studies on MPs have looked at MPs in marine environments compared to freshwater environments. Because the two systems have different hydrodynamics, physio-chemical, and species composition (Chen et al., 2019), it is imperative to examine how MPs affect freshwater systems separately. Anthropogenic activities (e.g., fertilizers, road deicers, leaking septic tanks) impact freshwater environments, decreasing freshwater quality. The plastisphere is often affected by high levels of nutrients and salinity (He et al., 2021). Nitrogen (N) and phosphorus (P) positively correlate with biofilm growth rates, while salinity negatively impacts the growth rates (Li et. al 2019). Given that urban lakes are susceptible to anthropogenic activities, including excess nutrients, salt runoff, and MPs, all of which may create both ecological and human health risks, it is important to better understand these stressors and how they interact with each other.

Chen (2020) demonstrated that the plastisphere was capable of assimilating and releasing N and P into surrounding waters depending on their development stage and ambient environmental conditions. Biofilms are key in cycling materials and energy in aquatic ecosystems. Impaired lakes may increase microbial activities on MPs from excessive in-land sources of nutrients. The extent of MPs impacts is unknown because of limited information on plastisphere dynamics in impaired urban water environments.

Study Site

My research examines biofilms growing on MPs in Church Lake, located in Grand Rapids, Michigan. Church Lake is a small kettle lake (surface area of ~7.7 ha and a maximum depth of 16 m) with residential housing on its south and west shorelines and is adjacent to the East Beltline (M-44) state highway to the east. An unnamed tributary flows underneath, and is fed by runoff from, the East Beltline highway; the tributary connects directly into Church Lake (Molloseau and Steinman, 2023). Previous studies on Church Lake have shown that the lake has high levels of chloride (Cl^-), calcium (Ca), phosphorus (P), and ammonia (NH_3) in the hypolimnion (Foley and Steinman, in press), but MP concentrations in the lake have not been studied. Currently, the only forms of protection to reduce runoff and erosion are vegetation buffers on some private properties. To prevent further pollutants, Church Lake homeowners banned fertilizers, motorboats, and switched to city sewers to avoid leaky septic systems. According to Foley and Steinman (2023), during snowmelt events road salt has been washing off the East Beltline highway into the tributary draining into Church Lake causing chloride levels to spike as high as 1,000 mg/L. This concentration exceeds the U.S. EPA chloride chronic toxicity threshold of 230 mg/L and the State of Michigan's more stringent final chronic threshold of 150 mg/L. High Cl^- levels in Church Lake prevent the lake from completely mixing in its deeper areas. The lake has a distinct chemocline at ~ 9 m that separates the epilimnion and hypolimnion zones. As a result, P has accumulated in the lake's hypolimnion, reaching ecologically alarming levels of 7 mg/L in some locations (Foley and Steinman, 2023). If Church Lake suddenly turned over and mixed, these high P concentrations would reach the lake surface where there is sufficient light for photosynthesis, and likely promote massive algal blooms. The long-term salt

buildup has prevented portions of the lake from seasonal mixing and as a result, high levels of P have accumulated at depth, which otherwise would have been gradually assimilated by photosynthetic algae and macrophytes. The increases in de-icing salt application and single-use plastics, combined with the proximity of major roads to lakes, have fostered an interest in studying microplastic interactions in salinized urban lakes.

My thesis research examines the influence of the plastisphere on P dynamics in Church Lake. To achieve this, we introduced MPs into Church Lake in retrievable flow-through containers (Steinman et al. 2020) to promote biofilm formation, brought the MPs back to the lab, and exposed them to a set of controlled environmental conditions. We measured P uptake and biofilm community structure. We selected Church Lake for three reasons: 1) its proximity to a major highway, which results in significant urban runoff; 2) its strong vertical salinity gradient (from salt deicer applications on the adjacent highway, allowing me to examine biofilm dynamics under very different environmental conditions in the hypolimnion vs. the epilimnion; and 3) prior studies on this lake, which provide baseline information. This work examines how microplastics from highway stormwater runoff affect nutrient dynamics in urban lakes and improves our understanding of potential impacts from MPs on aquatic ecosystems.

Purpose

Microplastics are a growing risk to freshwater ecosystems. Primary sources of MPs are derived from urban, agricultural, industrial, and wastewater treatment plant runoff (Guasch et al., 2022). Although urban areas are one of these four primary sources of MPs to freshwater environments, their impact in urban lakes is largely unknown. The potential ecological effects of MP in urban lakes need closer examination given the potential socio-economic costs to

lakefront homeowners and recreational uses of these lakes. This thesis research will examine microbial communities under different conditions and how this will influence nutrient dynamics. The significance of my research will reveal the interactions between highway-derived MPs, salinity, and the abundance, diversity, and nutrient dynamics of microbial communities found in an urban lake, providing key information to homeowners, the road and drain commission, and local municipalities.

Research Questions

Question 1: Are MPs entering Church Lake via the unnamed tributary coming off the East Beltline highway?

Hypothesis: We hypothesize that the East Beltline is a source of MPs entering Church Lake via the tributary.

Rationale: Storms and rain events are important mobilizers of a variety of non-point source contaminants, including sediment, fertilizers, and pathogens (Hitchcock, 2020). Similar mechanisms are thought to be involved in the mobilization and transportation of MPs. When it rains on road surfaces, numerous MPs from damaged road paint, tires, brake pad fragments, particles from air deposition, and degraded litter, may end up in stormwater systems (Lutz et al., 2021). Many MPs are likely to settle out and accumulate in the benthic environment in slow-moving conditions during dry periods of the year. During stormwater events, MPs are likely to have shorter residence time and be present in greater quantities in the tributary (Hitchcock, 2020). The 2022 traffic records from the Michigan Department of Transportation (MDOT, 2022) reported that the annual average daily traffic (AADT) passing

Church Lake is 44,270 vehicles (2022), which is an increase of 18% since 2020. Currently the only forms of protection to reduce runoff and erosion are vegetation buffers on some private properties. Pollution from the East Beltline highway will be a significant source of MPs to Church Lake via the tributary connecting East Beltline to the lake.

Question 2: How will algae and bacteria taxonomic composition differ on MPs grown in the hypolimnion (low light, high Cl^-, high P) vs. epilimnion (high light, low Cl^-, low P) in Church Lake?

Hypothesis: Algal communities growing on MPs in the hypolimnion (high salinity) will have lower species richness and abundance than those growing on MPs in the epilimnion (low salinity). However, bacteria will be better adapted to living in low light and anoxic environments found in the hypolimnion.

Rationale: Salinity, nutrients, and light are key abiotic factors influencing algae and bacterial species richness in lakes. Larson & Belovsky (2013) showed that salinity was a central abiotic factor influencing species richness in saline lakes. Many of the rarer algal taxa disappeared either as a result of being unable to physically overcome osmotic stress or because they were outcompeted by taxa that were less sensitive to it. At 10-m depth and below, algal species richness in Church Lake is expected to decrease in response to low light and osmotic stress from high salinity levels. In addition, bacterial communities found in the deeper, high Cl^- region of Church Lake may have developed osmotic adaptive strategies due to the yearlong abundance of high chloride levels found at 10-m, although salinity has been shown to reduce

the growth rate of biofilm (Li et al., 2019). Added nutrient abundance may allow species that are halotolerant or halophilic to thrive.

Question 3: Are the microbial communities growing on MPs removing P from Church Lake, and if so, is there a difference between the high vs. low salinity-grown communities?

Hypothesis A (microbial communities in their native habitat): Overall, the microbial communities found growing on MPs have a minimal impact on P removal in Church Lake due to the relatively low MP densities in the water column; however, P-uptake will be greater by low-salinity vs. high-salinity communities due to differences in abundance. P uptake per unit biomass will be lower in high-salinity communities.

Rationale: Colonized MPs will settle to the bottom due to their increased density. However, due to the lack of light in the deeper places, heterotrophic microbes predominate. It is uncertain how active these communities will be owing to the extreme salinity. Higher salinity environments will impose stress on these microbial communities, resulting in reduced metabolic demand. Previous studies have shown that salinity levels influence phytoplankton abundance (Larson & Belovsky, 2013); hence with reduced biofilm biomass in the high salinity hypolimnion area, we expect lower overall P uptake. However, bacterial species in the hypolimnion will be adapted to a high salinity/low light/P-rich environment. P is essential for living organisms given its role in energy metabolism (e.g., ATP), genetic material (nucleic acids), and membrane integrity (phospholipids). Bacteria tend to uptake P quicker in aerobic conditions compared to anoxic. Although Church Lake has high phosphorus in the hypolimnion, the area is anoxic.

Hypothesis B (microbial communities transferred from hypolimnion to epilimnion and vice versa): P uptake by transferred microbial communities will decline compared to uptake in control systems. The decline will be greater in communities transferred from the epilimnion to the hypolimnion than the hypolimnion to the epilimnion.

Rationale: The osmotic shock from the high salinity hypolimnetic water will outweigh the influence of more P, resulting in a slowing of microbial metabolism when epilimnetic microbes are placed in hypolimnetic water. A corollary for this is the transfer of microbial communities in the hypolimnion may be adapted to a high salinity environment, in which case their transfer to low salinity water may result in metabolic stress. If so, there may be an equivalent reduction in P uptake by both transferred communities.

References

Alimi, O. S., Farner Budarz, J., Hernandez, L. M., & Tufenkji, N. (2018). Microplastics and nanoplastics in aquatic environments: aggregation, deposition, and enhanced contaminant transport. Environmental Science and Technology, 52(4), 1704–1724. https://doi.org/10.1021/acs.est.7b05559

Amaneesh, C., Anna Balan, S., Silpa, P. S., Kim, J. W., Greeshma, K., Aswathi Mohan, A., Robert Antony, A., Grossart, H. P., Kim, H. S., & Ramanan, R. (2022). Gross negligence: Impacts of microplastics and plastic leachates on phytoplankton community and ecosystem dynamics. Environmental Science and Technology, 57 (1), 5-24. https://doi.org/10.1021/acs.est.2c05817

Chen, X., Chen, X., Zhao, Y., Zhou, H., Xiong, X., & Wu, C. (2020). Effects of microplastic biofilms on nutrient cycling in simulated freshwater systems. Science of the Total Environment, 719, 137-276. https://doi.org/10.1016/j.scitotenv.2020.137276

Chen, X., Xiong, X., Jiang, X., Shi, H., & Wu, C. (2019). Sinking of floating plastic debris caused by biofilm development in a freshwater lake. Chemosphere, 222, 856–864. https://doi.org/10.1016/j.chemosphere.2019.02.015

Dong, X., Zhu, L., Jiang, P., Wang, X., Liu, K., Li, C., & Li, D. (2021). Seasonal biofilm formation on floating microplastics in coastal waters of intensified marinculture area. Marine Pollution Bulletin, 171, 112914. https://doi.org/10.1016/j.marpolbul.2021.112914

Driedger, A. G. J., Dürr, H. H., Mitchell, K., & Van Cappellen, P. (2015). Plastic debris in the Laurentian Great Lakes: A review. Journal of Great Lakes Research, 41(1), 9–19. https://doi.org/10.1016/j.jglr.2014.12.020

Eadie, B. J., Schwab, D. J., Johengen, T. H., Lavrentyev, P. J., Miller, G. S., Holland, R. E., Leshkevich, G. A., Lansing, M. B., Morehead, N. R., Robbins, J. A., Hawley, N., Edgington, D. N., & Van Hoof, P. L. (2002). particle transport, nutrient cycling, and algal community structure associated with a major winter-spring sediment resuspension event in Southern Lake Michigan. Journal of Great Lakes Research, 28(3), 324–337. https://doi.org/10.1016/S0380-1330(02)70588-1

English, E., Wagner, C., Holmes, J. (2019). The effects of marine debris on beach recreation and regional economies in four coastal communities: a regional pilot study. National Oceanic and Atmospheric Administration Marine Debris Division, July 2019.

Foley, E., & Steinman, A. D. (In Press). Urban lake water quality responses to elevated road salt. Science of the Total Environment.

Guasch, H., Bernal, S., Bruno, D., Almroth, B. C., Cochero, J., Corcoll, N., Cornejo, D., Gacia, E., Kroll, A., Lavoie, I., J. Ledesma, J. L., Lupon, A., Margenat, H., Morin, S., Navarro, E., Ribot, M., Riis, T., Schmitt-Jansen, M., Tlili, A., . . . Martí, E. (2022). Interactions between microplastics and benthic biofilms in fluvial ecosystems: Knowledge gaps and future trends. Freshwater Science, 41(3). https://doi.org/10.1086/721472

He, S., Jia, M., Xiang, Y., Song, B., Xiong, W., Cao, J., Peng, H., Yang, Y., Wang, W., Yang, Z., & Zeng, G. (2021). Biofilm on microplastics in aqueous environment: Physicochemical properties and environmental implications. Journal of Hazardous Materials, 424 (B), 127286. https://doi.org/10.1016/j.jhazmat.2021.127286

Hitchcock, J. N. (2020). Storm events as key moments of microplastic contamination in aquatic ecosystems. Science of the Total Environment, 734, 139436. https://doi.org/10.1016/j.scitotenv.2020.139436

Hoellein T, Rojas M, Pink A, Gasior J, Kelly J (2014) Anthropogenic litter in urban freshwater ecosystems: distribution and microbial interactions, PLOS ONE 9(6): e98485. https://doi.org/10.1371/journal.pone.0098485

Johnson, K. A., Steinman, A. D., Keiper, W. D., & Ruetz, C. R. (2011). Biotic responses to low-concentration urban road runoff. Journal of the North American Benthological *Society*, *30*(3), 710–727. https://doi.org/10.1899/10-157.1

Kaushal, S. S., Reimer, J. E., Mayer, P. M., Shatkay, R. R., Maas, C. M., Nguyen, W. D., Boger, W. L., Yaculak, A. M., Doody, T. R., Pennino, M. J., Bailey, N. W., Galella, J. G., Weingrad, A., Collison, D. C., Wood, K. L., Haq, S., Newcomer-Johnson, T. A., Duan, S., & Belt, K. T. (2022). Freshwater salinization syndrome alters retention and release of chemical cocktails along flow paths: From stormwater management to urban streams. Freshwater Science, 41(3). https://doi.org/10.1086/721469

Kowalski, N., Reichardt, A. M., & Waniek, J. J. (2016). Sinking rates of microplastics and potential implications of their alteration by physical, biological, and chemical factors. Marine Pollution Bulletin, 109(1), 310–319. https://doi.org/https://doi.org/10.1016/j.marpolbul.2016.05.064

Larson, C. A., & Belovsky, G. E. (2013). Salinity and nutrients influence species richness and evenness of phytoplankton communities in microcosm experiments from Great Salt Lake, Utah, USA. Journal of Plankton Research, 35(5), 1154–1166. https://doi.org/10.1093/plankt/fbt053

Li, W., Zhang, Y., Wu, N., Zhao, Z., Xu, W., Ma, Y., & Niu, Z. (2019). Colonization characteristics of bacterial communities on plastic debris influenced by environmental factors and polymer types in the Haihe Estuary of Bohai Bay, China. Environmental Science and Technology, 53(18), 10763–10773. https://doi.org/10.1021/acs.est.9b03659

Lind, L., Schuler, M. S., Hintz, W. D., Stoler, A. B., Jones, D. K., Mattes, B. M., & Relyea, R. A. (2018). Salty fertile lakes: how salinization and eutrophication alter the structure of freshwater communities. Ecosphere, 9(9). https://doi.org/10.1002/ecs2.2383

Lutz, N., Fogarty, J., & Rate, A. (2021). Accumulation and potential for transport of microplastics in stormwater drains into marine environments, Perth region, Western Australia. Marine Pollution Bulletin, 168, 112362. https://doi.org/10.1016/j.marpolbul.2021.112362

Michigan Department of Transportation. (2022). Transportation Data Management System. https://mdot.public.ms2soft.com/tcds/tsearch.asp?loc=Mdot&mod=TCDS

Molloseau, J., & Steinman, A. D. (2023). Chloride and phosphorus retention and release in soils surrounding a salt-contaminated lake in West Michigan. Journal of Freshwater Ecology, 38(1). https://doi.org/10.1080/02705060.2023.2241478

Oberbeckmann, S., Kreikemeyer, B., & Labrenz, M. (2018). Environmental factors support the formation of specific bacterial assemblages on microplastics. Frontiers in Microbiology, 8, 1–12. https://doi.org/10.3389/fmicb.2017.02709

Scott, J. W., Gunderson, K. G., Green, L. A., Rediske, R. R., & Steinman, A. D. 2021. Perfluoroalkylated substances (PFAS) associated with microplastics in a lake environment. Toxics, 9(5), 106. https://doi.org/10.3390/toxics9050106

Steinman, A. D., Scott, J., Green, L., Partridge, C., Oudsema, M., Hassett, M., Kindervater, E., & Rediske, R. R. (2020). Persistent organic pollutants, metals, and the bacterial community composition associated with microplastics in Muskegon Lake (MI). Journal of Great Lakes Research, 46(5), 1444–1458. https://doi.org/10.1016/j.jglr.2020.07.012

Uzun, P., Farazande, S., & Guven, B. (2021). Mathematical modeling of microplastic abundance, distribution, and transport in water environments: A review. Chemosphere, 288(2), 132517. https://doi.org/10.1016/j.chemosphere.2021.132517

Verla, A. W., Enyoh, C. E., Verla, E. N., & Nwarnorh, K. O. (2019). Microplastic–toxic chemical interaction: a review study on quantified levels, mechanism, and implication. SN Applied Sciences, 1(11), 1–30. https://doi.org/10.1007/s42452-019-1352-0

Zettler, E. R., Mincer, T. J., & Amaral-zettler, L. A. (2013). Life in the “Plastisphere”: Microbial communities on plastic marine debris. Environmental Science & Technology, 47(13), 7137–714. https://doi.org/DOI: 10.1021/es401288x

Chapter 2: Characterization of Microplastics from Highway Runoff to Tributary to a Suburban Salinized Eutrophic Lake

Abstract

Storm events transport a range of non-point source pollutants such as sediment, road salt, nutrients, pathogens, and microplastics (MPs) from land to water bodies. Plastics' resistance to degradation can cause obstruction to natural rivers, streamflow, entangling marine/freshwater animals, and induce starvation from their consumption. The objective of this study was to investigate the role of an unnamed tributary in transporting MPs from a nearby highway into Church Lake, a small kettle lake located in Grand Rapids, Michigan. Specifically, this study aims to characterize the type of MPs present in the lake and tributary through water sampling over a one-year period, as well as sediment sampling in the spring. Water quality monitoring and weather data conducted in conjunction with sampling efforts were recorded to identify if storm events increase MPs found in the unnamed tributary. Results from this study verified the presence of MPs in both the tributary and lake. The majority of MPs found were black fragments of an unknown polymer with counts ranging from 61-16,390 counts #/L. Major spikes in MP concentration occurred in the winter for the lake and tributary (stormflow) during the Fall. These results indicate a need for road runoff to be considered as part of road infrastructure design to reduce potential environmental impacts to downstream receiving water bodies.

Introduction

Plastic materials have become necessary items for daily life. Due to their insulating qualities, durability, and low weight, plastics are versatile but also long-lasting. Plastic pollution is present throughout the globe because of the overproduction and mismanagement of plastic waste (OECD, 2022). In addition to plastic waste being unsightly when found in the environment, the synthetic material is capable of obstructing natural river or streamflow, entangling marine/freshwater animals, inducing starvation from consumption, and blocking sunlight from reaching photosynthetic organisms in the water column. As a function of their durability, the life span of plastic could take more than a human life time to completely degrade (Chamas et al., 2020). However, plastics can become brittle and fragment into tiny particles from mechanical, thermal, and biological processes (Chamas et al., 2020). Based on the size of plastic particles, these fragments can be grouped into five categories: nano-plastics (<1 μm), microplastics (MPs) (≥1 μm to <5 mm), meso-plastics (≥5 mm to 5 cm), macro-plastics (>5 to 50 cm), and mega-plastics (>50 cm) (Badea and Balas, 2023). MPs are of particular concern as they can travel easily through food webs and are small enough to obstruct internal passageways that can lead to death (Amaneesh et al., 2022; Wright et al., 2013).

MPs can be classified as either primary or secondary MPs. Primary MPs are manufactured into products (e.g., cosmetics, care products, medication, toothpaste). Secondary MPs are made up of fragments or particles generated after the physical, chemical, or biological breakdown of plastic products (e.g., bags, bottles, and food containers) (Badea and Balas, 2023). MPs come in many shapes and sizes and are characterized by their physical and chemical compositions. Physical characteristics of MPs include their size, shape, color, density, and

crystalline polymer particle structures (Badea and Balas, 2023). The chemical composition and surface chemistry of MPs describe a polymer's chemical property. The chemical byproducts, monomers, and additives that are incorporated into the manufacture of plastics, eventually become released into the environment (Alimi et al., 2018). These additives may leach from MPs when they decompose into the environment; hence the chemical and physical characteristics of MPs can have varying effects when ingested by aquatic organisms (Badea and Balas, 2023). In addition, MPs can serve as both the source and sink of contaminants as they move through the environment. Understanding the pathways that MPs take in the aquatic environment, their role as potential sources and sinks of chemicals and potential toxins, and the ultimate effects they have on the ecosystem are crucial for identifying the ecological impacts they potentially cause.

The most common sources of MPs are urban runoff, wastewater treatment plant inputs, sewage system overflows, and industrial inputs (Hitchcock, 2020). Discarded plastic materials eventually become MPs that can be transported from land to water sources. Rain and storm events transport a range of non-point source pollutants such as sediment, road salt, nutrients, pathogens, and MPs (Eadie et al., 2002; Hitchcock, 2020; Johnson et al., 2011; Kaushal et al., 2022). Often storm events hasten migration of MPs from land to water creating MP plumes (Liu et al., 2019). Urban lakes are particularly vulnerable to MPs due to their proximity to impervious surfaces that expedite urban runoff (He et al., 2021). Storm events pick up MPs through street dust from road surfaces, brake pads, car tires, and road paint (Alimi et al., 2018; Lutz et al., 2021). Once in waterways, the movement of MPs can be affected by water currents, wind patterns, and MP density. Seasonal wind patterns can result in areas of high MP concentrations (Alimi et al., 2018). Buoyant MPs can travel vast distances from where they

were discarded and eventually deposit into sediment when the density of the polymer becomes greater than water. The sinking velocity can be influenced by particle density, shape, biofouling, size, and fluid density of the water body (Kowalski et al., 2016). Lakes can act as temporary or long-term sinks for MPs (Alimi et al., 2018). High concentrations of MPs in lakes may bioaccumulate in zooplankton and benthic invertebrates because of their similarity to food sources, ultimately resulting in transfers through the trophic food web (Nair and Perumal, 2022; Setälä et al., 2014).

My study examines the dynamics of MPs running off a major highway into an urban lake in eastern Grand Rapids, Michigan. Road runoff from the East Beltline highway enters into storm drains located in the highway median, and then directly into a tributary flowing through a culvert under the highway, which then flows ~140 m before it drains into Church Lake (Molloseau and Steinman, 2023). The Lake is heavily salinized and has a distinct halocline in its deeper region, which formed after years of exposure to highway deicing salts (Foley and Steinman, 2023). Church Lake, located in Grand Rapids, Michigan is a small kettle lake (surface area of ~7.7 ha and a maximum depth of 16 m) with residential housing on its south and west shorelines and is adjacent to the East Beltline state highway to the east (Figure 2.1). Previous studies on Church Lake have shown that the lake has high levels of chloride (Cl^-), calcium (Ca), phosphorus (P), and ammonia (NH_3) in the hypolimnion (Foley and Steinman, 2023), but MP concentrations in the lake have not been studied.

The 2022 traffic records from the Michigan Department of Transportation (MDOT, 2022) reported that the annual average daily traffic (AADT) passing Church Lake is 44,270 vehicles (2022), which is an increase of 18% since 2020. Given the traffic density, it is anticipated that

runoff from the East Beltline highway will contribute a significant source of MPs to Church Lake via the tributary connecting East Beltline to the lake. Currently, the only forms of control to reduce runoff and erosion in the tributary are vegetation buffers on some private properties and a series of check dams in the tributary composed of steel sheets. These dams were constructed to reduce the velocity of water and control erosion of the downstream transport of sediment. Buoyant pollutants such as plastics can flow over and around these dams.

I examined the role of the unnamed tributary as a conduit for MPs entering Church Lake, and characterized the type and mass of the MPs entering the tributary. My goal was to identify if MPs are entering Church Lake and to characterize them; this information also helped determine the role of MPs in P dynamics in Church Lake (see chapter 4).

Methods

Study Site

Sampling occurred in Church Lake, an urban lake located in Kent County, Grand Rapids, Michigan (Figure 2.1). The lake is one of three lakes connected through marshy wetlands and groundwater in this area. This urban lake spans 7.7 ha and has a maximum depth of ~ 16.5 m. Runoff from a major highway (East Beltline) flows into an unnamed tributary that enters the east side of Church Lake. The deepest region of the lake does not mix seasonally due to a halocline (~9m) that has formed from deicing salt runoff from the East Beltline highway; a prior study on this lake showed that this road salt runs off into the unnamed tributary that flows under the highway, which in turn enters Church Lake resulting in excess Cl^- (Foley and Steinman, 2023).

MP Field Data Collection Methods

Water Collection

A total of 26 samples were taken, which included 7 lake water samples, 2 sediment samples with one sampling occurring in the tributary and one in the lake, 5 water samples taken from the tributary during a storm event, and 12 water samples taken from the tributary during baseflow each month (Figure 2.1). Lake samples were taken from June 2022- April 2023. A vertical Van Dorn was used to retrieve lake water samples from below the surface, at mid-depth, and 1m above the surface and then composited into a 1L glass container. Two lake samples were taken each season for 1 year (winter, fall, spring, summer) except for winter when only one sample was taken due to dangerous winter conditions, resulting in a total of 7 lake water samples. Two sediment samples were taken during the spring 2023, one sample from the lake and one sample from the tributary. A petite ponor was used to retrieve lake sediment samples at ~9m. The tributary is shallow, and I was able to retrieve sediment samples by pushing the 250 ml glass container into the sediment bed and covering the top with my hand to prevent any further penetration of water before capping the sample. Water samples were taken along the tributary once every month from May 2022-April 2023 for a total of 12 samples. Storm water sampling was conducted only if precipitation was preceded by 72 hours of dry weather and rain accumulation of > 0.25 cm. Five storm events were sampled from August 2022 - March 2023. Water samples were collected in 1L glass containers and used to collect water from the unnamed tributary and Church Lake to identify MPs present. Before closing the lid to the container, aluminum foil was placed on top of the glass container to prevent MP contamination from the cap. All water and sediment samples were collected at

randomly determined locations throughout the sampling time frame; this approach precluded measuring changes in the same location over time but provided a more robust estimate of MP distribution throughout the system. Water quality measurements were taken after water collection in the same area that water and sediment samples were taken for MP analysis on that day Precipitation data for storm events were obtained from the NOAA station website at the Gerald Ford International Airport (~ 13 km from Church Lake) weather station.

Water Quality

Water quality parameters were taken after every sampling event and included water temperature, pH, dissolved oxygen (DO), specific conductivity (Sp Cond), total dissolved solids (TDS), and turbidity (NTU) using a Yellow Springs Instruments (YSI) EXO multi-sensor sonde (Table 2.1). Water samples were placed in a cooler until they were brought to the lab and placed in the refrigerator (4℃) until MP analysis.

HOBO Data/Discharge Data

Stream flow was measured using SonTek FlowTracker 2 once a month for 1 year (May 2022-April 2023) at a permanently marked transect near the culvert closest to the highway. Water depth and velocity were measured at 6 equally spaced points at the transect using the velocity area method for discharge (Gore and Banning, 2017). Discharge was calculated by the SonTek FlowTracker 2. A HOBO logger device was placed near the unnamed tributary and recorded atmospheric pressure (kPa) and temperature (℃) every 10 minutes.

MP Quantification

Two 1-L water samples were taken from each sampling period. One was processed for MPs, while the other was processed for 6-PPD-Q (6PPD-quinone). 6PPD-Q is a toxic chemical formed when the tire preservative 6PPD reacts with ozone and contaminates water bodies through stormwater runoff (Bohara et al., 2024). It is highly toxic to aquatic life, particularly coho salmon, even at low concentrations (Bohara et al., 2024; Tian et al., 2022). Studies have shown that concentrations as low as 0.8 µg/L can cause acute toxicity and lead to significant mortality in coho salmon (Bohara et al., 2024; Tian et al., 2022). Water and sediment samples taken from the tributary and Church Lake were analyzed for MPs by Illinois Sustainable Technology Center (ISTC) following a modified version of NOAA laboratory methods for the analysis of microplastics in water and sediment (Masura et al., 2015; Scott et al., 2020). Brief descriptions are provided below.

Water Samples

Wet Sieving

This section describes the process of filtering water samples using a 5 µm mesh sieve to isolate MPs with specific densities, followed by vacuum filtration and thorough rinsing to ensure full recovery of MPs. Water samples were first filtered by using a stainless steel 5 µm mesh sieve to isolate MPs with density at 1.8 g/cm. A 5 µm mesh size was used instead of NOAA's 0.3mm filter because it captures smaller polymers such as polyvinyl chloride, polyester, and fluoropolymers (Scott et al., 2020). The aqueous samples were drawn through the unit using vacuum filtration due to the smaller pore sizes of these sieves. The sample container was

rinsed three times and filtered to ensure that all MPs were recovered. The debris that was left on the filter was rinsed into a glass beaker with ~ 25ml of deionized water (Scott et al., 2020).

Quality control consisted of laboratory blanks (10% of field samples or greater) and microplastic spike samples (positive controls); these controls were run alongside water and sediment samples. Laboratory blanks were subtracted from the field sample results. The laboratory blanks were produced by collecting 1000 ml of deionized water into a triple-rinsed flask and processed in the same manner as the rest of the field-collected water samples. A spike involved five pieces of PE, PP, and PVC added to 1000 ml of deionized water in a triple rinsed flask and processed in the same manner as the rest of the field collected water samples. Prior analyses have reported that laboratory blanks produce an average of 10 to 15 particles per liter.

Wet Peroxide Oxidation

This section explains the procedure of using aqueous Fe (II) solution and hydrogen peroxide to oxidize to remove natural organic material from the collected MPs. Twenty ml of aqueous Fe (II) solution was added to the beaker containing the 5 µm size fraction of collected solids, which was followed by the careful addition of 20 ml of 30% hydrogen peroxide. The solution was heated to 75°C on a hotplate. Once gas bubbles appeared at the surface, the beaker was removed from the hotplate and placed in a fume hood until boiling subsided. If necessary, distilled water was added to prevent overflow. The mixture was heated at 75°C for an additional 30 minutes. If natural organic material was still visible, another 20 ml of 30% hydrogen peroxide was added and the process repeated until no natural organic material was visible. Finally, approximately 6 g of salt (NaCl) per 20 ml of sample was added to increase the

density of the aqueous solution to around 5 M NaCl, and the mixture was heated again to 75°C until the salt dissolved (Masura et al., 2015).

Density Separation

This section outlines the process of transferring the oxidized solution to a density separator for isolating MPs from other materials in the sample. The wet peroxide oxidation solution was transferred to a density separation unit (Scott et al., 2020). A potassium iodide (KI) solution was poured into the density separator containing the sample until the volume was approximately 6 inches above the open valve (Scott et al., 2020). The density separator was loosely covered with aluminum foil, allowing the solids to settle overnight. The settled solids were examined visually for any MPs; if found, the settled solids were drained from the separator and MPs removed using forceps, then archived or discarded. By adding potassium iodide solution to the oxidized mixture, the density of the solution is increased, allowing the denser non-plastic particles to settle while the less dense microplastics remain suspended. This separation simplifies the recovery and examination of MPs, ensuring accurate identification and analysis.

After 24 hours, the valve was closed, and a laboratory vacuum system attached to a side-armed flask containing a gridded 0.45-µm filter, with a filtering apparatus attached using a clamp. The sample was poured from the density separator into the filtering apparatus, making sure the sides of the density separator were rinsed three times to recover all MPs, and then filtered (Scott et al., 2020). Finally, the filter was removed and placed into a petri dish and examined under the microscope.

Microscopy

Filters with MPs were observed under the Zeiss Stereo Zoom Discovery V.20 Light Microscope with Vision Research Micro eX4 Monochrome High-Speed Video Camera, which captured images of MP length, color, and shape. Thermo Infrared (IR) microscopic analysis identified microplastics greater than 20 µm in size and identified polymer type. Data reported for each sample includes counts per unit (#/L), size distribution, shape distribution, color distribution, and an estimate of total mass of MP present (Tables 2.2; 2.3; 2.4; 2.5). IR is very poor at identifying dark and black material; if a polymer ID match was not greater than 80% accurate, the ID of the polymer was classified as unknown.

Sediment Samples

Methods used to extract MPs from sediment followed NOAA protocols (Masura et al., 2015). Sediment samples were first prepped by weighing and labeling a clean and dry 800-ml beaker to the nearest 0.1 mg. Next, 400 g of wet sediment was weighed to the nearest 0.1 mg and added to the labeled beaker. Then, this mixture was dried at 90°C overnight or until completely dry and weighed. The mass of total solids was calculated by subtracting the mass of the tared beaker from the weight obtained. To disaggregate the dried bed sediments, 400 ml of potassium metaphosphate (5.5 g per liter of water) was added to the sediment sample, along with a stir bar. The sample was mixed for 1 hour at the high RPM setting, followed by wet sieving and transfer of sieved solids. Wet sieving followed the procedures described above; after rinsing, I removed and discarded any visible material larger than 5 mm with forceps. The solids retained on 0.3-mm sieves were transferred to tared 500-ml beakers using a metal spatula and then dried at 90°C for 24 hours or longer to ensure sample dryness. The beaker

with solids was then weighed on an analytical balance to the nearest 0.1 mg. Total solid mass was determined by subtracting the mass of the tared beaker.

For density separation, 300 ml of aqueous lithium metatungstate (d=1.6 g/ml) solution was added to the dried sediments in the beaker and stirred vigorously to float out the microplastics. The floating solids were transferred to a custom 5 µm sieve, which was transferred to a tared 500-ml beaker and dried at 90°C for 24 hours or longer to ensure sample dryness. The mass of all microplastics and natural materials was determined by subtracting the mass of the tared beaker.

Wet peroxide oxidation involved adding 20 ml of aqueous Fe (II) solution to the beaker containing the 5 µm size fraction of collected solids. Then, 20 ml of 30% hydrogen peroxide was added, allowing the mixture to stand at room temperature for five minutes before adding a stir bar, covering with a watch glass, heating to 75°C on a hotplate, and adding more hydrogen peroxide if natural organic material was visible, until no organic material was visible. About 6 g of salt (NaCl) was added per 20 ml of the sample to increase the density of the aqueous solution to ~5 M NaCl and the mixture was heated until the salt dissolved. Then this solution goes through the density separator again (repeating the previously mentioned steps). After the sample is dried it can be observed under the microscope.

6-PPD-Q

6-PPD-Q was analyzed separately from samples processed for MPs. One liter of sample was spiked with isotopically labeled 6PPD-Q so that its final concentration at 1 ml was 50 ng/ml (ppb). The samples were then passed through a pre-conditioned Oasis HLB solid phase

extraction column (P/N WAT106202), 200 mg). The columns containing the samples were then dried for 10 minutes. After drying, 6-PPD-Q was eluted from the columns with 10 ml of methanol. The eluates were then concentrated to a final volume of 1 ml under a gentle stream of nitrogen. In addition to the samples, a reagent blank and a reagent blank spike were processed with each batch to serve as additional quality control (Tian et al., 2022).

The extracts were analyzed by ultra-high performance liquid chromatography tandem mass spectrometry (Shimadzu LCMS 8050). Separation was achieved on a Water Acuity BEH Shield RP-18 analytical column (2.1 mm x 100 mm, 1.7 um particle size). The mobile phases consisted of 0.1% formic acid in water (Mobile Phase A) and methanol (mobile phase B). The gradient was initiated with 95% mobile phase A (5% mobile phase B). The mobile phase gradient was programmed to consist of 50% mobile phase A (50% mobile phase B) by 4 minutes into the run. Then at 10 minutes the mobile phase composition was set for 100% mobile phase B. By 13 minutes, the mobile phase composition was then set for 5% mobile phase A (95% mobile phase B). The sample injection volume was set at 10 microliters and the ionization mode was positive (Tian et al., 2022).

Statistical Analysis

All statistics and data visualization were conducted with R version 4.3.1 (2023-06-16 ucrt) using R studio (2022) version 4.2.2 (Integrated Development for R. RStudio, PBC, Boston, MA). A Shapiro-wilks test indicated that both discharge and MP mass were not normally distributed; as a result, a non-parametric test was used to determine the correlation between the two variables. A spearman's rank-order correlation was used to assess the strength and direction of the relationship between discharge and MP mass.

Results

Habitat: Lake

Environmental Conditions

Water samples taken from Church Lake began in the Summer of June 2022 and ended April of 2023 (Table 2.1). Samples were taken from randomly selecting coordinates in both the lake and the tributary to avoid sampling biases. Lake water samples were taken in the summer (n=2), fall (n=2), winter (n=1), and spring (n=2). Summer water samples were the warmest (24.7 ℃), DO was supersaturated in shallow regions and became hypoxic at ~ 10m, with relatively high conductivity in shallow areas (~ 2m: 841-864 µS/cm) and even higher in deeper regions (~ 10m: 1230-1312 µS/cm). pH was alkaline near the surface (8-9) and became circumneutral near the bottom. Turbidity was relatively low until ~10 m but this increase with depth may have been caused by disturbance of the sediment bed by the YSI sonde. Prior studies have shown that Church Lake thermally stratifies in summer months (Progressive AE, 2010; Foley and Steinman 2023); my data also show spring and summer thermal stratification (Table 2.1). The fall sampling was in more shallow locations, where oxygen levels were all >5 mg/L, even at the deepest site sampled (6 m). Conductivity was high in shallow areas (1 – 6 m), ranging from 847-867 µS/cm. pH remained high (8) until ~6m when it decreased very slightly. Only 1 winter sample was taken because of the thick ice sheet covering the lake from Dec-Feb; this shallow sample had high DO (12.8 mg/L) and conductivity (941 µS/cm), with low temps (2℃) and alkaline pH (8) (Table 2.1). During the spring months, temperatures were low (1m: 5-11℃), and DO was supersaturated closer to the surface (15 mg/L) but decreased with depth. Conductivity

was highest (866-941 µS/cm) in the shallower regions in the spring compared to the other seasons and increased with depth (979-1017 µS/cm).

MP Characteristics

MP density ranged from 61-880 counts/L in lake samples (Table 2.2). MP surface area ranged from 0.51 – 18.78 mm^2/L. MP mass ranged from 0.48-17.66 mg/L (Table 2.2). Overall, the largest density of MP was reported in January 2022 and the lowest in Sept 2022 (Table 2.2). A large but undefined portion of our MPs consisted of black particles that we were unable to classify because of the uncertainty of polymer identification, however, its suspected these unknown black polymer particles may be rubber fragments, potentially containing 6PPD-Q. 6-PPD-Q concentrations found in lake samples were all <1 ng/L.

The most common MP shape found in lake water (n=7) samples was fragments (59-783 counts/L), whereas the number of fibers found within our detectable size range of ~50 µm x 50 µm was 2-96 counts/L (Figure 2.2; Table 2.3). MP colors that were found in lake water samples were red (0-7 counts/L), yellow (0-72 counts/L), brown (0-172 counts/L), clear (0-53 counts/L), orange (0-22 counts/L), grey (0-407 counts/L), black (21-598 counts/L) (Figure 2.3; Table 2.4). This showed that black fragments were the most frequent material found in these lake water samples.

The following list of polymers and polymer additives were found in the lake and tributary: acrylic, polyvinylidene chloride, polyethylene, polyester, 6-PPD-Q polyamides, siloxane, ethylene vinyl alcohol, and silicone base; the rest were labeled unknown if there was a less than 80% certainty of identification (Figure 2.4; Table 2.5).

Polymer types were tabulated by surface area (mm^2/L) found in each sample. In lake samples, the majority of MPs were labeled unknown (0.25-18.78 surface area mm^2/L). The rest of the polymers found were polyamide (0-0.38 surface area mm^2/L), cellulosic (0-0.07 surface area mm^2/L), siloxane (0-0.42 surface area mm^2/L), ethylene vinyl alcohol (0-0.04 surface area mm^2/L), polyvinylidene chloride (0-0.006 surface area mm^2/L), polyethylene (0-0.06 surface area mm^2/L), and silicon (0-0.17 surface area mm^2/L) (Figure 2.4; Table 2.5).

Habitat: Tributary Baseflow

Environmental Conditions

Samples taken in the tributary (baseflow) (n=11) occurred once every month for one year from May 2022 to April 2023 (Table 2.1). The July sample was lost during MP analysis and was not included in water quality analysis or plots. Discharge was recorded at every tributary (baseflow) sampling event (Figure 2.5). Temperatures were warm from May – Sept (13-19 ℃), the rest of the sampling year was colder (4-8℃). The tributary (baseflow) maintained relatively high DO, which is expected of a moving stream. Conductivity was high (848-1799 µS/cm) nearly year-round, with an unexpected low value (240 µS/cm) in October; this is an unusually low value and may be related to instrument error. The pH was consistent year-round (~8) and NTU (Nephelometric Turbidity Unit) varied every month and may have been dependent on the location of sampling.

MP Characteristics

MP counts/L ranged from 127 - 1,293 in tributary (baseflow) samples. MP surface area ranged from 0.60 – 8.55 mm^2/L. MP mass ranged from 0.56-8.55 mg/L. 6-PPD-Q ranged from <1 -24 ng/L. The highest number of MPs occurred in October and the lowest occurred in May,

June, and Dec (Table 2.2). October also had the greatest 6-PPD-Q concentration; the only months with 6-PPD-Q values < 1 were May through October. Comparatively, MP counts, mass, and 6-PPD-Q were higher in the tributaries, even under baseflow, than in the lake (Table 2.2).

The majority of MPs found in tributary (baseflow) water (n=11) samples were in the shape of fragments (120-1,228 counts/L), followed by fibers, which within our detectable size range, were an order of magnitude more abundant than in lake water samples (8-293 counts/L) (Figure 2.3; Table 2.3). MP colors that were found in lake water samples were red (0-21 counts/L), yellow (0-82 counts/L), brown (0-187 counts/L), clear (0-87 counts/L), orange (0-43 counts/L), green (0-312 counts/L), grey (0-433 counts/L), and black (46-271 counts/L) (Figure 2.4). Similar to lake samples, black fragments were most abundant in tributary (baseflow) water samples.

Most of the MPs in the tributary (baseflow) water samples were composed of polymers that were unidentifiable and classified as unknown (0.23-6.58 surface area mm^2/L). The rest of the polymers were polyamide (0-0.14 surface area mm^2/L), cellulosic (0-0.23 surface area mm^2/L), siloxane (0-0.09 surface area mm^2/L), ethylene vinyl alcohol (0-0.06 surface area mm^2/L), acrylic (0-0.002 surface area mm^2/L), polyester (0-0.05 surface area mm^2/L), and silicon (0-1.88 surface area mm^2/L) (Figure 2.4).

Habitat: Tributary (Storm)

Environmental Conditions

A total of 5 tributary (storm) samples were taken from August 2022 – March 2023. Tributary (storm) sampling usually occurred a few days before baseflow sampling; this provided

insights into the immediate impacts of storm events on water quality, allowing a comparison of storm flow to baseflow conditions. In summer (8/17/22), stormflow was warmer than baseflow by ~3°C, presumably due to heated runoff from the road surface, which in turn resulted in lower DO levels. Conductivity declined by ~200 µS/cm, although absolute levels were still quite high, pH remained the same, but turbidity increased ~5-fold (Table 2.1). In fall (10/14/22), stormflow had a different effect, resulting in a 5°C decline in temperature, a slight increase in DO concentration, a 200 unit increase in conductivity (although much lower absolute levels than other seasons), and a decline in turbidity. The two-winter stormflow events (1/9/23 and 2/13/23) resulted in little change from baseflow in DO levels and pH, but a large decline (~500 units) in conductivity and a large increase (>20-fold) in turbidity, which was observed also in the early spring (3/27/23) sampling (Table 2.1).

MP Characteristics

There was a range of 482-16,390 counts/L of MPs found in storm samples. MP surface area ranged from 0.64 – 13.51 mm^2/L. MP mass ranged from 0.60-12.7 mg/L. 6-PPD-Q ranged from <1 -201 ng/L. The highest MP counts occurred in October and the lowest occurred in August (Table 2.2). 6-PPD-Q had the highest concentration overall during storm events. With the highest concentration of 6-PPD-Q occurring during October.

The majority of MPs measured in the stormflow (n=5) had the shape of fragments (472-15,734 counts/L); the number of fibers measured within our detectable size range was 0-655 counts/L (Figure 2.3; Table 2.3). MP colors that were found in stormwater samples were red (0-8 counts/L), yellow (16-145 counts/L), brown (0-820 counts/L), clear (0-33 counts/L), orange (0-

5 counts/L), grey (0-337 counts/L), black (28-15,472 counts/L) (Figure 2.4; Table 2.4). Most of the fragments found were black.

MP surface area samples in stormflow were dominated by items labeled as unknown (0.63-13.11 surface area mm^2/L). The rest of the polymer surface areas included polyamide (0-0.14 surface area mm^2/L), cellulosic (0-0.27 surface area mm^2/L), and polyethylene (0-0.42 surface area mm^2/L) (Figure 2.4). The polymers found in stormflow were less variable than the polymers that were found in baseflow.

Atmospheric pressure affects weather patterns such as precipitation, wind, and temperature, which in turn influences the movement and distribution of MPs. Variations in pressure can alter storm intensity and wind patterns, impacting MP transport. Precipitation plays a key role by transporting MPs into water bodies, with high precipitation leading to increased runoff and higher MP concentrations. Spikes in absolute pressure indicate high-pressure systems with calm weather and less runoff, while decreases signal low-pressure systems with stormier conditions and enhanced MP transport (Figure 2.5). Temperatures were warmer in mid-year and colder towards the end of 2022 and early 2023. Absolute pressure showed minor fluctuations from 98.37 kPa in May 2023 to 99.02 kPa in June 2022. Storm events were linked to higher MP concentrations, but no clear correlation was found between MP mass or counts and baseflow discharge in Church Lake (Figure 2.6; 2.7). Understanding these atmospheric conditions helps predict their impact on microplastic presence and movement.

Habitat: Sediment Samples

Environmental Conditions

Sediment samples were taken only in March 2023 (Table 2.1). One sample was taken in the lake and a second from the tributary near the end of the tributary. Water quality taken in the tributary before the sediment sample (tributary sediment) was collected revealed a cool temperature with high DO, high conductivity (940 µS/cm), basic pH, and low turbidity. Water sampled in the lake before sediment samples (lake sediment) were retrieved had a low temperature, relatively low DO, high conductivity (1017 µS/cm), slightly basic pH, and modest turbidity. Lake sediment sample was taken near the location where the PVC frames were deployed (Figure 2.1).

MP Characteristics

Overall, MPs were less abundant in the lake sediment than in the tributary sediment samples. The lake sediment sample had 3,016 MP counts/L, while sediment samples that came from the tributary had 8,736 MP counts/L (Table 2.2). MP surface area in the lake was 22.93 mm^2/L compared to 49.87 mm^2/L in the tributary; MP mass in sediment samples from the lake vs. the tributary was 21.55 vs. 45.27 mg/L, respectively.

The majority of MPs found in the tributary sediment (n=1) sample were as fragments (8,735 counts/L); no fibers were found (Figure 2.3). MP colors that were found in tributary sediment samples were red (9 counts/L), yellow (61 counts/L), brown (472 counts/L), clear (9 counts/L), green (9 counts/L), grey (5,730 counts/L), and black (2,437 counts/L) (Figure 2.4). The majority of MPs polymers were classified as unknown (48.09 surface area mm^2/L). The rest of

the polymers found were cellulosic (15.86 surface area mm^2/L), and polyethylene (1.90 surface area mm^2/L) (Figure 2.4; Table 2.5).

The most common MP shapes in lake sediment (n=1) samples were fragments (2,955 counts/L), followed by only a small number of fibers within our detectable size range (60 counts/L) (Figure 2.3; Table 2.3). MP colors that were found in lake sediment samples were red (3 counts/L), yellow (389 counts/L), brown (271 counts/L), clear (36 counts/L), orange (21 counts/L), grey (446 counts/L), and as observed in other samples, an abundance of black (1,852 counts/L) (Figure 2.4; Table 2.4). The majority of polymers in lake sediment MPs were classified as unknown (22.79 surface area mm^2/L). The rest of the polymers were cellulosic (1.28 surface area mm^2/L) and siloxane (0.01 surface area mm^2/L) (Figure 2.4; Table 2.5).

Discussion

In this study, I investigated the influx of MPs from an unnamed tributary that receives runoff from a major highway and flows into Church Lake. The goal was to assess MP abundance; characterize their shape, color, and type. By conducting monthly water sampling, complemented by spring sampling of the sediment, this study cataloged the concentrations and characteristics of MPs present in the tributary and Church Lake.

Samples in the current study from different habitats (lake and sediment) and media (water and sediment) revealed notable differences in both environmental conditions and MP characteristics (see below). The lake exhibited seasonal and spatial variations in temperature, DO levels, conductivity, and turbidity, indicative of thermal stratification and showed turnover patterns only in shallow areas of Church Lake. In contrast, the Tributary (baseflow) maintained

relatively stable conditions throughout the year, with consistently high DO and conductivity levels. Tributary (storm) sampling, typically conducted a few days before baseflow sampling, facilitated the comparison of storm flow conditions with baseflow conditions. Summer storm events were characterized by warmer temperatures, lower dissolved oxygen levels, and increased turbidity compared to baseflow, likely influenced by heated runoff from road surfaces. In contrast, fall and winter storm events led to varied effects on water quality parameters such as temperature, DO, conductivity, and turbidity, highlighting seasonal differences in stormwater dynamics. The lower conductivity values during stormflow compared to baseflow contrasted with prior results in this system (Foley and Steinman, 2023). It is possible that the time between sampling stormflow and baseflow (~ 1 week) may have altered conductivity; alternatively, different sampling locations were used when we sampled for Tributary (baseflow) and Tributary (storm). Random sampling was done to avoid any sampling biases and gave us a generalized idea of MP abundance in the tributary and lake. Water quality influences biofilm growth on MPs, and under favorable environmental conditions, increased biofilm growth can cause MPs to sink as a response to increases in biofilm mass (He et al., 2021; Semcesen & Wells, 2021). The different water quality characteristics among depths likely influenced the biofilm mass, which in turn, influenced the distribution and characteristics of MPs. This highlights the importance of understanding habitat-specific dynamics in assessing microplastic distribution.

The following list describes some of the purposes used for polymers and additives found in the tributary and lake and is not an exhaustive list of the possible usages for the polymers and their additives found in this study. Acrylics are transparent plastic material used for lenses,

acrylic nails, paint, security barriers, medical devices, LCD screens, and furniture. Cellulose is a natural biodegradable plastic made from cotton liners or wood pulp and used for the manufacture of cigarette filters, screwdriver handles, and ink pen reservoirs. Polyvinylidene chloride is used as a synthetic resin, commonly used in plastic food wraps because it is clear, flexible, and impermeable. Polyethylene is commonly used to produce grocery bags, agricultural mulch, wire, cable insulation, and toys. Polyester is a synthetic fiber derived from petroleum and found in most fabric materials. 6-PPD-Q is a stabilizing additive found in rubbers that is often leached from vehicle tires. Polyamides are highly durable water-resistant synthetic fibers. Siloxane is a modifying additive that improves surface characteristics such as a scratch resistant lubricant. Ethylene vinyl alcohol is a film used for food wrap and medical packaging to prevent gas transmissions. Silicone is a malleable rubber-like material that is flexible, temperature resistant, and water resistant. The most common sources of polymers and additives found in the tributary and lake are urban runoff and agricultural activities. Urban runoff includes materials from vehicle tires (6-PPD-Q), plastic food wraps (polyvinylidene chloride, ethylene vinyl alcohol), and household items (acrylics, polyethylene, silicone). Agricultural sources contribute materials like polyethylene used in agricultural mulch. The primary sources of MP pollution to Church Lake came from urban and agricultural runoff.

In comparing the MP characteristics across the four habitats (lake water, tributary (baseflow) water, tributary (storm) water, and sediment samples from both lake and tributary), several key differences emerged. Lake water samples generally exhibited lower MP counts, surface area, and mass compared to tributary (baseflow) and tributary (storm) water samples. However, sediment samples from both lake and tributary (baseflow) contained higher MP

counts, surface area, and mass compared to their respective water samples, with tributary (baseflow) sediment exhibiting the highest values. It was unknown where in the tributary MPs accumulated because the transport of MPs is influenced by water currents and retention structures, such as woody debris and vegetation (Semcesen & Wells, 2021; Vincent and Hoellhein, 2021). I infer that the majority of MPs entering the unnamed tributary were retained on or in the stream bed, reducing the amount that would otherwise reach Church Lake. These results are consistent with previously studied rates of settlement of MPs (Kowalski et al., 2016; Uzun et al., 2021; Vincent and Hoellein, 2021; Wu et al., 2019).

In terms of MP shapes, fragments were predominant across all habitats, followed by fibers, although their abundance varied. In comparison to similar studies, our results yielded larger quantities of fragments of MPs than other studies, but overall found that the proximity to a highway contributed to higher fragment counts than fiber (Table 2.6) (Leads & Weinstein, 2019; Monira et al., 2021; Shruti et al., 2021; Yano et al., 2021). In theory our results were influenced by the proximity to the highway and methodology used. MP counts vary among studies because of the different collection methods, size limitations, and density salts used for MPs analysis. MP concentrations reported among other studies have varied greatly since there are no established or harmonized methods for sampling, identifying, and quantifying MPs. Other studies examining tributaries have observed dominance by plastic fragments when runoff is coming from roads, whereas tributaries receiving runoff from wastewater treatment plants have largely fibers in the water and dry sediment (Leads & Weinstein, 2019; Werbowski et al., 2021; Yano et al., 2021). The source of runoff contributes a range of products, such as fiber-containing personal care products, paper goods, and textiles, to the wastewater stream. It is

not surprising that wastewater discharge has higher fiber concentrations than other sources of runoff because this type of effluent goes through extensive treatment that includes settling and removal of both buoyant and dense particles before the treated water is discharged to other streams. On the other hand, road surfaces, which collect wear-out from tires, artificial turf, brake wear, road marking paints, and litter (bottles, bags, etc.) are less likely to contain significant amounts of fibers, and are the main source of highway runoff (Monira et al., 2021; Werbowski et al., 2021).

Studies on MPs take color identification into account since colored MP particles can mislead aquatic organisms as food because they resemble prey (Shruti et al., 2021). While black MPs were consistently observed across all habitats, their proportions differed, with tributary (storm) water and tributary sediment samples showing higher counts of black MPs compared to lake water and lake sediment samples. Grey plastics were also predominately seen in both sediment samples in terms of counts in comparison with water samples, which may indicate that grey MPs entering the tributaries have higher densities than the rest of the polymers found. A large number of studies looking at MPs in tributaries near highways have observed black MPs from rubber eroded from car tires (Lange et al., 2021; Leads & Weinstein, 2019; Werbowski et al., 2021; Yano et al., 2021). The proximity to urban and stormwater runoff can influence the types of polymers present (Shruti et al., 2021). The most common polymers found in stormwater runoff from highways in other studies are PE, PP, PS, PET, acrylic, and polyamide (Lutz et al., 2021; Shruti et al., 2021). This study did not identify PP, PS, or PET among the polymers found in the tributary and Church Lake but maybe among the large quantity of unknown polymers we were unable to identify. In aquatic environments, the dispersion of MPs is influenced by the

density of the polymers. Studies have shown that the less dense polymers (PE, PP, and PS) are more common in the water column while higher density polymers (polyamide, polyester, PVC, and acrylic) are dominant in sediments (Driedger et al., 2015; Sang et al., 2021; Shruti et al., 2021). With the polymers we were able to identify sediment samples mostly composed of cellulosic and polyethylene. While water samples mostly contained polyester, cellulosic, siloxane, polyamide, and ethylene vinyl alcohol. Moreover, the diversity of polymer types was slightly higher in tributary (baseflow) sediment compared to lake sediment, suggesting potential differences in pollution sources or transport mechanisms between these habitats. MP color can also influence biofilm growth. The color of the MPs can affect the light absorption and chemical composition (Badea & Balas, 2023). Overall, these comparisons highlight the complex dynamics of MP distribution and composition within aquatic ecosystems, influenced by factors such as water flow, sedimentation, and habitat characteristics.

Although discharge measurements were made on a limited basis, the positive correlation between discharge and MP mass in water samples taken from tributary (baseflow) suggest that larger influxes of water into the tributary, such as storm events, could impact MP mass transportation. However, this correlation was not statistically significant, so more flow measurements are needed to confirm this suggestion.

This study showed that highway runoff can be a source of pollution to urban lakes, although factors such as distance from the road to water body, vehicular traffic density, and road infrastructure all play an important part in the volume and contents in the runoff. The presence of MPs in the water and sediment does not equate to whether they are having an

adverse impact on the biota. Specific studies are needed to test whether the densities, mass, and properties of the MPs in my study system are capable of generating an adverse impact. MP counts vary among studies because of the collection methods, size limitations, and density salts used for MPs analysis. MP concentrations reported among other studies vary greatly since there are no established or harmonized methods for sampling, identifying, and quantifying MPs. Hence, I am uncomfortable comparing my numbers to those of other studies. Nonetheless, based on the precautionary principle, I recommend that management actions are needed to detain or move water away from inflows to streams and lakes. Without these actions, stormwater pollution such as deicing salts and MPs will continue to enter systems such as Church Lake.

Future research in this system should measure not only discharge during storm events but also investigate tributaries and groundwater that connect Church Lake to the two urban lake areas downstream of Church (Middleboro and Westboro; Figure 2.1). The findings highlight the complex dynamics of MP pollution in freshwater ecosystems and underscore the need for continued monitoring and research to better understand the sources, fate, and impacts of MPs on aquatic biota and ecosystems. Additionally, efforts to mitigate plastic pollution should focus on identifying and addressing the primary sources of MPs and implementing effective management strategies to protect water quality and ecosystem health.

Conclusion

Based on the findings from the study conducted on Church Lake and its tributary, several key conclusions can be drawn:

1) MP abundance varied seasonally and between different habitats within the study area. Counts shown in each habitat at the time of sampling represent MPs present in the water column or sediment and may have been influenced by biotic and abiotic factors present during the time. The highest MP counts were recorded in the lake during the winter months; the tributaries showed higher MP counts during the fall and winter for Tributary (storm) and the Tributary (baseflow). Storm events were identified as hotspots for MP runoff, contributing to elevated MP levels in the tributaries.
2) The predominant MP shapes in both habitats were fragments, with stormflow samples exhibiting higher counts of fragments compared to baseflow samples. Similar results were seen in other studies observing stormwater runoff from highways to tributaries. In other studies, fragments were prevalent more in sediment than water (Lange et al., 2021; Leads & Weinstein, 2019; Werbowski et al., 2021; Yano et al., 2021). Although these studies identified rubber from tires as their dominant fragment particles, we were able to identify only black fragments as being dominant in the unnamed tributary that connects Church Lake.
3) Sediment samples in the tributary contained higher MP counts/ mass than lake samples, presumably because of closer proximity to the source of road runoff. As expected, there was a positive, albeit non-significant, correlation between discharge and MP counts/mass in water samples taken during baseflow in the tributary. Discharge is often low in small streams such as the tributary that connects to Church Lake and often does not show a correlation between discharge and MP counts; our data corresponds with the results of another study characterizing the plastic pollution in small streams

(Dikareva & Simon, 2019). The correlation likely would have been statistically significant if we were able to record discharge during storm events but dangerous storm conditions at the site precluded measurements. Other studies investigating MP transport have seen MP hot spots occurring during storm events (Liu et al., 2019; Lutz et al., 2021; Monira et al., 2021).

4) Given that different watersheds have distinct land use features that may significantly affect the amount and characteristics of MP present, location certainly influences the MPs found. Previous studies have seen that the proximity to highways or wastewater treatment plant runoff influences the MP shape, polymer types, and counts most commonly found in nearby tributaries (Grbić et al., 2020; Leads & Weinstein, 2019; Werbowski et al., 2021; Yano et al., 2021)
5) The study contributes to the growing body of research on plastic pollution, particularly in freshwater ecosystems. It highlights the prevalence of plastic debris in water bodies and the potential sources and transport mechanisms of MPs. MPs can accumulate in lakes sediments, shorelines and surfaces, causing the potential degradation of the environment and alteration of habitat (Driedger et al., 2015). Future research is needed to determine if the MPs in Church Lake are having these types of environmental impacts.

References

Alimi, O. S., Farner Budarz, J., Hernandez, L. M., & Tufenkji, N. (2018). Microplastics and nanoplastics in aquatic environments: aggregation, deposition, and enhanced contaminant transport. Environmental Science & Technology, 52(4), 1704–1724. https://doi.org/10.1021/acs.est.7b05559

Amaneesh, C., Anna Balan, S., Silpa, P. S., Kim, J. W., Greeshma, K., Aswathi Mohan, A., Robert Antony, A., Grossart, H. P., Kim, H. S., & Ramanan, R. (2022). Gross negligence: Impacts of microplastics and plastic leachates on phytoplankton community and ecosystem dynamics. Environmental Science and Technology. https://doi.org/10.1021/acs.est.2c05817

Arpia, A. A., Chen, W. H., Ubando, A. T., Naqvi, S. R., & Culaba, A. B. (2021). Microplastic degradation as a sustainable concurrent approach for producing biofuel and obliterating hazardous environmental effects: A state-of-the-art review. Journal of Hazardous Materials, 418(March), 126381. https://doi.org/10.1016/j.jhazmat.2021.126381

Badea, M. A., & Balas, M. (2023). Microplastics in freshwaters: implications for aquatic autotrophic organisms and fauna health. Microplastics, 39–59. https://doi.org/10.3390/microplastics2010003

Bohara, K., Timilsina, A., Adhikari, K., Kafle, A., Basyal, S., Joshi, P., & Yadav, A. K. (2024). A mini review on 6PPD quinone: A new threat to aquaculture and fisheries. Environmental Pollution, 340(P2), 122828. https://doi.org/10.1016/j.envpol.2023.122828

Canniff, P. M., & Hoang, T. C. (2018). Microplastic ingestion by Daphnia magna and its enhancement on algal growth. Science of the Total Environment, 633, 500–507. https://doi.org/10.1016/j.scitotenv.2018.03.176

Chamas, A., Moon, H., Zheng, J., Qiu, Y., Tabassum, T., Jang, J. H., Abu-omar, M., Scott, S. L., & Suh, S. (2020). Degradation rates of plastics in the environment. *ACS Sustainable Chemistry & Engineering*, *8* (9), 34943511. https://doi.org/10.1021/acssuschemeng.9b06635

Chen, X., Chen, X., Zhao, Y., Zhou, H., Xiong, X., & Wu, C. (2020). Effects of microplastic biofilms on nutrient cycling in simulated freshwater systems. Science of the Total Environment, 719, 137276. https://doi.org/10.1016/j.scitotenv.2020.137276

Dikareva, N., & Simon, K. S. (2019). Microplastic pollution in streams spanning an urbanisation gradient. Environmental Pollution, 250, 292–299. https://doi.org/10.1016/j.envpol.2019.03.105

Driedger, A. G. J., Dürr, H. H., Mitchell, K., & Van Cappellen, P. (2015). Plastic debris in the Laurentian Great Lakes: A review. Journal of Great Lakes Research, 41(1), 9–19. https://doi.org/10.1016/j.jglr.2014.12.020

Eadie, B. J., Schwab, D. J., Johengen, T. H., Lavrentyev, P. J., Miller, G. S., Holland, R. E., Leshkevich, G. A., Lansing, M. B., Morehead, N. R., Robbins, J. A., Hawley, N., Edgington, D. N., & Van Hoof, P. L. (2002). Particle transport, nutrient cycling, and algal community structure associated with a major winter-spring sediment resuspension event in Southern Lake Michigan. Journal of Great Lakes Research, 28(3), 324–337. https://doi.org/10.1016/S0380-1330(02)70588-1

Foley, E., & Steinman, A. D. (2023). Urban lake water quality responses to elevated road salt. Science of the Total Environment, 905, 167139. https://doi.org/10.1016/j.scitotenv.2023.167139

Gore, J.A, Banning, J. (2017). Discharge measurements and streamflow analysis. In: Hauer FR, Lamberti GA (eds) methods in stream ecology. 3rd ed. Elsevier Press 49-70.

Grbić, J., Helm, P., Athey, S., & Rochman, C. M. (2020). Microplastics entering northwestern Lake Ontario are diverse and linked to urban sources. Water Research, 174, 115623. https://doi.org/https://doi.org/10.1016/j.watres.2020.115623

He, S., Jia, M., Xiang, Y., Song, B., Xiong, W., Cao, J., Peng, H., Yang, Y., Wang, W., Yang, Z., & Zeng, G. (2021). Biofilm on microplastics in aqueous environment: Physicochemical properties and environmental implications. Journal of Hazardous Materials, 127286. https://doi.org/10.1016/j.jhazmat.2021.127286

Hitchcock, J. N. (2020). Tributary events as key moments of microplastic contamination in aquatic ecosystems. Science of the Total Environment, 734, 139436. https://doi.org/10.1016/j.scitotenv.2020.139436

Jeong, H., Novirsa, R., Nugraha, W. C., Addai-arhin, S., Dinh, Q. P., Fukushima, S., Fujita, E., Bambang, W., Kameda, Y., Ishibashi, Y., & Arizono, K. (2021). The distributions of microplastics (MPs) in the Citarum River Basin, West Java, Indonesia. *Journal of Environment and Safety*. *12*(2), 33–43.

Johnson, K. A., Steinman, A. D., Keiper, W. D., & Ruetz, C. R. (2011). Biotic responses to low-concentration urban road runoff. Journal of the North American Benthological Society, 30(3), 710–727. https://doi.org/10.1899/10-157.1

Kaushal, S. S., Reimer, J. E., Mayer, P. M., Shatkay, R. R., Maas, C. M., Nguyen, W. D., Boger, W. L., Yaculak, A. M., Doody, T. R., Pennino, M. J., Bailey, N. W., Galella, J. G., Weingrad, A., Collison, D. C., Wood, K. L., Haq, S., Newcomer-Johnson, T. A., Duan, S., & Belt, K. T. (2022). Freshwater salinization syndrome alters retention and release of chemical cocktails along flow paths: From stormwater management to urban streams. Freshwater Science, 41(3). https://doi.org/10.1086/721469

Kowalski, N., Reichardt, A. M., & Waniek, J. J. (2016). Sinking rates of microplastics and potential implications of their alteration by physical, biological, and chemical factors. Marine Pollution Bulletin, 109(1), 310–319. https://doi.org/https://doi.org/10.1016/j.marpolbul.2016.05.064

Lange, K., Österlund, H., Viklander, M., & Blecken, G.-T. (2021). Occurrence and concentration of 20–100 µm sized microplastic in highway runoff and its removal in a gross pollutant trap – Bioretention and sand filter stormwater treatment train. Science of The Total Environment, 151151. https://doi.org/10.1016/j.scitotenv.2021.151151

Leads, R. R., & Weinstein, J. E. (2019). Occurrence of tire wear particles and other microplastics within the tributaries of the Charleston Harbor Estuary, South Carolina, USA. Marine Pollution Bulletin, 145(February), 569–582. https://doi.org/10.1016/j.marpolbul.2019.06.061

Liu, F., Olesen, K. B., Borregaard, A. R., & Vollertsen, J. (2019). Microplastics in urban and highway stormwater retention ponds. Science of the Total Environment, 671, 992–1000. https://doi.org/10.1016/j.scitotenv.2019.03.416

Lutz, N., Fogarty, J., & Rate, A. (2021). Accumulation and potential for transport of microplastics in stormwater drains into marine environments, Perth region, Western Australia. Marine Pollution Bulletin, 168(April), 112362. https://doi.org/10.1016/j.marpolbul.2021.112362

Masura, J., et al. 2015. Laboratory methods for the analysis of microplastics in the marine environment: recommendations for quantifying synthetic particles in waters and sediments. NOAA Technical Memorandum, NOS-OR&R-48.

Molloseau, J., & Steinman, A. D. (2023). Chloride and phosphorus retention and release in soils surrounding a salt-contaminated lake in West Michigan. Journal of Freshwater Ecology, 38(1), 2241478. https://doi.org/10.1080/02705060.2023.2241478

Monira, S., Bhuiyan, M. A., Haque, N., Shah, K., Roychand, R., Hai, F. I., & Pramanik, B. K. (2021). Understanding the fate and control of road dust-associated microplastics in stormwater. Process Safety and Environmental Protection, 152, 47–57. https://doi.org/10.1016/j.psep.2021.05.033

Nair, H. T., & Perumal, S. (2022). Trophic transfer and accumulation of microplastics in freshwater ecosystem : Risk to food security and human health. International Journal of Ecology, Volume 2022. https://doi.org/10.1155/2022/1234078

OECD. (2022). Global plastics outlook: economic drivers, environmental impacts and policy options. OECD Publishing, Paris. https://doi.org/10.1787/de747aef-en.

Pazos, R. S., Maiztegui, T., Colautti, D. C., Paracampo, A. H., & Gómez, N. (2017). Microplastics in gut contents of coastal freshwater fish from Río de la Plata estuary. Marine Pollution Bulletin, 122(1–2), 85–90. https://doi.org/10.1016/j.marpolbul.2017.06.007

Ross, M. S., Loutan, A., Groeneveld, T., Molenaar, D., Kroetch, K., Bujaczek, T., Kolter, S., Moon, S., Huynh, A., Khayam, R., Franczak, B. C., Camm, E., Arnold, V. I., & Ruecker, N. J. (2023). *Estimated discharge of microplastics via urban stormwater during individual rain events*. *January*, 1–12. https://doi.org/10.3389/fenvs.2023.1090267

Sang, W., Chen, Z., Mei, L., Hao, S., Zhan, C., Zhang, W. bin, Li, M., & Liu, J. (2021). The

abundance and characteristics of microplastics in rainwater pipelines in Wuhan, China. Science of the Total Environment, 755, 142606. https://doi.org/10.1016/j.scitotenv.2020.142606

Scott, W.J., Green, L. Development and demonstration of a superior method for microplastic analysis: improved size detection limits, greater density limits, and more informative reporting. Illinois Sustainable Technology Center (2020). Report No: TR-078

Semcesen, P. O., & Wells, M. G. (2021). Biofilm growth on buoyant microplastics leads to changes in settling rates: Implications for microplastic retention in the Great Lakes. Marine Pollution Bulletin, 170(April), 112573. https://doi.org/10.1016/j.marpolbul.2021.112573

Setälä, O., Fleming-lehtinen, V., & Lehtiniemi, M. (2014). Ingestion and transfer of microplastics in the planktonic food web. Environmental Pollution, 185, 77–83. https://doi.org/10.1016/j.envpol.2013.10.013

Shruti, V. C., Pérez-Guevara, F., Elizalde-Martínez, I., & Kutralam-Muniasamy, G. (2021). Current trends and analytical methods for evaluation of microplastics in stormwater. Trends in Environmental Analytical Chemistry, 30. https://doi.org/10.1016/j.teac.2021.e00123

Steinman, A. D., Scott, W.J., Green, L., Partridge, C., Oudsema, M., Hassett, M., Kindervater, E., & Rediske, R. R. (2020). Persistent organic pollutants, metals, and the bacterial community composition associated with microplastics in Muskegon Lake (MI). Journal of Great Lakes Research, 46(5), 1444–1458. https://doi.org/10.1016/j.jglr.2020.07.012

Tian, Z., Gonzalez, M., Rideout, C. A., Zhao, H. N., Hu, X., Wetzel, J., Mudrock, E., James, C. A., McIntyre, J. K., & Kolodziej, E. P. (2022). 6PPD-Quinone: Revised Toxicity Assessment and Quantification with a Commercial Standard. Environmental Science and Technology Letters, 9(2), 140–146. https://doi.org/10.1021/acs.estlett.1c00910

Uzun, P., Farazande, S., & Guven, B. (2021). Mathematical modeling of microplastic abundance, distribution, and transport in water environments: A review. Chemosphere, 132517. https://doi.org/10.1016/j.chemosphere.2021.132517

Vincent, A. E., & Hoellein, T.J. (2021). Distribution and transport of microplastic and fine particulate organic matter in urban streams. Ecological Applications, 31(8), p.e 02429. https://doi.org/10.1002/eap.2429.

Werbowski, L. M., Gilbreath, A. N., Munno, K., Zhu, X., Grbic, J., Wu, T., Sutton, R., Sedlak, M. D., Deshpande, A. D., & Rochman, C. M. (2021). Urban stormwater runoff: a major pathway for anthropogenic particles, black rubbery fragments, and other types of microplastics to urban receiving waters. ACS ES and T Water, 1(6), 1420–1428. https://doi.org/10.1021/acsestwater.1c00017

Wright, S. L., Thompson, R. C., & Galloway, T. S. (2013). The physical impacts of microplastics on marine organisms: a review. Environmental Pollution (Barking, Essex : 1987), 178, 483–492. https://doi.org/10.1016/j.envpol.2013.02.031

Wu, Y., Guo, P., Zhang, X., Zhang, Y., Xie, S., & Deng, J. (2019). Effect of microplastics exposure on the photosynthesis system of freshwater algae. Journal of Hazardous Materials, 374(December 2018), 219–227. https://doi.org/10.1016/j.jhazmat.2019.04.039

Yano, K. A., Geronimo, F. K., Reyes, N. J., & Kim, L. H. (2021). Characterization and comparison of microplastic occurrence in point and non-point pollution sources. Science of the Total Environment, 797, 148939. https://doi.org/10.1016/j.scitotenv.2021.148939

Yu, H., Liu, M., Gang, D., Peng, J., Hu, C., & Qu, J. (2022). Polyethylene microplastics interfere with the nutrient cycle in water-plant-sediment systems. Water Research, 214(September 2021), 118191. https://doi.org/10.1016/j.watres.2022.118191

Zafar, R., Arshad, Z., Eun Choi, N., Li, X., & Hur, J. (2023). Unravelling the complex adsorption behavior of extracellular polymeric substances onto pristine and UV-aged microplastics using two-dimensional correlation spectroscopy. Chemical Engineering Journal, 470(June), 144031. https://doi.org/10.1016/j.cej.2023.144031

Zettler, E. R., Mincer, T. J., & Amaral-zettler, L. A. (2013). Life in the “ Plastisphere ” : Microbial Communities on Plastic Marine Debris. Environmental Science & Technology, 47(13), 7137–7146. https://doi.org/DOI: 10.1021/es401288x

Tables

Table 2.1. Water quality data taken before retrieving water/sediment samples for MP analysis. Habitat indicates the location where water/sediment samples were retrieved. Some lake samples have multiple rows in a single day because water was taken from multiple depths and then combined into a single sample. Date: MM/DD/YY; DEP: Depth in meters; °C: temperature is in Celsius; DO: dissolved oxygen, SPC: specific conductivity, NTU: turbidity.

Summer								
Habitat	Date	DEP m	°C	DO %	DO mg/L	SPC µS/cm	pH	NTU
Lake	6/17/2022	2	23.4	122.9	10.4	864.1	8.7	1
Lake	6/17/2022	10	8.9	9.9	1.1	1311.6	7	5.4
Lake	7/12/2022	2	24.7	105.4	8.8	840.8	8.6	1.6
Lake	7/12/2022	4	13.1	42.8	4.5	895.2	7.9	1.9
Lake	7/12/2022	10	5.1	4.2	0.5	1230	7.1	33
Trib (baseflow)	6/16/2022	-	18.9	77.7	7.2	906.7	7.9	5
Trib (baseflow)	8/17/2022	-	18.7	90.6	8.4	1424	8.2	2
Trib (storm)	8/3/2022	-	21.4	83.4	7.4	1225	8.2	15.7

Fall								
Habitat	Date	DEP m	°C	DO %	DO mg/L	SPC µS/cm	pH	NTU
Lake	9/23/2022	1	21.3	86.9	7.7	847	8.4	0.6
Lake	9/23/2022	2	21.3	85.8	7.6	849	8.4	0.6
Lake	9/23/2022	3	21.3	86.2	7.6	849	8.4	0.6
Lake	11/11/2022	1	11.6	92.3	10	862	8.4	1.1
Lake	11/11/2022	3	11	80.3	8.8	863	8.2	1.4
Lake	11/11/2022	6	10.8	57.6	6.4	867	7.9	2
Trib (baseflow)	9/23/2022	-	16.1	82.8	8.1	848	8.3	1.6
Trib (baseflow)	10/14/2022	-	16.2	93.7	9.2	240.7	8.2	15.3
Trib (baseflow)	11/11/2022	-	13.4	77.1	8	1682	7.8	5.1
Trib (storm)	10/11/2022	-	10.9	87.1	9.6	440.7	8.1	6

Winter								
Habitat	Date	DEP m	°C	DO %	DO mg/L	SPC µS/cm	pH	NTU
Lake	1/23/2023	1	2	92.7	12.8	941	8.3	2.5
Trib (baseflow)	12/9/2022	-	8.2	93.7	11	1586	8.1	4.2

Trib (baseflow)	1/9/2023	-	4	98.9	12.8	1423	8.3	1.2
Trib (baseflow)	2/13/2023	-	3.9	90.8	11.9	1586	8.1	3.7
Trib (storm)	1/16/2023	-	7	91.2	11.1	880	8.2	55.9
Trib (storm)	2/9/2023	-	3.8	93.1	12.2	932	7.9	52.4

Spring

Habitat	Date	DEP m	°C	DO %	DO mg/L	SPC µS/cm	pH	NTU
Lake	3/27/2023	1	5.8	119.6	14.9	940.6	8.7	3.4
Lake	3/27/2023	5	4.5	96.1	12.4	957.1	8.4	2.7
Lake	3/27/2023	9	4.3	58.9	7.6	1017.1	7.9	9.9
Lake	4/10/2023	1	11.8	145.1	15.7	866	9	3
Lake	4/10/2023	5	6.5	82.5	10.1	900.9	8.1	3
Lake	4/10/2023	8	4.5	23.4	3	979.3	7.5	3.1
Trib (baseflow)	5/31/2022	-	19.3	98.2	9	1504	8	7
Trib (baseflow)	3/27/2023	-	5.2	97.4	12.3	1178.5	8.1	10.2
Trib (baseflow)	4/10/2023	-	7.8	99.5	11.8	1799.2	8	4.3
Trib (storm)	3/25/2023	-	1.7	95.4	13.3	261.3	8.2	85.9
Trib Sediment	3/27/2023	-	5.8	119.6	14.9	940.6	8.7	3.4
Lake Sediment	3/27/2023	9	5.9	58.9	7.64	1017.1	7.89	9.88

Table 2.2. A summary of MP and 6-PPD-Q concentrations in Church Lake, the Trib (baseflow), during Trib (storm) events, and sediment. Habitat indicates the location of where the sample is taken. Date: MM/DD/YY, MP/L: MP Counts per Liter, MP mm^2/L: MP Surface Area mm^2/L, MP mg/L**:** MP Mass Estimate mg per liter, 6-PPD-Q ng/L**:** 6-PPD-QConcentration ng per L**,** 6-PPD-Q **%:** 6-PPD-Q Surrogate Recovery in %.

Summer						
Habitat	Date	Counts (MP/L)	Surface Area (mm^2/L)	Mass (mg/L)	6-PPD-Q (ng/L)	6-PPD-Q (%)
Lake	6/17/22	456	0.7	0.66	< 1	0.88
Lake	7/12/22	651	2	1.88	< 1	1.05
Trib (baseflow)	6/16/22	405	0.8	0.75	9.6	0.74
Trib (baseflow)	8/17/22	188	1.99	1.87	7.8	0.87
Trib (storm)	8/3/22	482	0.64	0.6	73	0.52

Fall						
Habitat	Date	Counts (MP/L)	Surface Area (mm^2/L)	Mass (mg/L)	6-PPD-Q (ng/L)	6-PPD-Q (%)
Lake	9/23/22	61	0.51	0.48	< 1	1.3
Lake	11/11/22	305.5	10.65	10.01	< 1	0.6
Trib (baseflow)	9/23/22	208	3.2	3.01	1.06	1.28
Trib (baseflow)	10/14/22	1293	2.03	1.91	24	1.18
Trib (baseflow)	11/11/22	266.5	2.37	2.23	< 1	0.94
Trib (storm)	10/11/22	16390	7	6.58	201	0.75

Winter						
Habitat	Date	Counts (MP/L)	Surface Area (mm^2/L)	Mass (mg/L)	6-PPD-Q (ng/L)	6-PPD-Q (%)
Lake	1/23/23	879.5	18.78	17.66	< 1	1.21
Trib (baseflow)	12/9/22	126.5	1.2	1.12	< 1	0.9
Trib (baseflow)	1/16/23	550.5	1.76	1.66	< 1	0.86
Trib (baseflow)	2/13/23	698.5	5.48	5.15	< 1	0.85
Trib (storm)	1/16/23	8208.5	12.06	11.34	28	0.23

Trib (storm)	2/9/23	9780.5	13.51	12.7	14	0.71

Spring Habitat	Date	Counts (MP/L)	Surface Area (mm^2/L)	Mass (mg/L)	6-PPD-Q (ng/L)	6-PPD-Q (%)
Lake	3/27/23	221.5	1.09	1.03	< 1	0.58
Lake	4/10/23	338.5	4.92	4.62	< 1	1.11
Trib (baseflow)	5/31/22	390	0.6	0.56	2.4	1.03
Trib (baseflow)	3/27/23	174.5	8.55	8.04	< 1	1.31
Trib (baseflow)	4/10/23	246.5	0.98	0.92	< 1	0.56
Trib (storm)	3/25/23	5321.5	8.37	7.87	< 1	0.04
Trib Sediment	3/27/23	8735.5	49.87	45.27	NA	NA
Lake Sediment	3/27/23	3015.5	22.93	21.55	NA	NA

Table 2.3. A summary of MP shape in the Trib (baseflow), during Trib (storm) events, sediment, and in Church Lake. Habitat indicates the location of where the sample is taken. Fragment and fiber are in terms of MP counts/ L (Table 2.2). MP ~ 50 µm x 50 µm or greater were considered fragments and MPs were considered fiber if they were ~ 50 µm x 50 µm < 20 µm. Date: MM/DD/YY.

Summer			
Habitat	Date	Fragment #/L	Fiber #/L
Lake	6/17/2022	447	9
Lake	7/12/2022	631	20
Trib (baseflow)	6/16/2022	393	12
Trib (baseflow)	8/17/2022	171	17
Trib (storm)	8/3/2022	472	10

Fall			
Habitat	Date	Fragment #/L	Fiber #/L
Lake	9/23/2022	59	2
Lake	11/11/2022	238	67
Trib (baseflow)	9/23/2022	168	40
Trib (baseflow)	10/14/2022	1228	65
Trib (baseflow)	11/11/2022	211	56
Trib (storm)	10/11/2022	15734	656

Winter			
Habitat	Date	Fragment #/L	Fiber #/L
Lake	1/23/2023	783	97
Trib (baseflow)	12/9/2022	105	22
Trib (baseflow)	1/16/2023	523	28
Trib (baseflow)	2/13/2023	405	293
Trib (storm)	1/16/2023	8209	0
Trib (storm)	2/9/2023	9781	0

Spring			
Habitat	Date	Fragment #/L	Fiber #/L
Lake	3/27/2023	215	7
Lake	4/10/2023	301	37
Trib (baseflow)	5/31/2022	382	8
Trib (baseflow)	3/27/2023	120	54
Trib (baseflow)	4/10/2023	212	35
Trib (storm)	3/25/2023	5322	0
Trib Sediment	3/27/2023	8736	0
Lake Sediment	3/27/2023	2955	60

Table 2.4. A summary of MP color in the Trib (baseflow), during Trib (storm) events, sediment, and in Church Lake. Habitat indicates the location of where the sample is taken. MP color type is in terms of MP counts/ L (Table 2.2). Date: MM/DD/YY.

Summer									
Habitat	Date	Red	Yellow	Brown	Clear	Orange	Green	Grey	Black
Lake	6/17/2022	3	14	12	19	1	0	18	389
Lake	7/12/2022	0	0	0	53	0	0	0	598
Trib (baseflow)	6/16/2022	1	49	13	64	0	0	0	271
Trib (baseflow)	8/17/2022	2	9	17	29	0	0	0	131
Trib (storm)	8/3/2022	0	145	0	0	0	0	308	28

Fall									
Habitat	Date	Red	Yellow	Brown	Clear	Orange	Green	Grey	Black
Lake	9/23/2022	6	22	0	11	1	0	0	21
Lake	11/11/2022	2	24	53	0	8	0	157	60
Trib (baseflow)	9/23/2022	1	72	13	49	0	0	1	72
Trib (baseflow)	10/14/2022	5	58	40	87	28	312	0	762
Trib (baseflow)	11/11/2022	1	82	36	24	0	0	77	46
Trib (storm)	10/11/2022	0	16	820	33	0	0	0	15472

Winter									
Habitat	Date	Red	Yellow	Brown	Clear	Orange	Green	Grey	Black
Lake	1/23/2023	7	11	172	3	22	0	407	258
Trib (baseflow)	12/9/2022	3	4	9	15	1	0	47	47
Trib (baseflow)	1/16/2023	21	0	0	28	0	0	433	68
Trib (baseflow)	2/13/2023	4	53	33	1	43	0	386	177
Trib (storm)	1/16/2023	8	25	90	16	0	0	337	7732
Trib (storm)	2/9/2023	0	20	59	0	0	0	49	9653

Spring									
Habitat	Date	Red	Yellow	Brown	Clear	Orange	Green	Grey	Black

Lake	3/27/2023	3	3	23	0	3	0	66	124
Lake	4/10/2023	2	72	23	0	4	0	180	57
Trib (baseflow)	5/31/2022	5	4	187	0	5	0	1	187
Trib (baseflow)	3/27/2023	0	2	20	0	2	0	80	70
Trib (baseflow)	4/10/2023	3	3	26	0	3	0	73	138
Trib (storm)	3/25/2023	0	21	11	0	5	0	101	5183
Trib Sediment	3/27/2023	9	61	472	9	0	9	5730	2437
Lake Sediment	3/27/2023	3	389	271	36	21	0	446	1852

Table 2.5. A summary of MP polymer ID (based on surface area: mm2/L/L) in Church Lake, the Trib (baseflow), during Trib (storm) events, and sediment. Habitat indicates the location of where the sample is taken. Date: MM/YY.

Summer											
Habitat	Date	Unknown	Polyamide	Cellulosic	Siloxane	Ethylene vinyl alcohol	Polyvinylidene chloride	Polyethylene	Acrylic	Polyester	Silicon
Lake	6/22	0.71	1.09	0.2	0.06	0	0	0	0	0	0
Lake	7/22	7.79	0	2.13	1.65	0.17	3.19	0.32	0	0	0
Trib (baseflow)	5/22	0.23	0.14	0.23	0	0	0	0	0	0	0
Trib (baseflow)	6/22	0.5	0	0.16	0.09	0.06	0	0	0.15	0	0
Trib (storm)	8/22	0.63	0	0	0.01	0	0	0	0	0	0

Fall											
Habitat	Date	Unknown	Polyamide	Cellulosic	Siloxane	Ethylene vinyl alcohol	Polyvinylidene chloride	Polyethylene	Acrylic	Polyester	Silicon
Lake	9/22	0.58	0.08	0.04	0	0	0	0	0	0	0
Lake	11/22	1.09	0	0	0	0	0	0	0	0	0
Trib (baseflow)	9/22	4.49	0.66	0.27	0	0	0	0	0	0	0
Trib (baseflow)	10/22	1.18	0	0.3	0	0	0	0	0.86	0	0
Trib (baseflow)	11/22	1.76	0	0	0	0	0	0	0	0	0
Trib (storm)	10/22	6.93	0.07	0	0	0	0	0	0	0	0

Winter											
Habitat	Date	Unknown	Polyamide	Cellulosic	Siloxane	Ethylene vinyl alcohol	Polyvinylidene chloride	Polyethylene	Acrylic	Polyester	Silicon
Lake	1/23	4.92	0	0	0	0	0	0	0	0	0
Trib (baseflow)	12/22	3.2	0	0	0	0	0	0	0	0	0
Trib (baseflow)	1/23	2.03	0	0.37	0	0	0	0	0	0	0
Trib (baseflow)	2/23	5.73	0	0.26	0	2.57	0	0	0	0	0
Trib (storm)	1/23	12.02	0	0	0	0	0.06	0	0	0	0
Trib (storm)	2/23	13.11	0.14	0.27	0	0	0	0	0	0	0

Spring

Habitat	Date	Unknown	Polyamide	Cellulosic	Siloxane	Ethylene vinyl alcohol	Polyvinylidene chloride	Polyethylene	Acrylic	Polyester	Silicon
Lake	3/27/2023	0.43	0	0.01	0	0	0	0	0	0	0.08
Lake	4/10/2023	18.78	0	0	0	0	0	0	0	0	0
Trib (baseflow)	5/31/2022	0.23	0.14	0.23	0	0	0	0	0	0	0
Trib (baseflow)	3/27/2023	0.75	0	0.01	0	0	0	0	0	0	0.21
Trib (baseflow)	4/10/2023	1.99	0	0	0	0	0	0	0	0	0
Trib (storm)	3/23	8.37	0	0	0	0	0	0	0	0	0

Figure Captions

Figure 2.1. Map of Church Lake. (a) Location of lake in lower peninsula of Michigan. (b.) Aerial view of Church Lake and the two other connecting lakes (Middleboro, Westboro). (c.) Close-up of Church Lake and the unnamed tributary that flows from the East Beltline to the urban Lake. The dots indicate the sampling locations; lake sampling points are labeled 1-7 and correspond to a specific date: 6/22 (1), 7/22(2), 9/22 (3), 11/22 (4), 1/23 (5), 3/23 (6), 4/23 (7). (d.) Bathymetry of Church Lake retrieved from Progressive AE (2010); the Lake has residential housing on its south and west shorelines and is adjacent to the East Beltline state highway on its east side. Depth contours are in ft.

Figure 2.2. The average concentration of the fragments and fibers found from Church Lake and tributary samples in both the water column and sediment. Tributary sediment was sampled under baseflow and storm flow. Site locations identified in Figure. 2.2 caption. Error bars indicate standard variation.

Figure 2.3. Average counts of MP/L per across different habitats. The bar plot shows the average MP counts for the top 4 colors in each habitat, with error bars indicating standard deviation. Site locations identified in Figure. 2.2 caption.

Figure 2.4. Relative abundance of the polymers sampled from sites identified in Figure. 2.2 caption. If polymer IDs could not be determined with greater than 80 % accuracy, the ID of the polymer is classified as unknown.

Figure 2.5. The upper panel plots MP counts (#/L)(left y axis) from water samples taken at the Trib (baseflow) each month (n=11) by discharge m^3/s (n=11) taken after each Trib (baseflow) sample was collected from May 2022- April 2023.The middle panel plot conveys MP mass (mg/L) (left y axis) from water samples taken at the Trib (baseflow) each month (n=11) by discharge m^3/s (n=11) taken after each Trib (baseflow) sample was collected from May 2022-April 2023.

Figure 2.6. Scatter plot displaying the lack of a relationship between discharge (m^3/s) and MP Mass from samples taken from the tributary (baseflow).

Figure 2.7. Scatter plot displaying the lack of a relationship between discharge (m^3/s) and MP counts #/L from samples taken from the tributary (baseflow).

Figures

Figure 2.1.

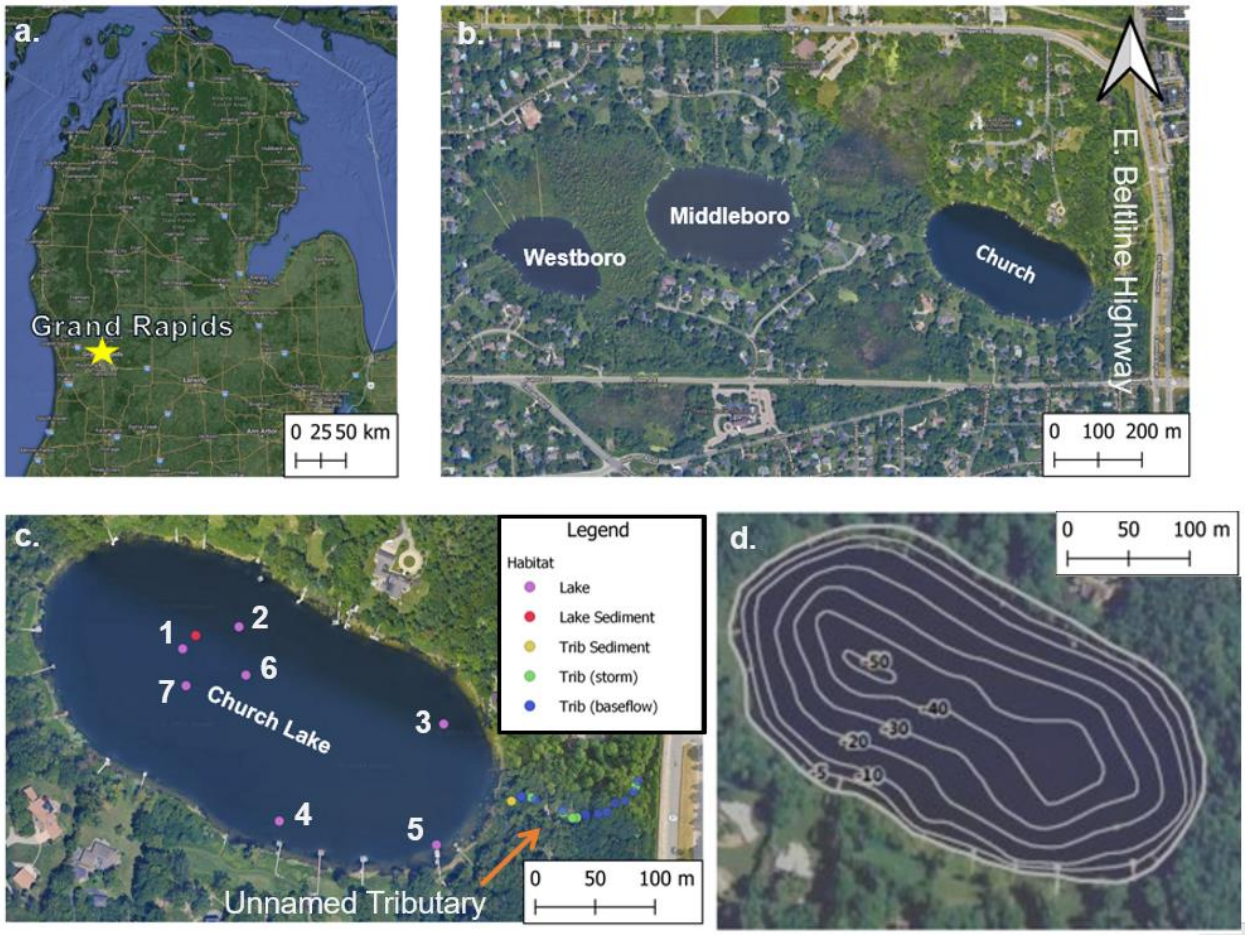

Figure 2.2.

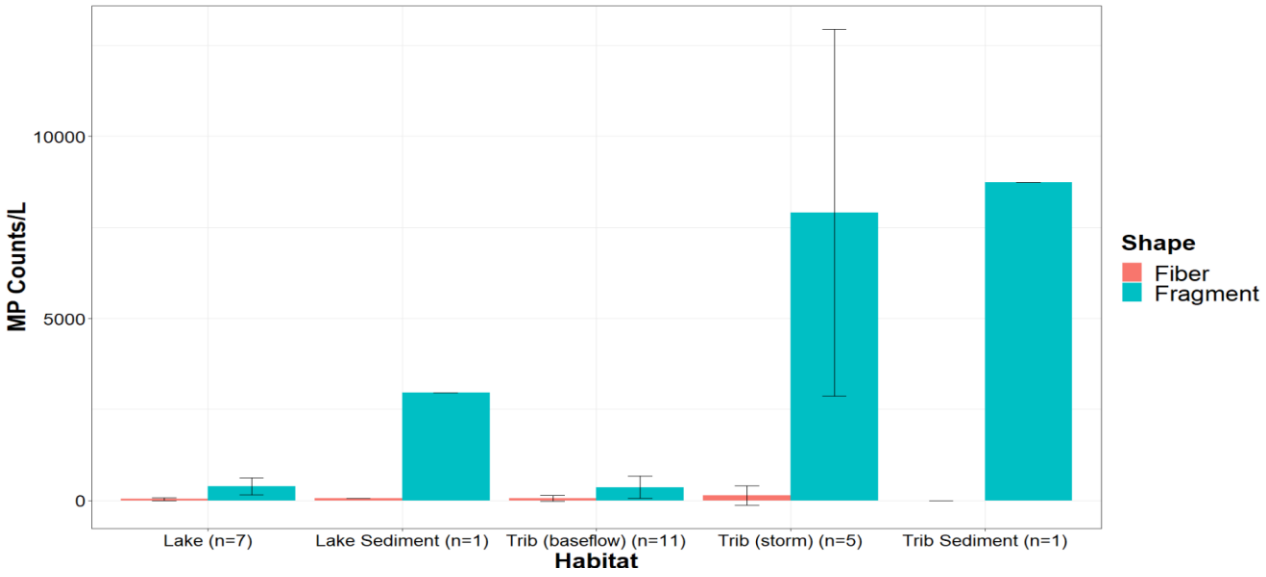
MP Counts/L
10000
5000
0
Lake (n=7)
Lake Sediment (n=1)
Trib (baseflow) (n=11)
Trib (storm) (n=5)
Trib Sediment (n=1)
Habitat
Shape
Fiber
Fragment

Figure 2.3.

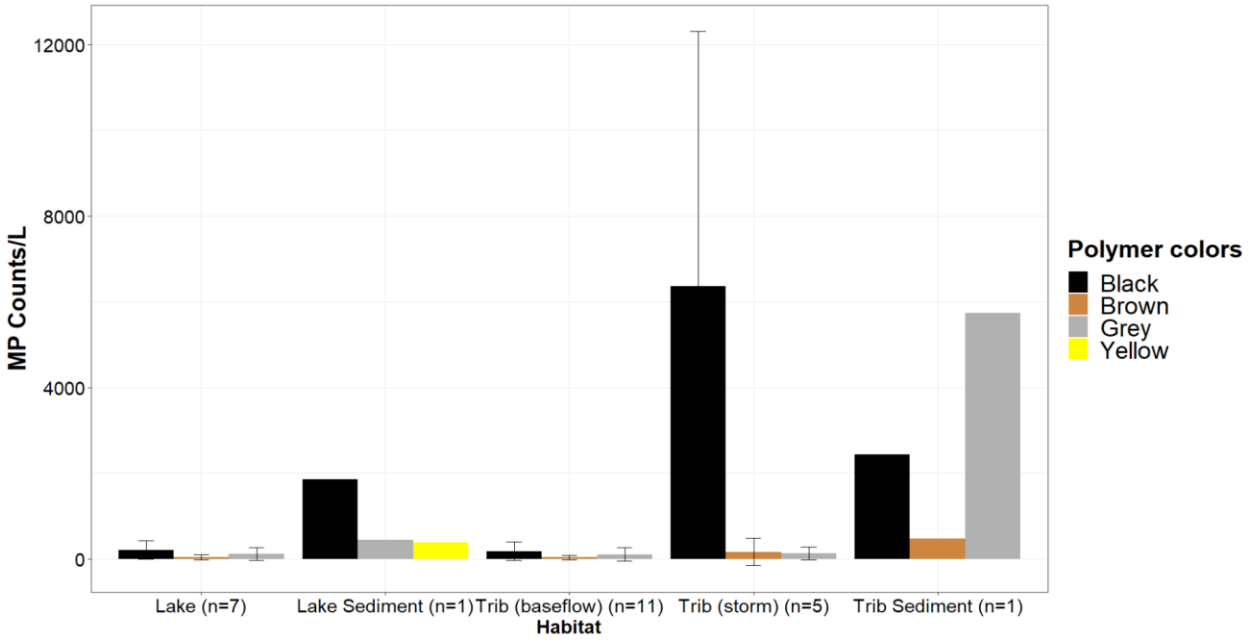
12000
8000
4000
0
MP Counts/L
Lake (n=7)
Lake Sediment (n=1)
Trib (baseflow) (n=11)
Trib (storm) (n=5)
Trib Sediment (n=1)
Habitat
Polymer colors
Black
Brown
Grey
Yellow

Figure 2.4.

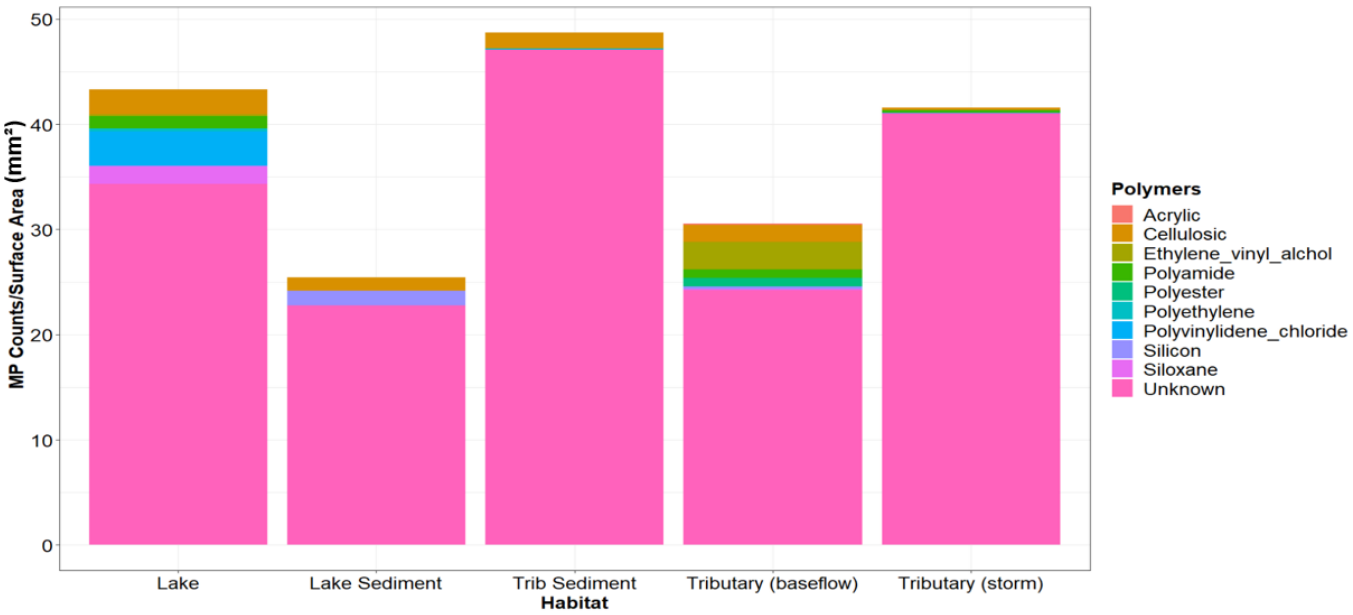
MP Counts/Surface Area (mm²)
50
40
30
20
10
0
Lake
Lake Sediment
Trib Sediment
Tributary (baseflow)
Tributary (storm)
Habitat
Polymers
Acrylic
Cellulosic
Ethylene_vinyl_alchol
Polyamide
Polyester
Polyethylene
Polyvinylidene_chloride
Silicon
Siloxane
Unknown

Figure 2.5.

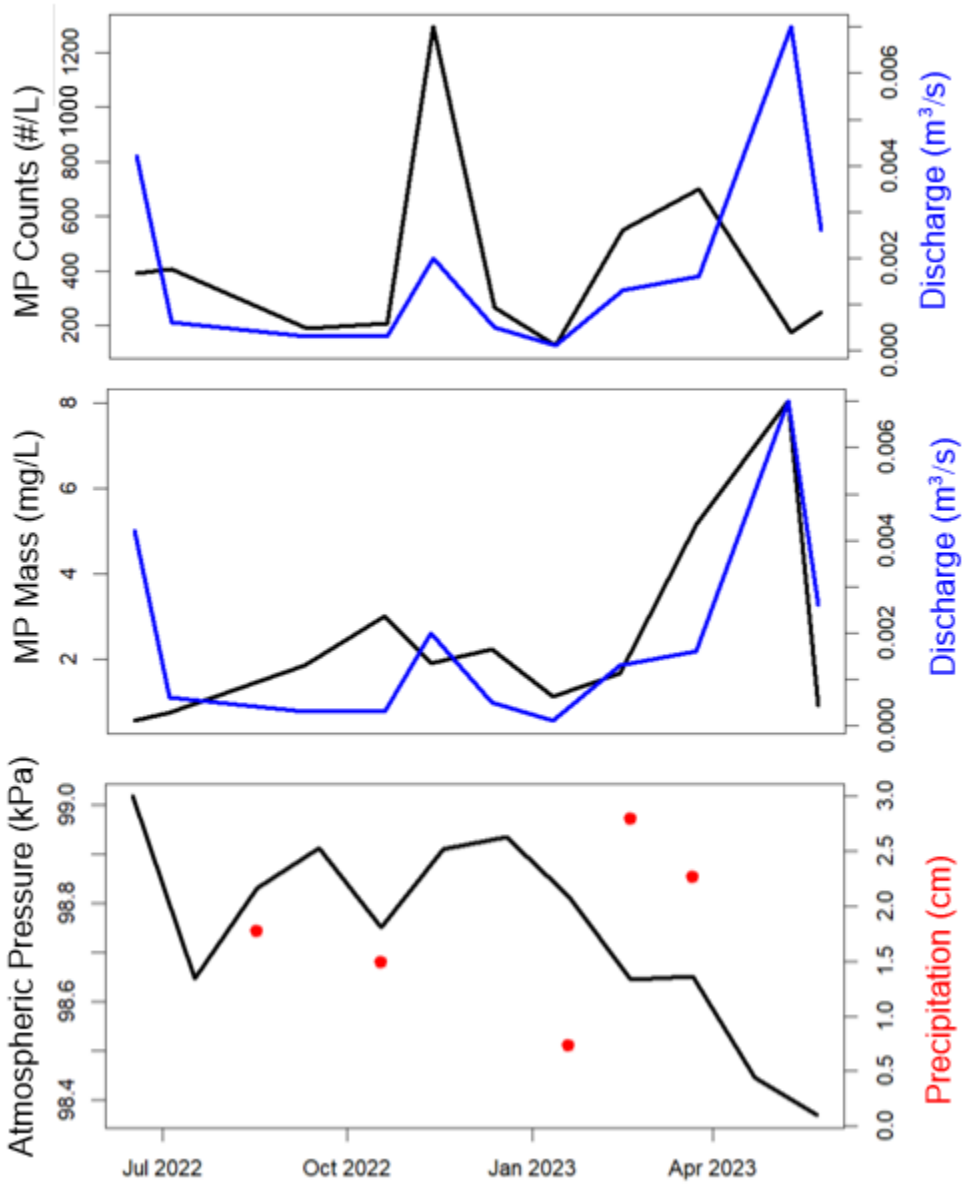
MP Counts (#/L)
200 400 600 800 1000 1200
0.000 0.002 0.004 0.006
Discharge (m³/s)
MP Mass (mg/L)
2 4 6 8
0.000 0.002 0.004 0.006
Discharge (m³/s)
Atmospheric Pressure (kPa)
98.4 98.6 98.8 99.0
0.0 0.5 1.0 1.5 2.0 2.5 3.0
Precipitation (cm)
Jul 2022
Oct 2022
Jan 2023
Apr 2023

Figure 2.6.

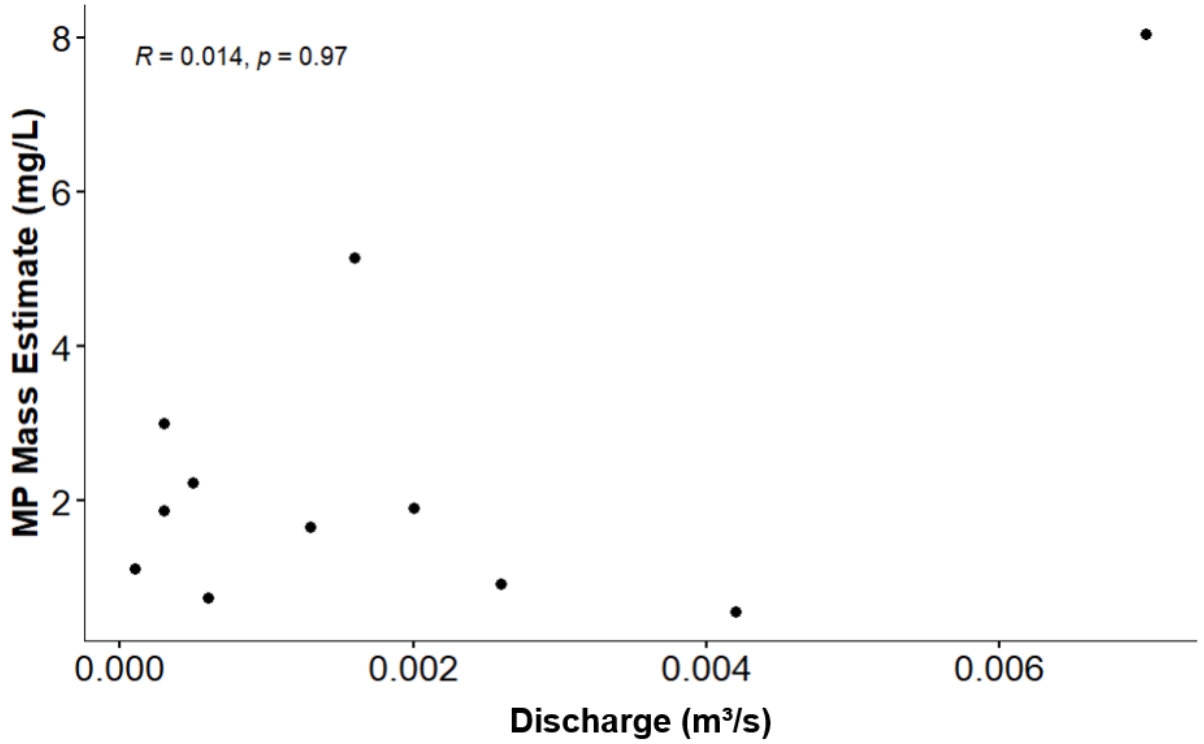
R = 0.014, p = 0.97
MP Mass Estimate (mg/L)
8
6
4
2
0.000
0.002
0.004
0.006
Discharge (m³/s)

Figure 2.7.

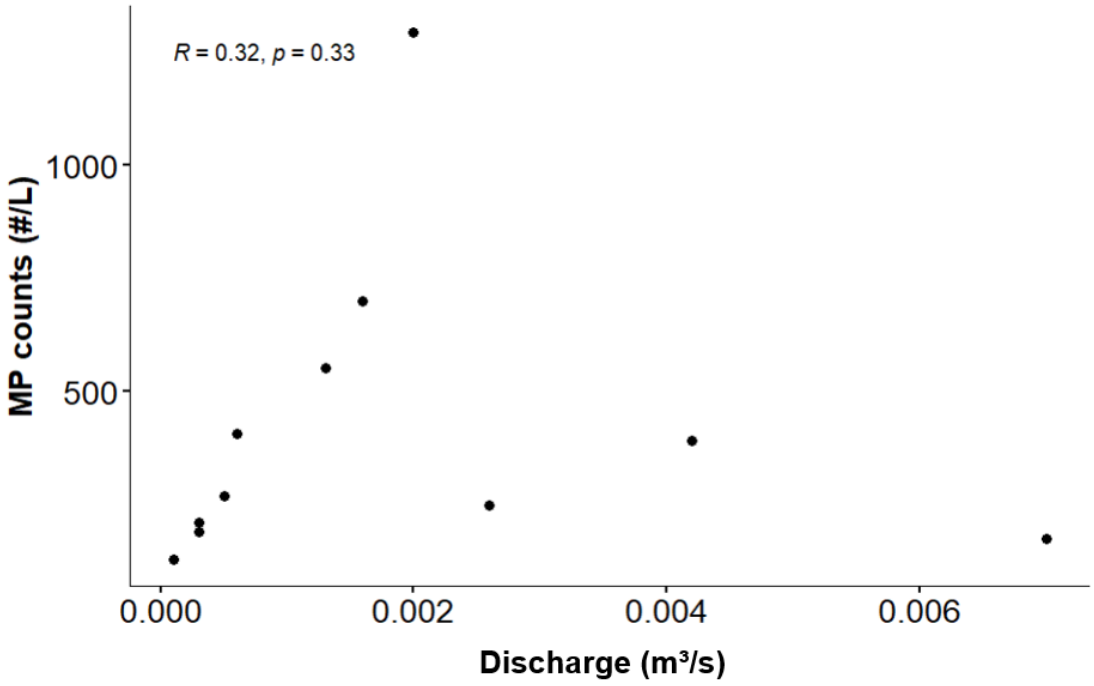
R = 0.32, p = 0.33
MP counts (#/L)
1000
500
0.000
0.002
0.004
0.006
Discharge (m³/s)

Chapter 3: The Biodiversity of Biofilm Found on Microplastics in a Meromictic Lake

Abstract

Since the introduction of plastics, an ecological niche called the plastisphere has garnered interest due to its relatively new presence in the environment and unknown long-term effects on the aquatic ecosystem. My research is interested in examining the biodiversity of algae and bacteria between two microplastic (MP) polymers in a eutrophic, salinized, partially meromictic lake. To achieve this, unweathered MPs were incubated in Church Lake in retrievable flow-through containers to promote biofilm formation on polypropylene (PP) and polyethylene terephthalate (PET). After incubation, MPs were brought back to the lab and were exposed to a set of controlled environmental conditions. The experimental design consisted of two treatments: 1) MPs initially incubated in the low P, low salinity, high light epilimnion of Church Lake, then retrieved and in the lab placed in either its ambient water or placed in the water from the hypolimnion, which is high P, high salinity, and low light; and 2) the reverse treatment using MPs initially incubated in the hypolimnion of Church Lake, and placed in either ambient conditions or epilimnetic water. This design allowed us to examine the responsiveness of the biofilm to new environmental conditions should the lake fully turn over in the future. Amplicon sequencing targeting the 16S rRNA regions was performed on biofilm growing on MPs, while algal identification was conducted separately through light microscopy. The findings indicate that environmental factors, as opposed to the kind of polymer utilized, significantly influence the composition of microbial communities. Bacterial communities in the epilimnion exhibited higher diversity and a more varied taxonomic composition compared to the hypolimnion. Algal communities showed a similar trend, with greater diversity in the epilimnion. Overall, depth-

specific conditions significantly influenced both bacterial and algal community structures. Hence, the impact of turnover on the plastisphere in Church Lake, should it occur, will strongly be influenced by the initial community composition. For those plastisphere communities capable of responding to species specific desirable environmental conditions, the increase in phosphorus and salinity from hypolimnetic water will increase the abundance of algae on MPs in the photic zone, possibly causing increased settling rates.

Introduction

The breakdown of plastic materials by manufacturers or through gradual degradation processes from the environment form microplastics (MPs), defined as plastics ranging from 1 µm to 5 mm in length (Hitchcock, 2020). Poor waste management efforts since the introduction of plastics, combined with their mobility in water and air, have resulted in MPs being found in every biome on Earth (Blettler et al., 2018). The necessity of plastics in our everyday lives has led to MPs becoming a chronic contaminant in the environment. The most common sources of MPs are urban runoff, wastewater treatment plant inputs, sewage system overflows, and industrial inputs (Hitchcock, 2020). From manufacture to disposal, MPs travel a great distance from atmosphere to land, and from land to rivers and estuaries into lakes and marine ecosystems. Rain and storm events transport a range of non-point source pollutants such as sediment, road salt, nutrients, pathogens, and MPs (Eadie et al., 2002; Hitchcock, 2020; Johnson et al., 2011; Kaushal et al., 2022). Following MPs entry into the water column, MPs become a carrier for colonizing microbial communities.

Once MPs enter aquatic ecosystems, their density determines whether they will float or sink, with denser MPs settling into sediments. In these environments, MPs act as carriers for microbial communities, providing synthetic substrates for colonization. This biofilm, termed the "plastisphere," comprises a diverse array of microorganisms including bacteria, algae, fungi, and protozoa (He et al., 2021; Zettler et al., 2013). Biofilm development on MPs is influenced by various environmental factors such as pH, salinity, nutrients, flow, temperature, and light (Chen et al., 2020). MPs are unique in that their buoyancy and surface characteristics facilitate the adsorption of both organic and inorganic pollutants, forming a conditioning membrane that supports microbial colonization (Holmes et al., 2014; Verla et al., 2019).

Microbial colonization on MPs can lead to the formation of biofilms that secrete extracellular polymeric substances (EPS), which provide protection and facilitate the adhesion of particles from the surrounding environment (He et al., 2021; Zafar et al., 2023). The presence of such biofilms not only protects MPs from degradation but also increases the longevity of MPs. Considering MPs can act as carriers for bacterial colonization and the propagation of potentially harmful microorganisms (Wang et al., 2020), the increased longevity of these MP can lead to heightened exposure to harmful microorganisms and contribute to bioaccumulation in aquatic biota.

MPs differ from naturally occurring substrates in several ways, including their chemical composition, surface characteristics, and the potential to serve as vectors for pollutants. These differences influence the microbial community structure, often leading to distinct microbial assemblages on plastics compared to other surfaces (He et al., 2021; Oberbeckmann et al.,

2014; Okeke et al., 2022). Studies have also shown that bacterial richness on MPs can be higher than on natural substrates, with Proteobacteria and Cyanobacteria being the most commonly observed phyla in freshwater environments (Miao et al., 2019; Okeke et al., 2022; Zettler et al., 2013). This underscores the need to identify microbes that preferentially colonize plastic surfaces to better understand their role in aquatic ecosystems and their potential impact on water quality, including nutrient cycling and pollutant degradation.

Microorganisms benefit from living in biofilms in several ways, including nutrient accumulation, stable matrix connection, protection from hazardous substances, and horizontal gene transfer (Okeke et al., 2022). Within the biofilm exists a potentially symbiotic relationship between algae and bacteria. Algal photosynthesis provides oxygen and carbon substrates for bacteria to utilize while algae in return assimilate the carbon dioxide respired by bacteria. The ecological functions that algae and bacteria provide in biofilm aid in biogeochemical cycling. Algae and bacteria are structural pillars in ecosystems, and it is unknown how these two microbial groups adapt to living on MPs in impacted urban lakes.

My study aims to investigate the species richness and composition of microbial communities on MPs (specifically polypropylene (PP) and polyethylene terephthalate (PET)) in Church Lake, a salinized, eutrophic, and partially meromictic lake affected by highway deicing salts and fertilizers (Foley and Steinman, 2023). The research focuses on comparing the microbial communities on MPs in the hypolimnion (characterized by high salinity and low light) versus the epilimnion (characterized by low salinity and higher light). This study addresses key

questions about how these environmental conditions influence microbial colonization on MPs and the potential implications for ecosystem health and water quality.

I hypothesize that *algal* communities growing on MPs in the hypolimnion will exhibit lower species richness and abundance compared to those in the epilimnion due to the stressful conditions of high salinity and low light observed in the hypolimnion of Church Lake. Conversely, I expect *bacterial* communities in the hypolimnion to demonstrate greater species richness and abundance, as they are better adapted to the low light and anoxic conditions found in this layer. To test these hypotheses, MPs were placed in flow-through containers in Church Lake to facilitate biofilm formation and then subjected to controlled environmental treatments in the laboratory. This design allowed us to examine the responsiveness of the biofilm to new environmental conditions should the lake fully turn over in the future. The results will provide insights into the adaptability and ecological roles of microorganisms in response to varying environmental conditions on MPs in salinity-impacted urban lakes.

Methods

Study Site

The sampling occurred in Church Lake, an urban lake located in Grand Rapids (Kent County), Michigan (Figure 3.1). The lake represents one of three lakes connected through marshy wetlands and groundwater in this area (Molloseau and Steinman, unpubl. data). Church Lake spans 7.7 hectares and has a maximum depth of ~ 16.5m. Runoff from a major highway (East Beltline) flows into an unnamed tributary that enters the east side of Church Lake. The deepest region of the lake, approximately 3-5% of total lake volume, does not seasonally mix

due to a chemocline (~9m) that has formed from deicing salt runoff from the East Beltline highway (Foley and Steinman, 2023).

Microplastic Type

I used two polymers in this experiment: PP and PET. PP and PET are the most common polymers found in urban areas (Driedger et al., 2015; Lutz et al., 2021). PP is found in auto parts and food containers while PET is found in textiles and water bottles. I sourced PP and PET pellets from Plastic Pellets 4 Fun (High Point, NC). The bulk material was sieved, resulting in a size range of 2– 4 mm.

Incubation: Frame Deployment and Retrieval

I placed unweathered MPs in flow-through tubes based on a design by Steinman et al. (2020), allowing biofilms to grow on the MPs (Figure. 3.2). I placed ~46 g of MP pellets in each incubation tube. The incubation tubes are made from Harvel Clear^{TM} Rigid PVC (outer diameter of 7.62 cm) cut into 15 cm-long sections. I drilled six evenly spaced holes (5 cm diameter) along the sides of the tubes to allow for the passage of lake water. The section holding the microplastics is made of a clear PVC pipe lined with stainless steel wire cloth (mesh size 1 mm) forming a sleeve. The wire cloth prevented microplastics from leaving incubation tubes. I placed clear PVC slip caps on the ends of each incubation tube and then inserted a 0.64 cm threaded rod in the center of each tube and through holes drilled in the center of each slip cap. Washers and metal locknuts secured both the slip cap and an automotive brake line tab to both sides of each tube. The assembled incubation tube was attached via the brake line tab to double loop chains along each attachment frame with a metal quick link. The chains allow the incubation

tubes to move with wave motion while still attached to the frame and for easy removal at the end of deployment (Steinman et al., 2020).

I deployed the frames in June of 2022 during the growing season and retrieved them two weeks after deployment. The deployment period was selected because microbial communities grow quickly (Wang et al., 2020), and two weeks should be sufficient to obtain biofilm growth. Frames were attached to a buoy and deployed at ~2-m (oxic) and 10-m (hypoxic) depths at a site used in a prior study (Foley and Steinman, 2023). I chose the deployment depths to examine the effects of salinity and phosphorus on microbial community structure and function; MPs in tubes near the lake surface (epilimnion) were exposed to lower salinity water, higher light, higher levels of dissolved oxygen, and lower mean conductivity and phosphorus concentrations (see below) compared to those deployed deeper (hypolimnion) (Table 3.1; see also Foley and Steinman, 2023).

I removed and filtered 72 L of lake water (36 L from each depth) after deploying the frames to use in the laboratory experiment. Zooplankton and other floating organisms were removed from the epilimnion and the hypolimnion by a two-step sequential filtration process first using 1 µm filters, followed by 0.2 µm filters (Watertec QMC1-10NPCS and 0.2-10NPCS, respectively). After the two-week incubation period, lake water was collected from the 2-m and 10-m depths via Van Dorn samplers to measure microbial community structure, conductivity, total phosphorus (TP), and soluble reactive phosphorus (SRP).

Water and Sediment Sample Collection

Before the microcosm experiment started, samples were taken from the water column and littoral zone and used to compare bacterial and algal communities found in the water column at Church Lake to what were attached to our MP pellets. To compare communities found in Church Lake to MP pellets, two integrated water samples were taken of ~ 500 ml at 2-m and 10-m depths using a vertical Van Dorn and poured into a 1 L brown bottle then placed on ice in a cooler. Two sediment samples were taken by delineating an area with a petri dish and then sediment and water was sucked up within the circle using a turkey baster to collect the top layer of the sediment and water. The sediment and water sample were placed into a 250 ml brown container. MP pellets were retrieved from each frame at 2 and 10-m depths after the 2-week deployment (Figure 3.3). Roughly 1 gram of MP pellets from both depths were taken for later algae and microbial analysis. One sample out of the two replicates for each sampling event were stored at -20 ℃ when we arrived back to the lab. MP pellets were stored in 50 ml centrifuge tubes with DI water and immediately frozen at -20 ℃. This allowed for a comparison of microbial communities found on the MP pellets before the microcosm experiment was conducted. One sample out of the two replicates for each sampling event was preserved using Lugol's iodine, this allows for the preservation and staining of cell shape/structure for later identification of algae; 2-3 ml of Lugol's iodine was used for every 100 ml of sample (Bellinger et al., 2015). MP pellets were stored in 50 ml centrifuge tubes with DI water and wrapped in electrical tape before storage. All samples taken for algae identification were stored at 4℃ until analysis.

Water Chemistry

I measured the following water quality parameters at each sampling event during the initial and retrieval events for frame incubation period: water temperature, pH, dissolved oxygen (DO), specific conductivity (Sp Cond), total dissolved solids (TDS), and turbidity, using a Yellow Springs Instruments (YSI) EXO multi-sensor sonde. I estimated chloride concentrations from conductivity using the equation y=0.296x-184 (r^2= 0.92; n=51), established previously at this site (Foley and Steinman, 2023).

Laboratory Experiment

All items deployed were retrieved successfully. The laboratory (microcosm) experiment involved the collection of MPs incubated at the 2-m and 10-m depths in Church Lake, which were then placed in 1-L beakers in the lab under the environmental conditions present at either 1) the water and depth at which they were collected or 2) the water and conditions at the alternate depth. This design allowed us to examine the responsiveness of the biofilm to new environmental conditions should the lake fully mix in the future. Environmental conditions from prior sampling efforts defined the conditions in the microcosms. Conditions at the deployment site in the epilimnion during summer included: average water temperature of 16 °C; mean irradiance of 190 µmol/m^2/s; mean conductivity of 865 µS/cm; and mean SRP and TP concentrations of 5 µg/L and 13 µg/L, respectively. Light levels in the growth chamber were lower than ambient conditions because of bulb limitations, resulting in an irradiance of ~34.5 µmol/m^2/s. Conditions in the hypolimnion had mean water temperature of 5°C; mean irradiance of 0.03 µmol/m^2/s; mean conductivity: 1315 µS/cm; and mean SRP and TP concentrations of 500 and 450 µg/L, respectively. Iron in the water samples collected in Church

Lake's hypolimnion caused interference during TP analysis, resulting in lower TP than SRP values in treatments receiving hypolimnetic water. Following digestion, the samples showed obvious floc and an orange tint. Similar problems have previously affected TP and SRP sampling from prior Church Lake research (Brian Scull, pers. comm.). Given that TP cannot be less than SRP in nature, I replaced the 450 µg/L value with 500 µg/L, which is equivalent to the SRP concentration and the minimum possible value for TP, thereby providing a conservative estimate for the starting concentration in the hypolimnion.

To evaluate how environmental conditions influenced the microbial and algal communities on the MP, the experimental design consisted of six different treatments. One-L beakers served as the experimental units. Each beaker contained 750 mL of filtered water (two-step sequential filtration:1 µm filter-Watertec QMC1-10NPCS and 0.2 µm filter-0.2-10NPCS) from Church Lake. The six treatment groups included (Table 3.1): Treatment group 1 (T-1) had MPs incubated in the lake epilimnion under ambient conditions (mean temperature: 16 °C; mean irradiance: 190 µmol/m^2/s; mean conductivity: 865 µS/cm; mean SRP and TP: ~5 and ~13 µg/L) transferred to hypolimnetic water and maintained at summer hypolimnetic conditions (mean temperature: 5°C; mean irradiance: 0.03 µmol/m^2/s; mean conductivity: 1315 µS/cm; mean SRP ~500 and TP ~500 µg/L) in the growth chamber. Treatment group 2 (T-2) had MPs incubated in the lake hypolimnion and transferred to epilimnetic water in the growth chamber. Treatment group 3 (T-3) had MPs incubated in the lake epilimnion and transferred to epilimnetic water in the growth chamber. Treatment group 4 (T-4) had MPs incubated in the lake hypolimnion and transferred to hypolimnetic water in the growth chamber. Control group one (C-1) had no MPs added to epilimnetic water, put in hypolimnetic conditions. Control group

2 (C-2) had no MPs added to hypolimnetic water, put in epilimnetic conditions. The four treatments with MPs had 5 replicates each and the 2 control treatments (no MPs) had 4 replicates each. This design was conducted for each of the two polymers being used in the experiment. Hence, a total of 48 beakers were used ([5 reps × 4 MP treatments] × 2 polymer types) + [4 reps × 2 controls]).

Beakers were placed in Precision Plant Growth Chambers (Power Scientific, Inc.) that coincided with each treatment's environmental factors. Photoperiod was set at a 15:9 light: dark cycle for treatments simulating epilimnetic conditions (i.e., treatment #'s 2, 3, C-2; Table 3.1) to reflect ambient conditions; treatments simulating hypolimnetic conditions (i.e., 1, 4, C-1; Table 3.1) were kept in the dark. The temperatures in the growth chambers reflect the average summer temperature at 2m and 10m depths.

Biofilm Calculation

The pellets from each treatment were retrieved and pooled for total biofilm biomass (ash-free dry mass: AFDM) at the end of the 25-day experiment, and measured by gravimetric analysis (Steinman et al., 2017). MP pellets were subsampled for biofilm by placing 8 g of MP pellets into a 50 ml centrifuge tube with DI water. Plastic pellets were sonicated for 10 seconds to remove biofilm attached to the surface of the pellets (Chen et al., 2020). Randomly selected pellets were checked microscopically for remaining biofilm after sonication; if biofilm remained, pellets were sonicated again. If no biofilm was found on the surface of the pellets, sonication was stopped, and the liquid was filtered. If the randomly selected MP pellets were clean, the total MP pellets were assumed to be clean. The biofilm retained on the filter was dried at 105 °C for 48 h and then placed in a muffle furnace at 550 °C for 1 h. AFDM was calculated as the

difference between the dry weight and the ashed weight. Biomass was log-transformed before application of analysis of variance (ANOVA) and followed by a Tukey HSD post hoc test.

DNA Extraction and 16S rRNA Amplicon Sequencing

After the conclusion of the microcosm experiment, 8 g of MPs was taken from each beaker and divided into centrifuge tubes filled with DI water and then stored at -20 °C until DNA extraction. DNA was extracted using the Macherey-Nagel NucleoSpin® Soil DNA extraction kit (Macherey-Nagel, Bethlehem, PA). Genomic DNA was extracted from water columns, sediments, and biofilm on MP pellets following protocols from the Macherey-Nagel NucleoSpin® Soil user manual (Düren, Germany). MP pellets went through a bead beating step prior to DNA extraction. A two-step PCR process was used following protocols outlined in Illumina MiSeq Systems 16S Metagenomic Sequencing Library Preparation. The 16S rRNA v4 region was amplified using the 515F/806R primer set (Callahan et al., 2016). Libraries were normalized to 4 nM using a QIAseq® normalization kit per their instructions (Qiagen, Germantown, MD). The quality of the individual libraries was checked on an Agilent Bioanalyzer (Agilent, Santa Clara, CA). Libraries passing the quality check were pooled, and the amplicons were sequenced using a 2 x 250 bp format, along with a 20% spike-in of Phi-X, on the Illumina MiSeq System (Illumina, San Diego, CA).

Sequence Data Quality Assessment and Taxonomic Assignment

Before analyzing bacterial biodiversity data, the sequence reads were filtered based on quality scores, sequencing errors were estimated, paired reads were merged, chimeras were removed, and amplicon sequence variants (ASVs) were identified using the package dada2 in R

Studio (2022) version 1.30.0 (Callahan et al., 2016). Taxonomic assignments were based on aligning merged paired reads to the SILVA 138 SSU database (Quast et al, 2013).

I identified ASVs that were potential contaminants using the "prevalence" method in the R package decontam R package version 1.22.0 (Davis et al., 2018). This method compares how often a sequence appears in blank samples (blank and PCR no template controls) to how often it appears in the true positive samples. ASVs that appear more often in the blank sample are considered contaminants and are removed from the analysis.

16S Amplicon Microbial Biodiversity Statistical Analysis

To visualize the dominant microbial community assemblages across the samples, I examined the top 20 most abundant genera present across samples and evaluated their relative abundance for each of our environmental (water, sediment, PET-2 m, PP-2 m, PP-10 m)(Figure 3.10) and mesocosm samples (T-1, T-2, T-3, T-4, C-1, C-2)(Figure 3.11). To estimate alpha and beta diversity, I rarified all of the samples to the lowest read depth of 20,000. Prior to rarefication, I removed some sample replicates (T-3, C-2) because they had much lower read counts compared to other replicates of the same treatment. Including them in the rarefaction step would result in subsampling all samples to a low read count and would not fully capture the microbial communities present.

Shannon's diversity index was used to estimate alpha diversity for each polymer per treatment. For this analysis, we observed only trends since some samples had n<3 and statistical analyses could not be performed. Beta diversity was assessed by using a Principal Coordinate Analysis (PCoA) to identify how microbial communities differed between mesocosm

treatments and samples collected from the lake. Like the alpha diversity estimates, a statistical analysis of bacteria biodiversity was not done between individual treatments because of the limited sample size among treatments (N≤3).

Since the PCoA showed that the largest differences in mesocosm microbial communities were driven by where microplastics were originally incubated (see results), a DESeq *(*Differential Expression Analysis for Sequence count data) analysis (Love et al., 2014) was used to examine microbial genera that significantly differed in abundance between plastics first incubated in the hypolimnion and those initially incubated in the epilimnion. For the analysis, only ASVs with read counts greater than 100 across all mesocosm treatments and ASVs present in at least 3 of the samples were considered. This removes ASVs that have very low read counts or would have just been present in one replicate. To look at differences only between samples that were initially incubated in the epilimnion and those initially incubated in the hypolimnion, I pooled the PP and PET samples together. This meant that all PP Epi-Epi (T-3), PP Epi-Hypo (T-1), PET Epi-Epi (T-3), and PET Epi-Hypo (T-1) became the initial Epi group, and the PP Hypo-Hypo (T-4), PP Hypo-Epi (T-2), PET Hypo-Hypo (T-4), and PET Hypo-Epi (T-2) became the initial Hypo group. The DESeq package tests for significant differences using a negative binomial generalized linear model, where the initial hypolimnion samples were set as the reference. An alpha value of 0.01 was used to determine significance.

Algal Preservation Methods and Algal Species Counts

After the 25-day microcosm experiment, 8 g of MP pellets were taken from each beaker and placed in centrifuges tubes. Plastic pellets were vortexed on the highest setting for 10 seconds to detach biofilm from the surface of the pellets. Randomly selected pellets were

checked microscopically for remaining biofilm after vortexing; if biofilm remained, pellets were vortexed for 10s again. If no biofilm was found on the surface of the pellets, vortexing stopped, and the pellets were removed. If the randomly selected MP pellets were clean, the total MP pellets were assumed to be clean. Vortexing was used to avoid damaging cell structure during removal (Amritha et al., 2023). Samples were concentrated prior to enumeration in Sedgewick Rafter counting chambers. Samples were concentrated following algal sedimentation methods (Bellinger et al., 2016). Before sedimentation began, each sample container was dropped onto a hard surface from a height of about 1.5 meters (m). The sudden increase in pressure as the bottle hits the floor collapses gas vacuoles in cells usually common in buoyant cyanobacteria taxa. Concentrating was conducted by allowing sample containers to sit for 72 hours in a dark vibration-free surface at 4℃. After 3-days, MP pellets were removed and 90 % of the supernatant was removed without disturbing the settled biomass.

Algal Community Evaluation

Algal communities were identified to genera using a Nikon Eclipse Ni-U DIC inverted microscope. Sedgwick Rafter slides were used to evaluate cell density and genera diversity. Before the identification of algae, I prepared the slides by concentrating cells in each sampling container. Concentrated samples were placed in a refrigerator to prevent shaking for 24 hours then samples sat on the lab counter for 15 mins at room temperature to allow the iodine to equilibrate. The sample was homogenized before 1 ml of sample was placed under the coverslip placed across the Sedgwick Rafter slide. The algal cells were left to settle at the bottom of the chamber for 15 minutes and then examined at 400x magnification on an inverted microscope. Cell counts were identified and recorded if they were alive before preservation.

Algal colonies were counted individually as single units. Filamentous algae were counted by dividing the final length (µm) within the square by 10. A taxonomic photo library was compiled of known and unknown genera found in both the environment (Sediment, Water, PET at 2 and 10m, PP at 2 and 10m) and mesocosm samples (treatment 1, 2, 3 ,4, C-1, C-2). Any algal cells that could not be identified to genus were renamed after observed characteristics and listed with phylum. Cell density was calculated where U is the total number of Taxon A units counted in all grids; A is the area of the grid used (0.01 cm^2); G is the number of grids counted; C is volume of Sedgwick-Rafter chamber used (1 ml); B is the total basal area of the Sedgwick-Rafter (10 cm^2); and CF is the concentration factor (0.01)

$$\text{Individual Cell density (cells/ml)} = CF\left(\frac{U}{A*G*\frac{C}{B}}\right)$$

Algal Biodiversity Statistical Analysis

All statistics and data visualization were conducted with R version 4.3.1 (2003-06-16 ucrt) using R studio (2022) version 4.2.2 (Integrated Development for R. RStudio, PBC, Boston, MA). A bubble plot was used to show the 20 most abundant genera present in the experiment. A nonmetric multidimensional scaling (NMDS) ordination was used to identify similarities or dissimilarities between the algal communities growing in Church Lake (Sediment, Water) and initial biofilm community on MPs at different depths before treatment (PP-2m, PP-10m, PET-2m, PET-10m) and treatment groups (T- 1,T-2,T-3,T-4,C-1,C-2; see Table 3.1) using R package vegan v. 2.6-4. NMDS ordinations were based on dissimilarity matrices calculated from cell density for each sample and Bray-Curtis's distance measures. Then an ANOSIM test was performed to determine if there was a difference in abundance between Lake and treatment

groups. When P-value was significant, a pairwise adonis test (package pairwiseAdonis v. 0.4.1) was used to find which groups were significantly more abundant than the others. Next, an indicator species analysis was used to find which genera were driving the community in the lake and treatment groups using R package indicspecies v.1.7.14. Lastly, species diversity was measured using Shannon diversity index to identify species richness and evenness between each treatment and lake samples. A Kruskal-Wallis test was used to assess whether there was a significant difference among the sample groups (PP-2m, PP-10m, PET-2m, PET-10m,T- 1,T-2,T-3,T-4,C-1,C-2; see Table 3.1) and polymers; if the p-value was significant, it was followed by a Dunn post hoc test.

Results

Biofilm quickly colonized MPs pellets incubated in Church Lake during the 2-week incubation of the frames at 2 and 10 meters during the summer. The 2-m and 10-m depths in Church Lake showed clearly different environmental conditions; the former was warm, supersaturated with DO, and had lower P concentrations (SRP: 5 µg/L, TP: 13 µg/L; Table 3.2), while the latter was cold, extremely hypoxic, and had higher P concentrations (SRP: 606 µg/L, TP: 555 µg/L; Table 3.2). The experimental conditions in the lab mimicked the differences in water quality between the hypolimnion and epilimnion in Church Lake, thereby providing a reasonable platform to test my hypothesis regarding the impacts of shifting species richness in the plastisphere from a low P, lower Cl^-, high light conditions to high P, high Cl^-, low light depth to demonstrate the influence of turnover on the plastisphere.

Environmental Conditions

Church Lake conditions at the time of MP frame retrieval were consistent with conditions at the start of the deployment (Table 3.2). The 2-m depth water was relatively warm and supersaturated with DO, and characterized by relatively high conductivity, and relatively low turbidity (NTU: 1.52). Mean SRP and TP concentrations at 2-m were ~ 5 and 13 µg/L, respectively (Table 3.2). In contrast, water at the 10-m depth was cold and hypoxic, with high conductivity, a circumneutral pH, and turbidity that is more than double that at 2-m (NTU: 3.45). At 10-m, SRP and TP concentrations averaged 606 and 555 µg/L, respectively (Table 3.2). Turbidity conditions at 2 and 10m were not replicated for any of the beakers. Turbidity remained low in all treatment beakers throughout the experiment (data not reported). Phosphorus concentration was more than 100 times higher in the hypolimnion than in the epilimnion in both the lake and experimental conditions. TP values were lower than SRP values in water samples taken from hypolimnetic zone, presumably because of the interference by iron in the water samples taken in the hypolimnion of Church Lake (Brian Scull, pers. comm.), for this experiment TP was set to 500 µg/L as a conservative value (see Methods).

Biofilm Biomass

The range of biomass on each polymer was from 0.23- 0.76 mg/g on PET and from 0.17 to 0.49 mg/g on PP (Figure 3.4; Table 3.3). There was no statistically significant difference in AFDM between PP and PET ($p = 0.20$; $df = 1$; F-value 1.62). In general, the amount of AFDM that developed on both polymers was greater on pellets that were incubated in the epilimnion than in the hypolimnion, irrespective of whether they were transferred to hypolimnetic water or maintained in epilimnetic water (Table 3.3).

PP Biomass: Biofilm AFDM on PP was significantly different among the 4 treatment groups ($p < 0.01$; df = 3; F-value = 4.54). The two significant differences based on a Tukey post-hoc HSD test both involved treatment 2 (Hypo→Epi): treatment 2 AFDM was significantly lower than treatment 1 (Epi→Hypo), and treatment 3 biomass was significantly greater than treatment 2 (Hypo→ Epi) (Table 3.4).

PET Biomass: AFDM growing on PET was significantly different among treatments ($p < 0.0001$; df = 3; F-value = 28.29). A Tukey post hoc test showed that treatment 1 (Epi→Hypo) was greater than all other treatments, and treatment 3 (Epi→ Epi) AFDM was greater than AFDM in both treatments 2 (Hypo→Epi) and 4 (Hypo→Hypo) (Table 3.5).

Bacterial Community Biodiversity

The number of times a particular sequence variant occurs in a sample is referred to as the "abundance" of an ASV in the context of amplicon sequencing. This measure provides an estimate of the relative quantity of a particular microbial taxon within the microbial community of that sample. Samples taken from the lake had a diverse phylum but were abundant largely in Proteobacteria and Bacteroidota (Figure 3.5). Water samples taken from the water column were abundant in *Chlorobium* but were not found in any other samples. BSV13 was only found in the water and sediment, but not on MPs. Sediment samples were most abundant with *Luteolibacter and Dechloromonas*; these genera were not seen or in very low abundance on MP pellets at 2m. PP-2m pellets were very abundant in both *Inhella and Aquabacterium.* At a depth of 10m, PP pellets were abundant with *Inhella,* and the overall diversity and abundance decreased at 10-m.

In the 25-day microcosm experiment, Proteobacteria and Bacteroidota continued to be the dominant phyla in all treatments (Figure 3.6). MP pellets initially incubated in the epilimnion had predominantly Cyanobacteria. Patterns of relative abundance for MP treatments in the mesocosm experiment tended to be similar across treatments that started in the same type of water. For instance, both T-1 (Epi→Hypo) and T-3 (Epi→Epi) started in the epilimnion and had similar microbial communities on both polymers. *Pirellula* was found only on T-1 and T-3 samples regardless of plastic type. T-2 (Hypo→Epi) and T-4 (Hypo→Hypo) both show similar patterns of relative abundance across the different genera, such as high abundance of *Flavobacterium, Rhdoferax, Methylotenera*. In comparison to lake samples and microcosm MP pellets, there was an increase in relative abundance when MP samples were transferred from the lake to the microcosms. The top five genera shifted when we transferred MP pellets into the microcosm experiment, except for Methylotenera.

Shannon's Diversity Index

Shannon's diversity index shows the potential difference between microplastics incubated in the hypolimnion (high salinity) and the epilimnion (low salinity) (Figure 3.7). The data indicate that Treatments 1 (Epi →Hypo) and 3 (Epi →Epi) had higher diversity in both PET and PP compared to the treatments that began in the hypolimnion. While the limited sample sizes prevented assessing statistical significance to these differences, the biomass results reflect similar patterns as the Shannon diversity index.

PCoA

Bacterial community beta diversity was compared among samples using a PCoA, which measures dissimilarity among communities based on Bray–Curtis distance matrix (Figure 3.8).

The first two principal components explained 64.9 % of community variance; the first axis explained 52.6% of the total variance and the second axis explained 12.3%. The largest separation across axis 1 was between the treatments that began in the epilimnion (positive position) and the treatments that began in the hypolimnion (negative position). Treatment 1 (Epi → Hypo) and 3 (Epi → Epi) had similar community structures to one another. Treatment groups 2 (Hypo → Epi), 4 (Hypo → Hypo), C-1(Epi → Hypo), and C-2 (Hypo → Epi) to a lesser degree clustered together. Along axis 2, the most distinct separation was between the T-3 PP samples and the T-3 PET samples. A PERMANOVA was not used to compare bacterial composition among treatments because of the low sample size (N≤3).

Differential Abundance Analysis

The most distinct differences observed in the PCoA was between mesocosm samples initially incubated in the epilimnion and samples incubated in the hypolimnion. I used a DESeq to evaluate which genera were statistically differentially abundant between the two depths (Table 3.6; Appendix Table 3.1). A total of 186 distinct ASVs were identified. Of these, only a few ASVs were significantly dominant in the hypolimnion. In the epilimnion, 165 ASVs were more abundant (Appendix Table 3.1). It appears that a select few families account for the majority of the plastisphere microbial community more abundant in the hypolimnion. Sulfurimonadaceae, Oxalobacteraceae, Pseudomonadaceae, Shewanellaceae, Alteromonadaceae, and Sphingobacteriaceae are among the families that were more abundant in samples that started out in the hypolimnion. Proteobacteria was the dominant phylum at both depths. The analysis revealed that microbial communities differed significantly between

the epilimnion and hypolimnion, with certain families being more abundant in the hypolimnion and Proteobacteria dominating at both depths.

Algae Community Biodiversity

The dominant phyla in Church Lake were Bacillariophyta, Cyanobacteria, and Chlorophyta (Figure 3.9). Sediment samples were composed of mostly Bacillariophyta and Chlorophyta. Water samples had less biodiversity than sediment and MP pellets incubated in the epilimnion. MP pellets incubated in the epilimnion had the highest diversity and abundance than any of the lake samples taken. Both polymers incubated in the epilimnion showed a high abundance in Chlorophyta and Cyanobacteria. MP pellets incubated in the hypolimnion showed low biodiversity and high relative abundance in Bacillariophyta and Cyanobacteria.

The dominant phyla in treatments from the microcosm experiment were Bacillariophyta, Chlorophyta, and Cyanobacteria (Figure 3.10). The dominant genera shifted slightly after being transferred from the lake to the microcosms. *Phormidium, Spirulina, Woronichinia, Dolichospermum, Coelastrum*, and a naviculoid diatom were no longer the dominant algal genera present. The cyanobacteria *Leptolyngbya* and *Pseudanabaena* were the most dominant genera present across all treatments and polymers. Treatment 1 (Epi→Hypo) had a noticeably higher abundance in genera than the other treatments and controls. Charophyta was present only in samples that were initially incubated in the epilimnion. In comparison to Lake samples, the Cyanobacteria continued to be the dominant phylum after transitioning from Church Lake to the lab experiment.

Shannon Diversity Index

The results from the Shannon diversity index results measured the biodiversity among samples in the Lake and microcosm (Figure 3.11). Controls C-1 and C-2 show low diversity, as would be expected of filtered water samples in the absence a plastisphere. Moderate diversity was predominately found in samples that were taken from the hypolimnion (T-2-PP, T-2-PET, T-3-PET, T-4-PET, T-4-PP, water column, PP-10m, PET-10m). Mesocosm samples had the highest diversity in T-1 on both PP and PET. Lakes samples with the highest diversity came from the sediment, PET-2m, PP-2m. A Kruskal-Wallis analysis indicates that there was a significant difference in diversity among treatments and polymers (chi-squared = 33.123, df = 5, p-value = < 0.001; chi-squared = 17.717, df = 2, p-value = <0.001, respectively). Following the significant p-value, a dunn post hoc test revealed that treatment 1 (Epi→Hypo) was significantly different from T-2 (Hypo→Hypo; n=5), T-3 (Epi→Epi; n=5), and T-4 (Hypo→Hypo; n=5), C-1 (Epi→Hypo; n=4), C-2 (Hypo→Epi; n=4) (Table 3.9). Both PP and PET algal communities were significantly different than samples that had no MP pellets, but algal diversity on the polymers used were not significantly different from each other (Table 3.10).

NMDS

The NMDS showed that the community composition among both treatments (T-1, T-2, T-3, T-4) and MPs (PP, PET) were similar to one another (Figure 3.12). Most samples look very similar to each other with the exception of T-1, which deviates slightly from the rest of the group. Lake samples were removed during the ANOSIM statistical test because only one sample was taken per environment (sediment, water, PP-2m, PP-10m, PET-2m, PET-10m). ANOSIM was performed to determine if there was a difference in algal community structure among

treatments. There was a significant difference in cell density among our polymers and treatments ($p< 0.05$). The ANOSIM statistic R showed a value of 0.24, indicating a moderate degree of dissimilarity in algae cell density found on MPs. A pairwise test indicated significant differences (adjusted $p < 0.05$) in community composition between PET and PP (p. adjusted = 0.024), PET and controls (C-1, C-2) (p. adjusted = 0.003), and PP and controls (p. adjusted = 0.003) (Table 3.7). The ANOSIM results indicate significant differences ($p \leq 0.05$) between treatment groups in multiple pairwise comparisons. Specifically, significant differences were found between T-1 (Epi →Hypo) and all other treatments (Table 3.8). Lastly, there was also a statistically significant difference between the community composition on MPs initially incubated in the epilimnion and hypolimnion (R = 0.1434, p-value = 0.0022).

An indicator species analysis was used to identify which algal genera were strongly associated with specific environmental conditions (T1= Epi→Hypo; T2= Hypo→Epi; T3= Epi→ Epi; T4=Hypo→Hypo) and substrate (PP, PET, Water). The results from the indicator species analysis imply that Diatom C is more common or abundant in group T-1 (Epi →Hypo), whereas *Leptolyngbya* is present in significant amounts in all three groups combined (T-1, T-2, and T-3). At the 0.05 significance level, no genus demonstrated a significant correlation with T-4 (Hypo →Hypo) or a combination containing T-4. With respect to PP and PET, there was a strong correlation between *Fragilaria* and the PET group, as evidenced by the significant connection (p-value= 0.009). There also was a strong correlation between *Achnanthidium* and the PP group (p-value= 0.0404).

Discussion

This study compared algal and bacterial communities growing on MPs in the epilimnion (low salinity, low P) and those growing on MPs in the hypolimnion (high salinity, high P) to observe species diversity and abundance influenced by environmental conditions if turnover occurred. In summary, this study is important because it provides insights into how environmental factors influence the microbial communities associated with MPs, which is essential for understanding ecological impacts and developing effective management strategies.

Water quality data from Church Lake showed distinct differences between environmental conditions at 2 and 10-m. The epilimnion's warmer temperatures, light availability, and high DO levels supported higher biofilm biomass on MPs. The highest biomass occurred on MPs that were initially incubated in the epilimnion (T-1 and T-3) suggesting that these conditions were conducive to microbial growth. The colder, more saline, hypoxic conditions of the hypolimnion contributed to significantly lower biomass and diversity of both algae and bacteria, as seen in T-2 (Hypo → Epi) and T-4 (Hypo → Hypo). Polymer type had minimal to no influence on the plastisphere, with microbial communities largely shaped by environmental conditions. The effectiveness of MP physiochemical properties and their influence on biomass often varies among studies, with some studies seeing higher biomass in high-density MPs (PVC and PET) and decreases in biomass in low-density MPs (PP), while others see no affect (Miao et al., 2021; Nava et al., 2021). The inconsistent results are believed to be influenced by the different environmental conditions between experiments in different laboratories (Miao et al., 2021).

Studies have shown that the biodiversity of the plastisphere is highest when the biodiversity of the microbial communities in the surrounding water and naturally occurring substrate are also high, a finding that is consistent in this study (Amaneesh et al., 2022; González-Pleiter et al., 2021; Zettler et al., 2013). The high conductivity (mostly as chloride; Foley and Steinman, 2023) in the hypolimnion can be stressful to many organisms, leading to lower biomass and diversity. Lower nutrient concentrations in the epilimnion can limit excessive algal blooms but may still support a balanced and diverse microbial community. Lower but not extremely low P levels in the epilimnion likely created a more favorable system for a range of taxa, as opposed to the hypolimnion, where the very high P environment promotes the growth of specific bacteria and algae adapted to nutrient-rich environments (Vadstein et al. 1988). The presence of high nutrients has been shown to strongly influence the community structure of microplastic biofilms (Nava et al., 2021; Oberbeckmann et al., 2018). The substantial presence of cyanobacterial genera such as *Leptolyngbya* and *Pseudanabaena* occurred in both the epilimnion and hypolimnion, showing the adaptability of these cyanobacteria.

In the present study, when MPs incubated in the epilimnion were introduced to hypolimnetic water with high P and chloride, the abundance of algal genera remained high regardless of the high salinity concentration, as seen in T-1 (Epi→ Hypo). The Shannon diversity index indicated significantly higher biodiversity in this treatment compared to others (Figure 3.11). Treatment 1 (Epi→ Hypo) had significantly higher biodiversity compared to other treatments. A similar study found that phosphate concentration was the dominant driver for algae assemblage regardless of high or low conductivity (Nava et al., 2021). Lower salinity and

phosphorus in the epilimnion typically supported a broader range of freshwater microorganisms. Groups like Chlorophyta are highly adaptable to low nutrient and low salinity conditions depending on species and can support higher diversity and abundance (Bellinger et al., 2016). But Chlorophyta are limited by low light and dissolved organic carbon levels (Bellinger et al., 2016). Cyanobacteria can thrive in high P and salinity concentrations (Bellinger et al., 2016), but at low light levels, photosynthetic algae will become growth limited.

I accept the hypothesis that algal communities growing on MPs in the hypolimnion have lower species richness and abundance compared to those in the epilimnion. However, I reject the hypothesis that bacterial communities in the hypolimnion have greater species richness and abundance, as the observed results do not support this prediction. Higher salinity levels in the hypolimnion can stress many freshwater organisms but may be more suitable for certain salt-tolerant or halophilic bacteria. DESeq analysis highlighted differences in bacterial genera abundance between the epilimnion and hypolimnion, with a majority of ASVs appearing in the epilimnion-grown plastisphere. Families such as Sulfurimonadaceae, Oxalobacteraceae, and Pseudomonadaceae were more abundant to the hypolimnion, indicating their adaptation to those harsher environmental conditions. Overall, the results showed that there was a great influence on the initial location in which the bacteria in the plastisphere colonized.

Conclusions

I hypothesized that algal communities on MPs in the hypolimnion of Church lake would have lower biodiversity and abundance compared to those in the epilimnion due to stress from high salinity and low light, whereas bacterial communities would thrive in the hypolimnion's low-light, low DO conditions. To test this, MPs were incubated in Church Lake and later exposed

to controlled lab environments that contrasted with the initial environment in which the MPs were incubated. This allowed me to assess biofilm adaptability and how these organisms responded to differing environmental conditions, which could provide insights if the lake experiences a full turnover.

In summation, my study revealed that microbial community composition is influenced much more by environmental conditions rather than by the type of polymer used. At the epilimnion, bacterial communities were diverse, dominated by Proteobacteria and Bacteroidota, and had higher diversity compared to the hypolimnion. The hypolimnion, while hosting fewer genera, saw an increase in specific families like Sulfurimonadaceae and Oxalobacteraceae favoring the high salinity and low light conditions. Similarly, Algae in the epilimnion showed higher diversity and abundance, with dominance by Cyanobacteria and Chlorophyta. In contrast, the hypolimnion had lower algal biodiversity but higher relative abundance of Bacillariophyta and Cyanobacteria.

The hypolimnion of Church Lake has extremely high P concentrations, which are conducive to eutrophication, a process that leads to excessive algal blooms and can degrade water quality. If Church Lake completely mixes, then the introduction of high nutrients may stimulate biomass growth on MPs (assuming the salinity levels are diluted to the point that they do not inhibit growth). Based on the results from this study, the biofilm is likely to start out diverse on epilimnetic MPs relative to hypolimnetic MPs, but it is unclear if this diversity would be maintained over longer time periods, as phosphorus-enhanced growth on the MPs will result in greater density and MP sinking, inter-specific competition within the plastisphere matrix for resources such as nutrients and light, and susceptibility to grazers.

References

Alimi, O. S., Farner Budarz, J., Hernandez, L. M., & Tufenkji, N. (2018). Microplastics and nanoplastics in aquatic environments: aggregation, deposition, and enhanced contaminant transport. Environmental Science & Technology, 52(4), 1704–1724. https://doi.org/10.1021/acs.est.7b05559

Amaneesh, C., Anna Balan, S., Silpa, P. S., Kim, J. W., Greeshma, K., Aswathi Mohan, A., Robert Antony, A., Grossart, H. P., Kim, H. S., & Ramanan, R. (2022). Gross Negligence: Impacts of Microplastics and Plastic Leachates on Phytoplankton Community and Ecosystem Dynamics. *Environmental Science and Technology*. https://doi.org/10.1021/acs.est.2c05817

Amritha, P. S., Veena, V., & Harathi, P. B. (2023). Model periphyton biofilms: biological system of bioremediation of synthetic plastics. Microbiology, 92(5), 686–694. https://doi.org/10.1134/s002626172260358x

Bellinger, Edward G., and David C. Sigee. Freshwater algae: identification, enumeration and use as bioindicators, John Wiley & Sons, Incorporated, 2015. ProQuest eBook Central, http://ebookcentral.proquest.com/lib/gvsu/detail.action?docID=1895748.

Blettler, M. C. M., Abrial, E., Khan, F. R., Sivri, N., & Espinola, L. A. (2018). Freshwater plastic pollution: Recognizing research biases and identifying knowledge gaps. Water Research, 143, 416–424. https://doi.org/10.1016/j.watres.2018.06.015

Callahan, B., McMurdie, P., Rosen, M. *et al.* (2016). DADA2: High-resolution sample inference from Illumina amplicon data. *Nat Methods* 13, 581–583. https://doi.org/10.1038/nmeth.3869

Chen, X., Chen, X., Zhao, Y., Zhou, H., Xiong, X., & Wu, C. (2020). Effects of microplastic biofilms on nutrient cycling in simulated freshwater systems. Science of the Total Environment, 719, 137276. https://doi.org/10.1016/j.scitotenv.2020.137276

Davis, N. M., Proctor, D., Holmes, S. P., Relman, D. A., & Callahan, B. J. (2017). Simple statistical identification and removal of contaminant sequences in marker-gene and metagenomics data. bioRxiv, 221499. https://doi.org/10.1101/221499

Driedger, A. G. J., Dürr, H. H., Mitchell, K., & Van Cappellen, P. (2015). Plastic debris in the Laurentian Great Lakes: A review. Journal of Great Lakes Research, 41(1), 9–19. https://doi.org/10.1016/j.jglr.2014.12.020

Eadie, B. J., Schwab, D. J., Johengen, T. H., Lavrentyev, P. J., Miller, G. S., Holland, R. E., Leshkevich, G. A., Lansing, M. B., Morehead, N. R., Robbins, J. A., Hawley, N., Edgington, D. N., & Van Hoof, P. L. (2002). Particle transport, nutrient cycling, and algal community structure associated with a major winter-spring sediment resuspension event in southern Lake Michigan. Journal of Great Lakes Research, 28(3), 324–337. https://doi.org/10.1016/S0380-1330(02)70588-1

Foley, E., & Steinman, A. D. (2023). Urban lake water quality responses to elevated road salt. Science of the Total Environment, 905, 167139. https://doi.org/10.1016/j.scitotenv.2023.167139

González-Pleiter, M., Velázquez, D., Casero, M. C., Tytgat, B., Verleyen, E., Leganés, F., Rosal, R., Quesada, A., & Fernández-Piñas, F. (2021). Microbial colonizers of microplastics in an Arctic freshwater lake. Science of the Total Environment, 795. https://doi.org/10.1016/j.scitotenv.2021.148640

Guasch, H., Bernal, S., Bruno, D., Almroth, B. C., Cochero, J., Corcoll, N., … Martí, E. (2022). Interactions between microplastics and benthic biofilms in fluvial ecosystems: knowledge gaps and future trends. Freshwater Science, 41(3), 442-458. https://doi.org/10.1086/721472

Harrison, J. P., Schratzberger, M., Sapp, M., & Osborn, A. M. (2014). Rapid bacterial colonization of low-density polyethylene microplastics in coastal sediment microcosms. BMC Microbiology, 14(1). https://doi.org/10.1186/s12866-014-0232-4

He, S., Jia, M., Xiang, Y., Song, B., Xiong, W., Cao, J., Peng, H., Yang, Y., Wang, W., Yang, Z., & Zeng, G. (2021). Biofilm on microplastics in aqueous environment: Physicochemical properties and environmental implications. Journal of Hazardous Materials, 127286. https://doi.org/10.1016/j.jhazmat.2021.127286

Hitchcock, J. N. (2020). Storm events as key moments of microplastic contamination in aquatic ecosystems. Science of the Total Environment, 734, 139436. https://doi.org/10.1016/j.scitotenv.2020.139436

Holmes, L. A., Turner, A., & Thompson, R. C. (2014). Interactions between trace metals and plastic production pellets under estuarine conditions. Marine Chemistry, 167, 25–32. https://doi.org/10.1016/j.marchem.2014.06.001

Johnson, K. A., Steinman, A. D., Keiper, W. D., & Ruetz, C. R. (2011). Biotic responses to low-concentration urban road runoff. Journal of the North American Benthological Society, 30(3), 710–727. https://doi.org/10.1899/10-157.1

Kaur, K., Reddy, S., Barathe, P., Oak, U., Shriram, V., Kharat, S. S., Govarthanan, M., & Kumar, V. (2021). Microplastic-associated pathogens and antimicrobial resistance in environment. Chemosphere, October, 133005. https://doi.org/10.1016/j.chemosphere.2021.133005

Kaushal, S. S., Reimer, J. E., Mayer, P. M., Shatkay, R. R., Maas, C. M., Nguyen, W. D., Boger, W. L., Yaculak, A. M., Doody, T. R., Pennino, M. J., Bailey, N. W., Galella, J. G., Weingrad, A., Collison, D. C., Wood, K. L., Haq, S., Newcomer-Johnson, T. A., Duan, S., & Belt, K. T. (2022). Freshwater salinization syndrome alters retention and release of chemical cocktails along flowpaths: From stormwater management to urban streams. Freshwater Science, 41(3). https://doi.org/10.1086/721469

Lazrak, K., Nothof, M., Tazart, Z., Filker, S., Berger, E., Mouhri, K., & Loudiki, M. (2024). Salt stress responses of microalgae biofilm communities under controlled microcosm

conditions. Algal Research, 78(October 2023), 103430. https://doi.org/10.1016/j.algal.2024.103430

Liu, F., Olesen, K. B., Borregaard, A. R., & Vollertsen, J. (2019). Microplastics in urban and highway stormwater retention ponds. Science of the Total Environment, 671, 992–1000. https://doi.org/10.1016/j.scitotenv.2019.03.416

Loch, T.P., Faisal, M. (2015). Emerging flavobacterial infections in fish: A review. J Adv Res. May;6(3):283-300. doi: 10.1016/j.jare.2014.10.009.

Love, M.I., Huber, W., Anders, S. (2014) Moderated estimation of fold change and dispersion for RNA-seq data with DESeq2. Genome Biology, 15:550. 10.1186/s13059-014-0550-8

Lutz, N., Fogarty, J., & Rate, A. (2021). Accumulation and potential for transport of microplastics in stormwater drains into marine environments, Perth region, Western Australia. Marine Pollution Bulletin, 168(April), 112362. https://doi.org/10.1016/j.marpolbul.2021.112362

Miao, L., Wang, P., Hou, J., Yao, Y., Liu, Z., Liu, S., & Li, T. (2019). Distinct community structure and microbial functions of biofilms colonizing microplastics. Science of the Total Environment, 650, 2395–2402. https://doi.org/10.1016/j.scitotenv.2018.09.378

Mulholland, P.J., Steinman, A.D., Palumbo, A.V., Elwood, J.W., & Kirschtel, D.B. (1991) Role of nutrient cycling and herbivory in regulating periphyton communities in laboratory streams. Ecology, 72(3), 966-982. https://doi.org/10.2307/1940597

Nava, V., Matias, M. G., Castillo-Escrivà, A., Messyasz, B., & Leoni, B. (2021). Microalgae colonization of different microplastic polymers in experimental mesocosms across an environmental gradient. Global Change Biology. https://doi.org/10.1111/gcb.15989

Numberger, D., Zoccarato, L., Woodhouse, J., Ganzert, L., & Sauer, S. (2022). Urbanization promotes specific bacteria in freshwater microbiomes including potential pathogens. Science of the Total Environment, 845(February), 157321. https://doi.org/10.1016/j.scitotenv.2022.157321

Oberbeckmann, S., Kreikemeyer, B., & Labrenz, M. (2018). Environmental factors support the formation of specific bacterial assemblages on microplastics. Frontiers in Microbiology, 8(JAN), 1–12. https://doi.org/10.3389/fmicb.2017.02709

Oberbeckmann, S., Loeder, M. G. J., Gerdts, G., & Osborn, M. A. (2014). Spatial and seasonal variation in diversity and structure of microbial biofilms on marine plastics in Northern European waters. FEMS Microbiology Ecology, 90(2), 478–492. https://doi.org/10.1111/1574-6941.12409

Okeke, E. S., Prince, T., Ezeorba, C., Chen, Y., Mao, G., Feng, W., & Wu, X. (2022). Ecotoxicological and health implications of microplastic - associated biofilms: a recent review and prospect for turning the hazards into benefits. Environmental Science and Pollution Research, 0123456789. https://doi.org/10.1007/s11356-022-22612-w

Quast C, Pruesse E, Yilmaz P, Gerken J, Schweer T, Yarza P, Peplies J, Glöckner FO (2013) The SILVA ribosomal RNA gene database project: improved data processing and web-based tools. Opens external link in new windowNucl. Acids Res. 41 (D1): D590-D596.

Sánchez-Fortún, A., Fajardo, C., Martín, C., D'ors, A., Nande, M., Mengs, G., Costa, G., Martín, M., & Sánchez-Fortún, S. (2021). Effects of polyethylene-type microplastics on the growth and primary production of the freshwater phytoplankton species Scenedesmus armatus and Microcystis aeruginosa. Environmental and Experimental Botany, 188(May). https://doi.org/10.1016/j.envexpbot.2021.104510

Scott, J. W., Gunderson, K. G., Green, L. A., Rediske, R. R., & Steinman, A. D. (2021). Perfluoroalkylated substances (Pfas) associated with microplastics in a lake environment. In Toxics (Vol. 9, Issue 5). https://doi.org/10.3390/TOXICS9050106

Steinman, A. D., Lamberti, G. A., Leavitt, P. R., & Uzarski, D. G. (2017). Biomass and pigments of benthic algae. In F. R. Hauer & G. A. Lamberti (Eds.), Methods in Stream Ecology, Volume 1 (Third Edition), pp. 223–241). Academic Press. https://doi.org/https://doi.org/10.1016/B978-0-12-416558-8.00012-3

Steinman, A. D., Scott, J., Green, L., Partridge, C., Oudsema, M., Hassett, M., Kindervater, E., & Rediske, R. R. (2020). Persistent organic pollutants, metals, and the bacterial community composition associated with microplastics in Muskegon Lake (MI). Journal of Great Lakes Research, 46(5), 1444–1458. https://doi.org/10.1016/j.jglr.2020.07.012

Vadstein, O., Jensen, A., Olsen, Y. and Reinertsen, H., 1988. Growth and phosphorus status of limnetic phytoplankton and bacteria. Limnology and Oceanography 33(4): 489-503.

Verla, A. W., Enyoh, C. E., Verla, E. N., & Nwarnorh, K. O. (2019). Microplastic–toxic chemical interaction: a review study on quantified levels, mechanism, and implication. SN Applied Sciences, 1(11), 1–30. https://doi.org/10.1007/s42452-019-1352-0

Wang, L., Luo, Z., Zhen, Z., Yan, Y., Yan, C., Ma, X., Sun, L., Wang, M., Zhou, X., & Hu, A. (2020). Bacterial community colonization on tire microplastics in typical urban water environments and associated impacting factors. Environmental Pollution, 265, 114922. https://doi.org/10.1016/j.envpol.2020.114922

Wu, Y., Guo, P., Zhang, X., Zhang, Y., Xie, S., & Deng, J. (2019). Effect of microplastics exposure on the photosynthesis system of freshwater algae. Journal of Hazardous Materials, 374(December 2018), 219–227. https://doi.org/10.1016/j.jhazmat.2019.04.039

Zafar, R., Arshad, Z., Eun Choi, N., Li, X., & Hur, J. (2023). Unravelling the complex adsorption behavior of extracellular polymeric substances onto pristine and uv-aged microplastics using two-dimensional correlation spectroscopy. Chemical Engineering Journal, 470(June), 144031. https://doi.org/10.1016/j.cej.2023.144031

Zettler, E. R., Mincer, T. J., & Amaral-zettler, L. A. (2013). Life in the "plastisphere": microbial communities on plastic marine debris. Environmental Science & Technology, 47(13), 7137–7146. https://doi.org/DOI: 10.1021/es401288

Tables

Table 3.1. Environmental conditions in Church Lake at 2m and 10m compared to experimental treatment conditions in the laboratory. Treatment #1: MPs incubated in lake epilimnion transferred to hypolimnetic water. Treatment #2: MPs incubated in lake hypolimnion transferred to epilimnetic water. Treatment #3: MPs incubated in lake epilimnion and transferred to epilimnetic water. Treatment #4: MPs incubated in lake hypolimnion and transferred to hypolimnetic water. C-1: No MPs were added to epilimnetic water put in hypolimnetic conditions. C-2: No MPs were added to hypolimnetic water put in epilimnetic conditions. Spec. Cond: specific conductivity.

Treatment #	Initial Conditions (Lake)				Treatment Conditions (Lab)				
	Spec. Cond µS/cm	STDEV.P	Light	P	Spec. Cond µS/cm	STDEV.P	Light	P	MPs
#1-Epi→Hypo	865	4	High	Low	1178	11	Low	High	Present
#2-Hypo→Epi	1315	100	Low	High	880	5	High	Low	Present
#3-Epi→Epi	865	4	High	Low	873	2	High	Low	Present
#4Hypo→Hypo	1315	100	Low	High	1200	2	Low	High	Present
C-1-Epi→Hypo	865	4	High	Low	877	2	Low	High	Absent
C-2-Hypo→Epi	1315	100	Low	High	1187	4	High	Low	Absent

Table 3.2. Water quality data from the experiment. Samples labeled retrieval are measurements taken from the Church Lake water column at 2 and 10 meters after the 2-week frame incubation period. Remaining rows are water quality samples from the beakers taken on the final day of the experiment (excluding P values which are from first day of the microcosm experiment [see below]) after removing MP pellets (except Controls, where no pellets were present). SRP and TP values are means (± SD) from each treatment taken at the beginning of the experiment regardless of polymer (n = 10). SRP and TP values labeled "retrieval" were sampled from Church Lake after the 2-week frame incubation period and had no replicates. SRP values are higher than TP values in the hypolimnion because of interference from high iron concentrations in the hypolimnion. DO: dissolved oxygen, SPC: specific conductivity.

Treatment	Temp (°C)	DO (%)	DO (mg/L)	pH	SPC (µS/cm)	SRP (µg/L)	TP (µg/L)
Retrieval-2m	24	134	11.24	8	865	5	13
Retrieval-10m	4	2.6	0.33	6	1315	606	555
T1-Epi→Hypo	5	2.6	0.33	8	1177.5	504±37	500±23*
T2-Hypo→Epi	16	134	11.24	8	880	5±0	10±1
T3-Epi→Epi	16	134	11.24	8	873	5±0	10±1
T4-Hypo→Hypo	5	2.6	0.33	8	1199.5	504±37	500±23*
C-1- Epi→Hypo	5	2.6	0.33	8	877	5±0	10±1
C-2- Hypo→Epi	16	134	11.24	8	1187	502±34	500±25*

*TP values set at 500 µg/L to match SRP values (see CH 3 methods for explanation)

Table 3.3. Minimum, maximum and mean (± SD, n = 5) AFDM values in each treatment. The average was taken from replicates of biofilm biomass for each treatment measured on the 25th day. (T1= Epi→Hypo; T2= Hypo→Epi; T3= Epi→ Epi; T4=Hypo→Hypo)

	AFDM (mg/g)		
Treatment	Min	Max	Mean
T-1-PET-Epi→Hypo	0.40	0.76	0.59 ± 0.14
T-1-PP-Epi→Hypo	0.33	0.49	0.40 ± 0.07
T-2-PET-Hypo→Epi	0.23	0.31	0.26 ± 0.03
T-2-PP-Hypo→Epi	0.17	0.31	0.24 ± 0.05
T-3-PET-Epi→Epi	0.41	0.49	0.44 ± 0.03
T-3-PP-Epi→Epi	0.31	0.40	0.36 ± 0.03
T-4-PET-Hypo→Hypo	0.23	0.34	0.28 ± 0.04
T-4-PP-Hypo→Hypo	0.18	0.41	0.33 ± 0.09

Table 3.4. Tukey multiple comparisons for differences in the mean values of biofilm biomass on PP microplastics between 4 treatments. A negative value indicates the first treatment in the treatment pair was significantly lower than the second treatment in the pair. Asterisks indicate level of significance: *** $p < 0.0001$, ** $p < 0.01$, * $p < 0.05$. Diff stands for the differences in means between two groups being compared. lwr stands for lower confidence interval and describes the lower bound of the confidence interval for the differences in means. Upr stands for upper confidence interval and describes the upper bound of the confidence interval for the differences in means.

Treatment	diff	lwr	upr	p.adj
T2PP-T1PP	-0.50	-0.91	-0.09	0.01**
T3PP-T1PP	-0.09	-0.50	0.32	0.91
T4PP-T1PP	-0.20	-0.61	0.21	0.50
T3PP-T2PP	0.40	-0.005	0.81	0.05*
T4PP-T2PP	0.29	-0.12	0.7	0.21
T4PP-T3PP	-0.11	-0.52	0.30	0.86

Table 3.5. Tukey multiple comparisons for differences in the mean values of biofilm biomass on PET microplastics between 4 treatments. A negative value indicates the first treatment in the treatment pair was significantly less than the second treatment in the pair. Asterisks indicate level of significance: *** $p < 0.0001$, ** $p < 0.01$, * $p < 0.05$. Diff stands for the differences in means between two groups being compared. Lwr stands for lower confidence interval and describes the lower bound of the confidence interval for the differences in means. Upr stands for upper confidence interval and describes the upper bound of the confidence interval for the differences in means.

Treatment	diff	lwr	upr	p.adj
T2PET-T1PET	-0.81	-1.10	-0.52	3.4E-06***
T3PET-T1PET	-0.29	-0.58	0.006	0.05*
T4PET-T1PET	-0.74	-1.03	-0.45	1.09E-05***
T3PET-T2PET	0.53	0.23	0.82	0.001***
T4PET-T2PET	0.07	-0.22	0.37	0.89
T4PET-T3PET	-0.45	-0.75	-0.16	0.002**

Table 3.6. DESeq results showed 186 ASVs that were differentially abundant. This table shows the 21 ASVs that were significantly more abundant in the hypolimnion.

ASVs	log2FoldChange	p.adj	Phylum	Family	Genus
ASV185	9.19	1.83E-29	Proteobacteria	Comamonadaceae	*Polaromonas*
ASV431	7.58	9.97E-38	Campylobacterota	Sulfurimonadaceae	*Sulfuricurvum*
ASV592	7.55	2.88E-34	Proteobacteria	Rhodocyclaceae	*Dechloromonas*
ASV7	7.53	7.18E-18	Proteobacteria	Comamonadaceae	*Rhodoferax*
ASV126	7.49	1.56E-19	Proteobacteria	Oxalobacteraceae	*Janthinobacterium*
ASV176	7.45	2.12E-13	Proteobacteria	Oxalobacteraceae	*Massilia*
ASV24	7.38	2.46E-21	Proteobacteria	Pseudomonadaceae	*Pseudomonas*
ASV324	7.34	1.20E-23	Proteobacteria	Oxalobacteraceae	*[Aquaspirillum] arcticum group*
ASV32	7.33	7.66E-19	Proteobacteria	Methylomonadaceae	*Crenothrix*
ASV540	7.04	4.42E-26	Proteobacteria	Moraxellaceae	*[Agitococcus] lubricus group*
ASV249	7.03	1.36E-17	Proteobacteria	Shewanellaceae	*Shewanella*
ASV110	6.97	8.70E-16	Proteobacteria	Methylomonadaceae	NA
ASV250	6.89	4.59E-19	Proteobacteria	Oxalobacteraceae	*Undibacterium*
ASV16	6.52	1.24E-12	Proteobacteria	Methylomonadaceae	*Methylobacter*
ASV900	5.03	8.48E-09	Proteobacteria	Methylomonadaceae	*Methylomonas*
ASV151	4.35	4.80E-05	Proteobacteria	Alteromonadaceae	*Rheinheimera*

ASV437	3.84	7.50E-07	Bacteroidota	Sphingobacteriaceae	*Pedobacter*
ASV416	3.51	0.00099	Proteobacteria	Pseudohongiellaceae	*Pseudohongiella*
ASV5	2.88	0.008024	Proteobacteria	Comamonadaceae	*Inhella*
ASV10	2.48	7.16E-05	Proteobacteria	Methylophilaceae	*Methylotenera*
ASV165	1.82	0.004975	Proteobacteria	Caulobacteraceae	*Caulobacter*

Table 3.7. Pairwise comparison of algae cell density (cells/ml) between MPs (PP, PET, Water). Df stands for degrees of freedom. SumOfSqs stands for sum of squares. F. Model stands for F-statistics. R2 stands for R-squared. Asterisks indicate level of significance: *** p < 0.0001, ** p < 0.01, * p < 0.05.

Polymer	Df	SumsOfSqs	F. Model	R2	p. adjusted	
PET vs PP	1	0.60	2.99	0.07	0.02	*
PET vs Water	1	1.48	7.54	0.22	0.003	***
PP vs Water	1	1.26	6.25	0.19	0.003	***

Table 3.8. Pairwise comparison of algae cell density (cells/ml) between treatments. Df stands for degrees of freedom. (T1= Epi→Hypo; T2= Hypo→Epi; T3= Epi→ Epi; T4=Hypo→Hypo). Lake samples were removed due to insufficient sample size. SumOfSqs stands for sum of squares. F. Model stands for F-statistics. R2 stands for R-squared, R2 helps you understand how well the independent variables explain the variability in the dependent variable for each pair of groups being compared. Asterisks indicate level of significance: *** p < 0.0001, ** p < 0.01, * p < 0.05.

Treatment	Df	SumsOfSqs	F. Model	R2	p. adjusted	
T-1 vs T-2	1	1.16	7.08	0.28	0.02	*
T-1 vs T-3	1	1.44	10.23	0.36	0.02	*
T-1 vs T-4	1	1.77	10.13	0.36	0.02	*
T-1 vs C-1	1	1.44	8.76	0.42	0.02	*
T-1 vs C-2	1	1.57	7.80	0.39	0.03	*
T-2 vs T-3	1	0.40	3.23	0.15	0.23	
T-2 vs T-4	1	0.46	2.92	0.14	0.33	
T-2 vs C-1	1	0.67	4.88	0.29	0.06	
T-2 vs C-2	1	1.16	6.61	0.36	0.08	
T-3 vs T-4	1	0.49	3.65	0.17	0.15	
T-3 vs C-1	1	0.62	6.08	0.34	0.02	*
T-3 vs C-2	1	1.21	8.69	0.42	0.02	*
T-4 vs C-1	1	0.23	1.47	0.11	1.00	
T-4 vs C-2	1	0.62	3.25	0.21	0.21	
C-1 vs C-2	1	0.26	1.39	0.19	1.00	

Table 3.9. Dunn Test Pairwise Comparisons with Bonferroni Correction comparing Shannon algal diversity index values among treatments. (T1= Epi→Hypo; T2= Hypo→Epi; T3= Epi→ Epi; T4=Hypo→Hypo).

Treatments	z-Score	p-Value	
C-1 vs C-2	0.05	1	
C-1 vs T-1	-4.43	0.0001	***
C-1 vs T-2	-2.36	0.14	
C-1 vs T-3	-2.30	0.16	
C-1 vs T-4	-1.52	0.97	
C-2 vs T-1	-4.49	0.0001	***
C-2 vs T-2	-2.42	0.11	
C-2 vs T-3	-2.36	0.14	
C-2 vs T-4	-1.58	0.86	
T-1 vs T-2	2.74	0.04	*
T-1 vs T-3	2.82	0.03	*
T-1 vs T-4	3.86	0.0009	***
T-2 vs T-3	0.08	1	
T-2 vs T-4	1.119737	1	
T-3 vs T-4	1.039755	1	

Table 3.10. Dunn Test Pairwise Comparisons with Bonferroni Correction comparing Shannon algal diversity index values among Polymers. Water indicates samples that contained no MP pellets.

Polymers	z-Score	p-Value	
PET vs PP	0.95	0.51	
PET vs Water	4.16	0.0004	***
PP vs Water	3.44	0.0009	***

Figure Captions

Figure 3.1 Map of Church Lake. (a) Location of lake in lower peninsula of Michigan. (b) Aerial view of Church Lake and the two other connecting lakes (Middleboro, Westboro). (c) Close-up of Church Lake and the unnamed tributary that flows from the East Beltline to the urban Lake. (d) Bathymetry of Church Lake retrieved from Progressive AE (2010); the Lake has denser residential housing on its south and west shorelines and is adjacent to the East Beltline state highway on its east side. Depth contours are in ft.

Figure 3.2. PVC frame holding Incubation tubes before deployment (after Steinman et al., 2020).

Figure 3.3. Urban lake water column. View through the water column and frame setup in portion of lake with established chemocline.

Figure 3.4. Bar plot of the average AFDM values in each treatment for PP (A) and PET (B) (± SD, n = 5). The average was taken from replicates (n=5) of biofilm biomass for each treatment measured on the 25th day. (T1= Epi→Hypo; T2= Hypo→Epi; T3= Epi→ Epi; T4=Hypo→Hypo).

Figure 3.5. Bubble plot of the relative abundance of bacteria genus-level ASVs found in Church Lake before the microcosm experiment was conducted. The bubble plot represents the top 20 most abundant genera found, with the highest abundant genus occurring at the top of the graph to the lowest abundance genus occurring towards the bottom. The size of the bubbles represents the relative abundance of each genus in each sample. The phylum of each genus is represented by color. The "Lake" plot shows water samples taken from 2-m and 10-m in Church lakes water column with no known MPs present combined to form an integrated water sample of the water column(water)(n=1). Samples taken from the sediment were taken from Church lakes littoral and had no known MPs present (sediment)(n=1). After the two-week frame incubation period in Church Lake, the MP pellets (PP, PET) were taken from each depth (2-m, 10-m) (n=1 each). PET-10m was lost during PCR sequencing.

Figure 3.6. The relative abundance of bacteria genus-level ASVs identified from MP Pellets after the microcosm experiment. The data is split into treatments with no MPs "Water" (C-1, C-2) (n=3; 3) , treatments that had PET (T-1, T-2, T-3, T-4) (n=5; 2; 5; 1) and treatments that had PP (T-1, T-2, T-3, T-4) (n=5; 3; 4; 2) (T1= Epi→Hypo; T2= Hypo→Epi; T3= Epi→ Epi; T4=Hypo→Hypo; C-1= Epi→ Hypo; C-2= Hypo → Epi). The bubble plot represents the top 20 most abundant genera found, with the highest abundant genus occurring at the top of the graph to the lowest abundance genus occurring towards the bottom. The size of the bubbles represents the relative abundance of each genus in each sample. The phylum of each genus is represented by color.

Figure 3.7. Alpha diversity estimates based on Shannon's Diversity Index for the bacteria genera present on MP pellets after the microcosm experiment.

Figure 3.8. Principal coordinate analysis (PCoA) shows the profiles the plastisphere and water communities on the basis of the Bray−Curtis distance matrix calculated at the genus level comparing biofilms on MPs (T-1, T-2, T-3, T-4) and no MPs (C-1, C-2) for each sample.

Figure 3.9. Bubble plot displaying the cell density of algae found in "Lake" samples (Sediment, Water, PP-2m, PP-10m, PET-2m, PET-10m). The top 20 most abundant genera found, with the most abundant genus occurring at the top of the graph to the lease abundant genus occurring towards the bottom. The size of the bubble represents genus abundance. The phylum of each genus is represented by color. (T1= Epi→Hypo; T2= Hypo→Epi; T3= Epi→ Epi; T4=Hypo→Hypo).

Figure 3.10. Bubble plot displaying the cell density found in microcosm samples (T-1, T-2, T-3, T-4, C-1, C-2) on PP and PET. The top 20 most abundant genera found, with the most abundant genus occurring at the top of the graph to the least abundant genus occurring towards the bottom. The size of the bubble represents genus abundance. The phylum of each genus is represented by color. (T1= Epi→Hypo; T2= Hypo→Epi; T3= Epi→ Epi; T4=Hypo→Hypo).

Figure 3.11. Non-metric Multidimensional Scaling (NMDS) of cell density abundance between sample type and treatments. (T1= Epi→Hypo; T2= Hypo→Epi; T3= Epi→ Epi; T4=Hypo→Hypo) (see Table 3.1).

Figure 3.12. Shannon diversity measurements showing the richness and evenness of the algal genera present in samples taken from the lake and MP pellets before and after the microcosm experiment.

Figures

Figure 3.1.

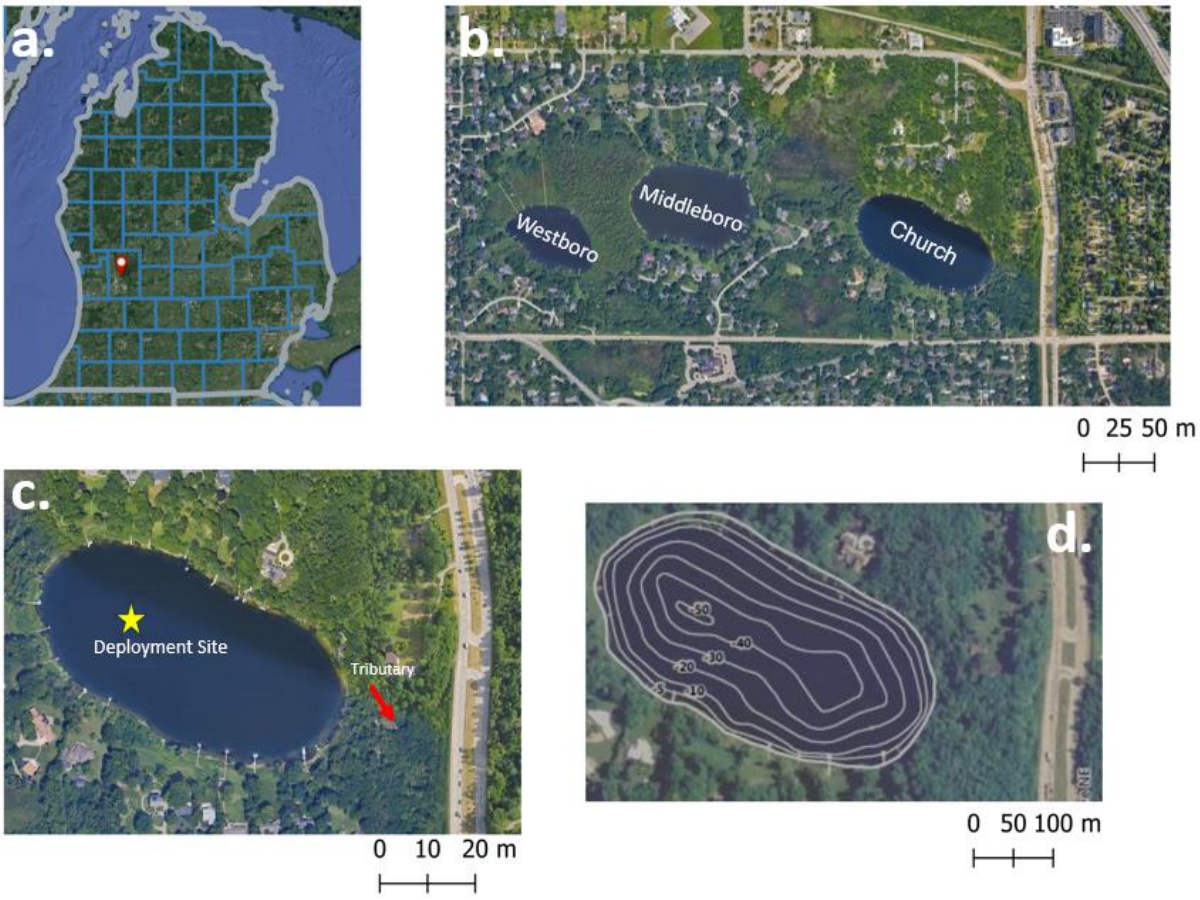

Figure 3.2.

Figure 3.3.

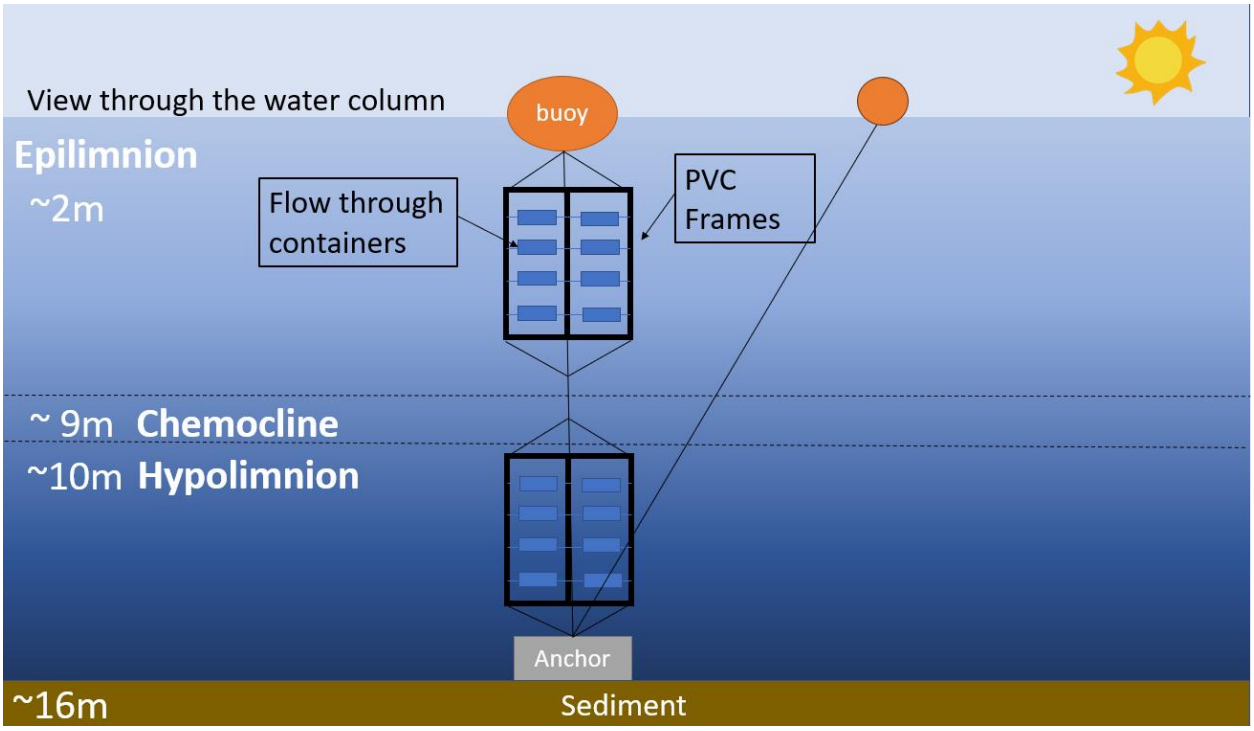
View through the water column
buoy
Epilimnion
~2m
Flow through containers
PVC Frames
~ 9m Chemocline
~10m Hypolimnion
Anchor
~16m
Sediment

Figure 3.4.

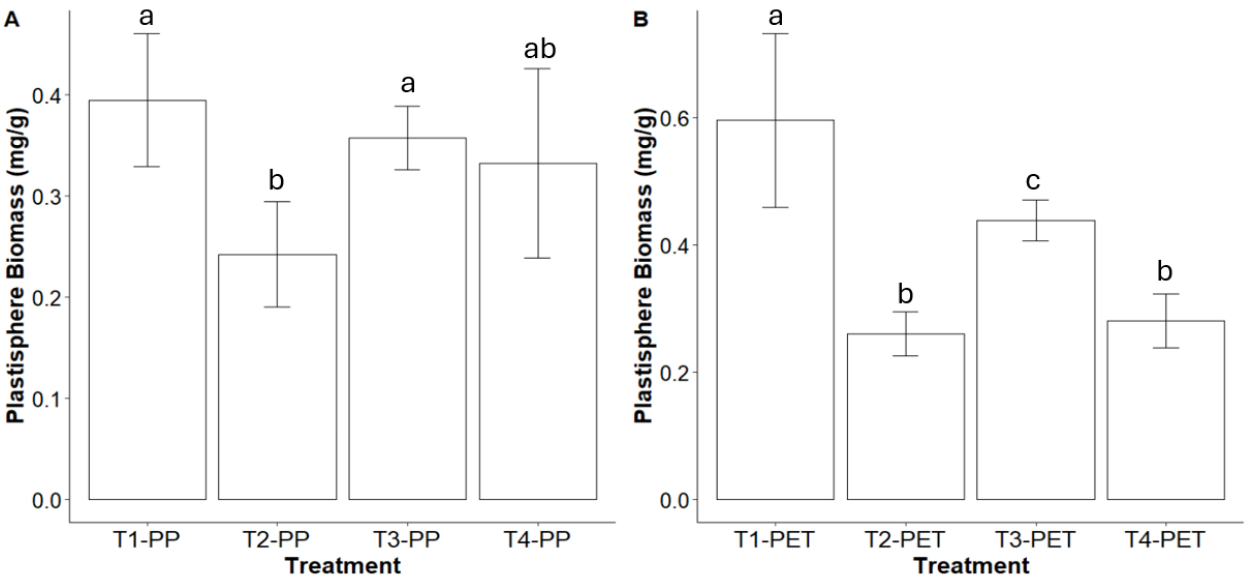
A
a
b
a
ab
Plastisphere Biomass (mg/g)
0.0
0.1
0.2
0.3
0.4
T1-PP
T2-PP
T3-PP
T4-PP
Treatment
B
a
b
c
b
Plastisphere Biomass (mg/g)
0.0
0.2
0.4
0.6
T1-PET
T2-PET
T3-PET
T4-PET
Treatment

Figure 3.5.

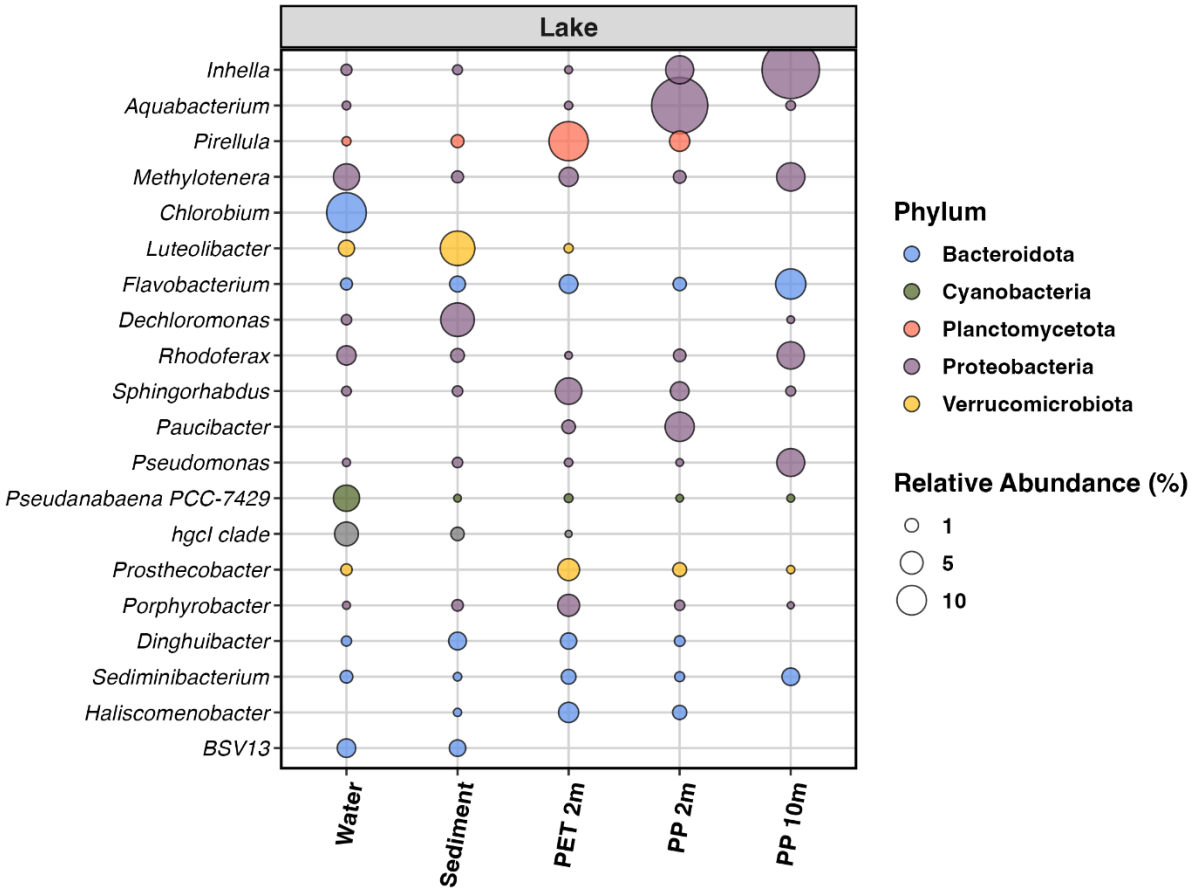
Lake
Inhella
Aquabacterium
Pirellula
Methylotenera
Chlorobium
Luteolibacter
Flavobacterium
Dechloromonas
Rhodoferax
Sphingorhabdus
Paucibacter
Pseudomonas
Pseudanabaena PCC-7429
hgcI clade
Prosthecobacter
Porphyrobacter
Dinghuibacter
Sediminibacterium
Haliscomenobacter
BSV13
Water
Sediment
PET 2m
PP 2m
PP 10m
Phylum
Bacteroidota
Cyanobacteria
Planctomycetota
Proteobacteria
Verrucomicrobiota
Relative Abundance (%)
1
5
10

Figure 3.6.

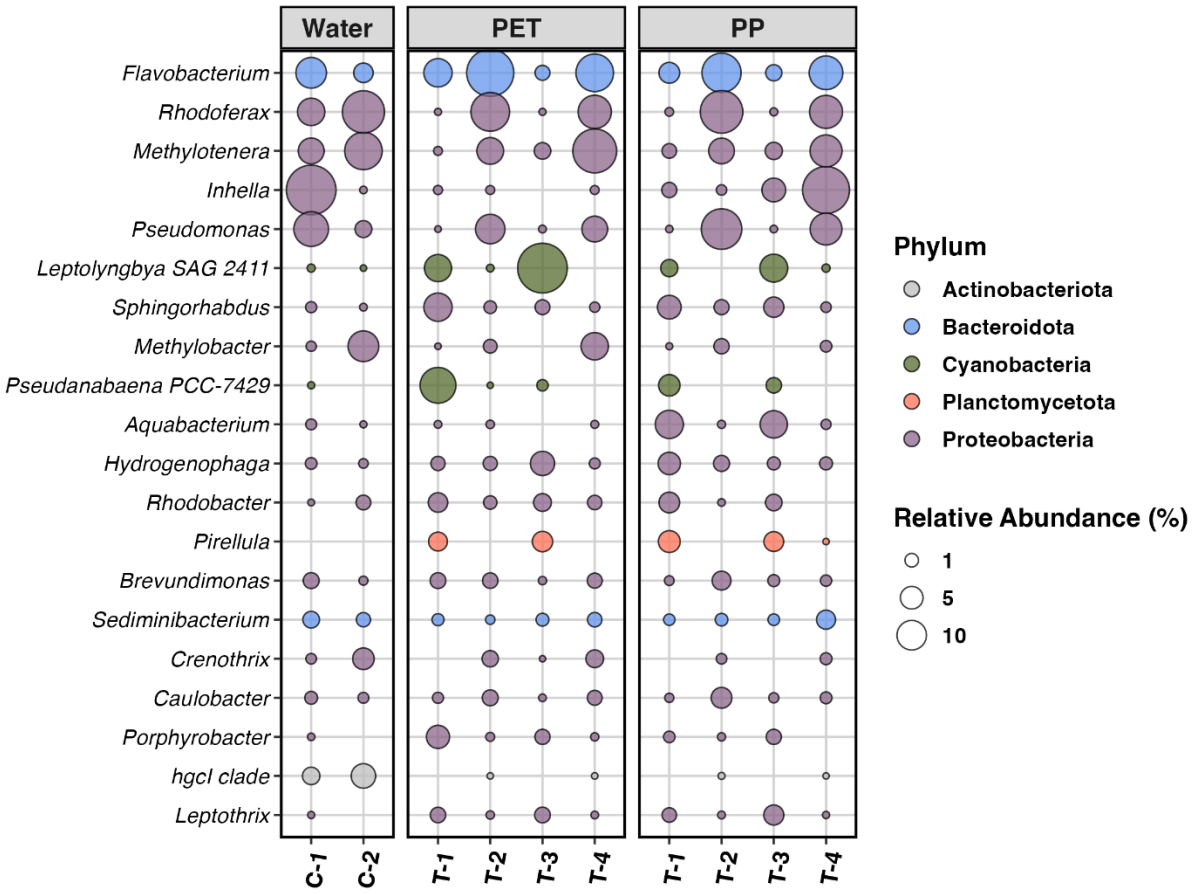
Water
PET
PP
Flavobacterium
Rhodoferax
Methylotenera
Inhella
Pseudomonas
Leptolyngbya SAG 2411
Sphingorhabdus
Methylobacter
Pseudanabaena PCC-7429
Aquabacterium
Hydrogenophaga
Rhodobacter
Pirellula
Brevundimonas
Sediminibacterium
Crenothrix
Caulobacter
Porphyrobacter
hgcI clade
Leptothrix
C-1
C-2
T-1
T-2
T-3
T-4
T-1
T-2
T-3
T-4
Phylum
Actinobacteriota
Bacteroidota
Cyanobacteria
Planctomycetota
Proteobacteria
Relative Abundance (%)
1
5
10

Figure 3.7.

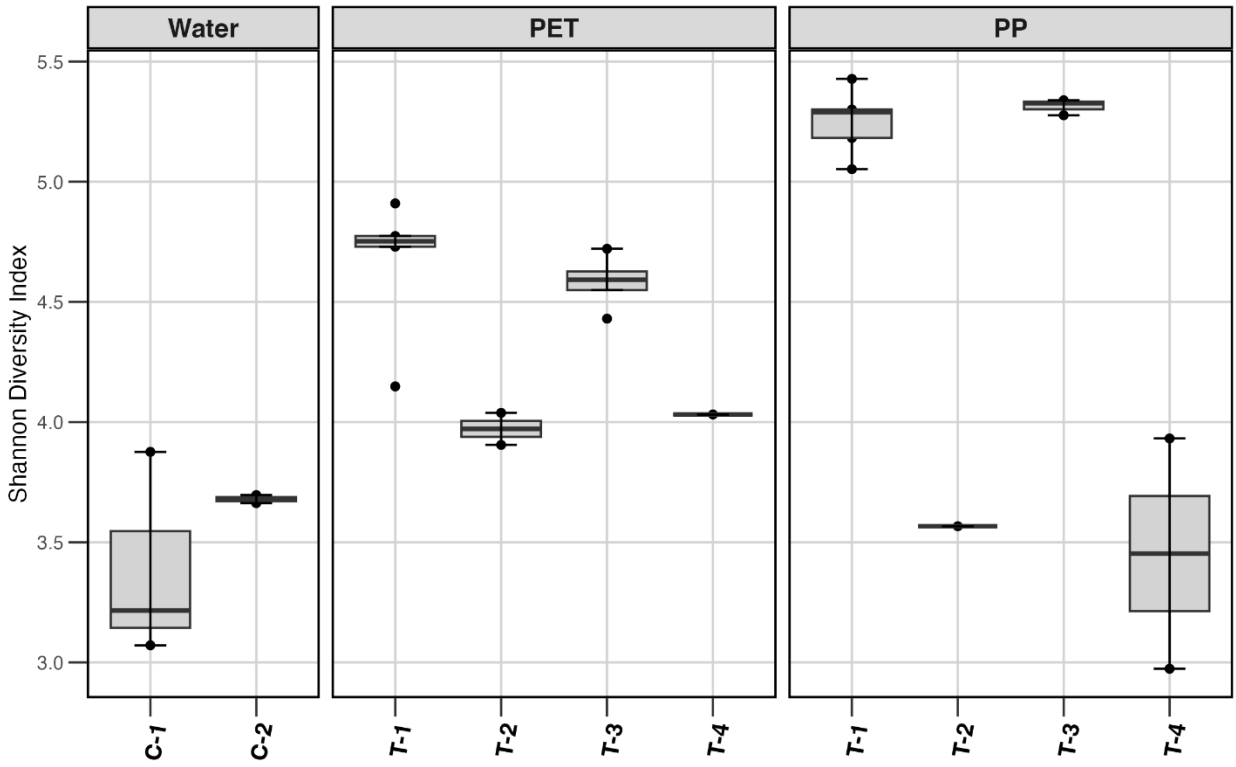
Water
PET
PP
Shannon Diversity Index
5.5
5.0
4.5
4.0
3.5
3.0
C-1
C-2
T-1
T-2
T-3
T-4
T-1
T-2
T-3
T-4

Figure 3.8.

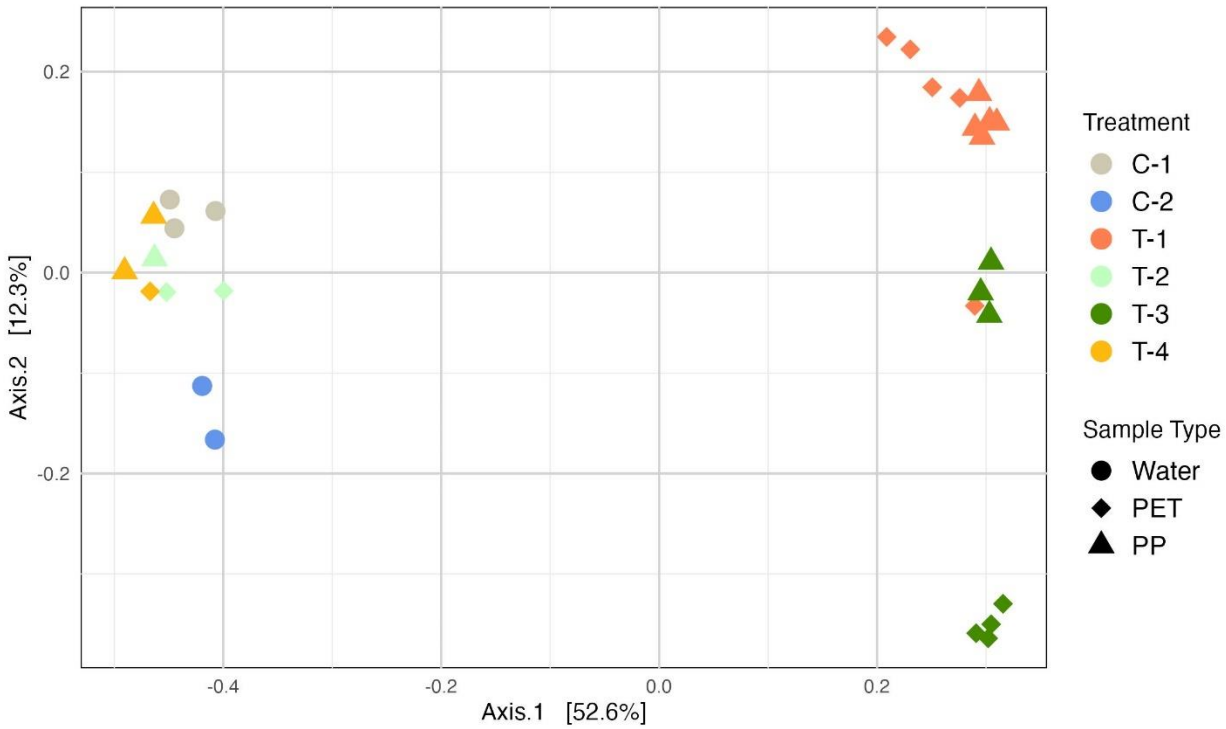
0.2
0.0
-0.2
Axis.2 [12.3%]
-0.4
-0.2
0.0
0.2
Axis.1 [52.6%]
Treatment
C-1
C-2
T-1
T-2
T-3
T-4
Sample Type
Water
PET
PP

Figure 3.9.

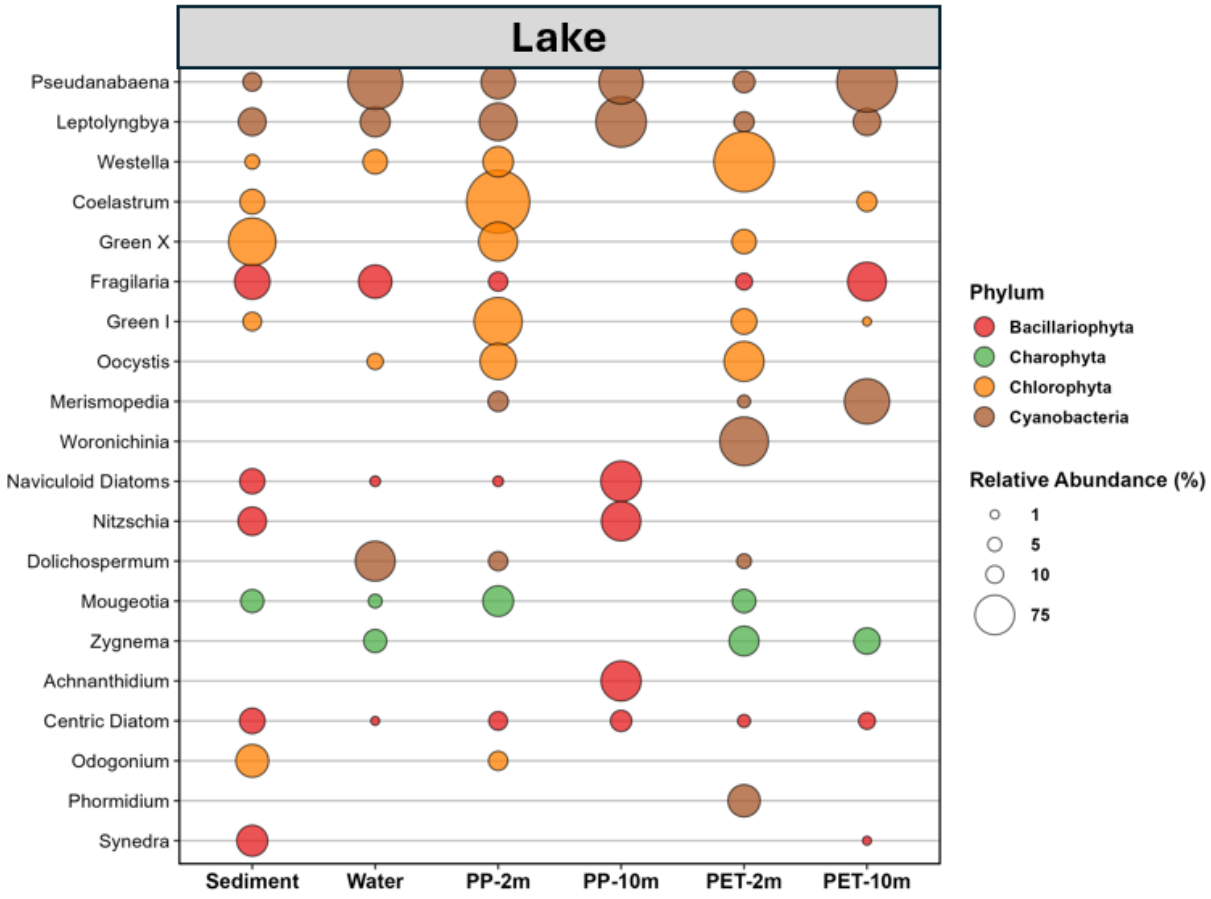
Lake
Pseudanabaena
Leptolyngbya
Westella
Coelastrum
Green X
Fragilaria
Green I
Oocystis
Merismopedia
Woronichinia
Naviculoid Diatoms
Nitzschia
Dolichospermum
Mougeotia
Zygnema
Achnanthidium
Centric Diatom
Odogonium
Phormidium
Synedra
Sediment
Water
PP-2m
PP-10m
PET-2m
PET-10m
Phylum
Bacillariophyta
Charophyta
Chlorophyta
Cyanobacteria
Relative Abundance (%)
1
5
10
75

Figure 3.10.

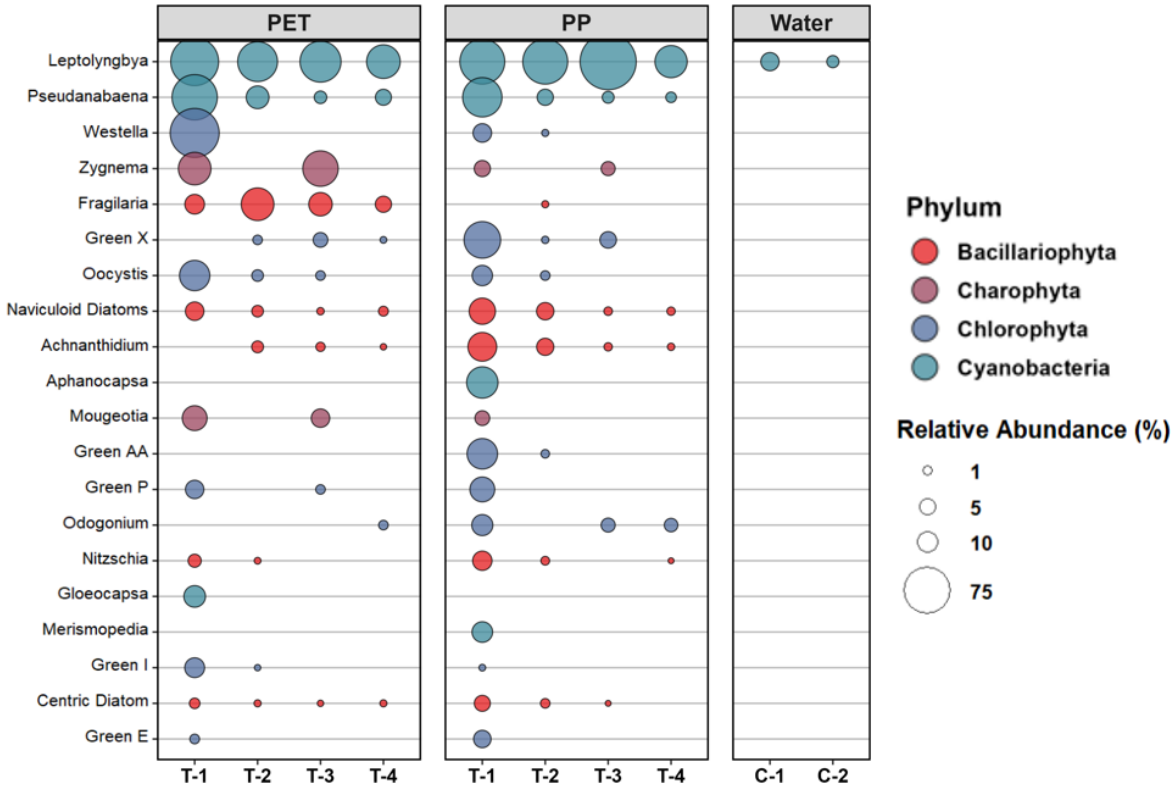
PET
PP
Water
Leptolyngbya
Pseudanabaena
Westella
Zygnema
Fragilaria
Green X
Oocystis
Naviculoid Diatoms
Achnanthidium
Aphanocapsa
Mougeotia
Green AA
Green P
Odogonium
Nitzschia
Gloeocapsa
Merismopedia
Green I
Centric Diatom
Green E
T-1
T-2
T-3
T-4
T-1
T-2
T-3
T-4
C-1
C-2
Phylum
Bacillariophyta
Charophyta
Chlorophyta
Cyanobacteria
Relative Abundance (%)
1
5
10
75

Figure 3.11.

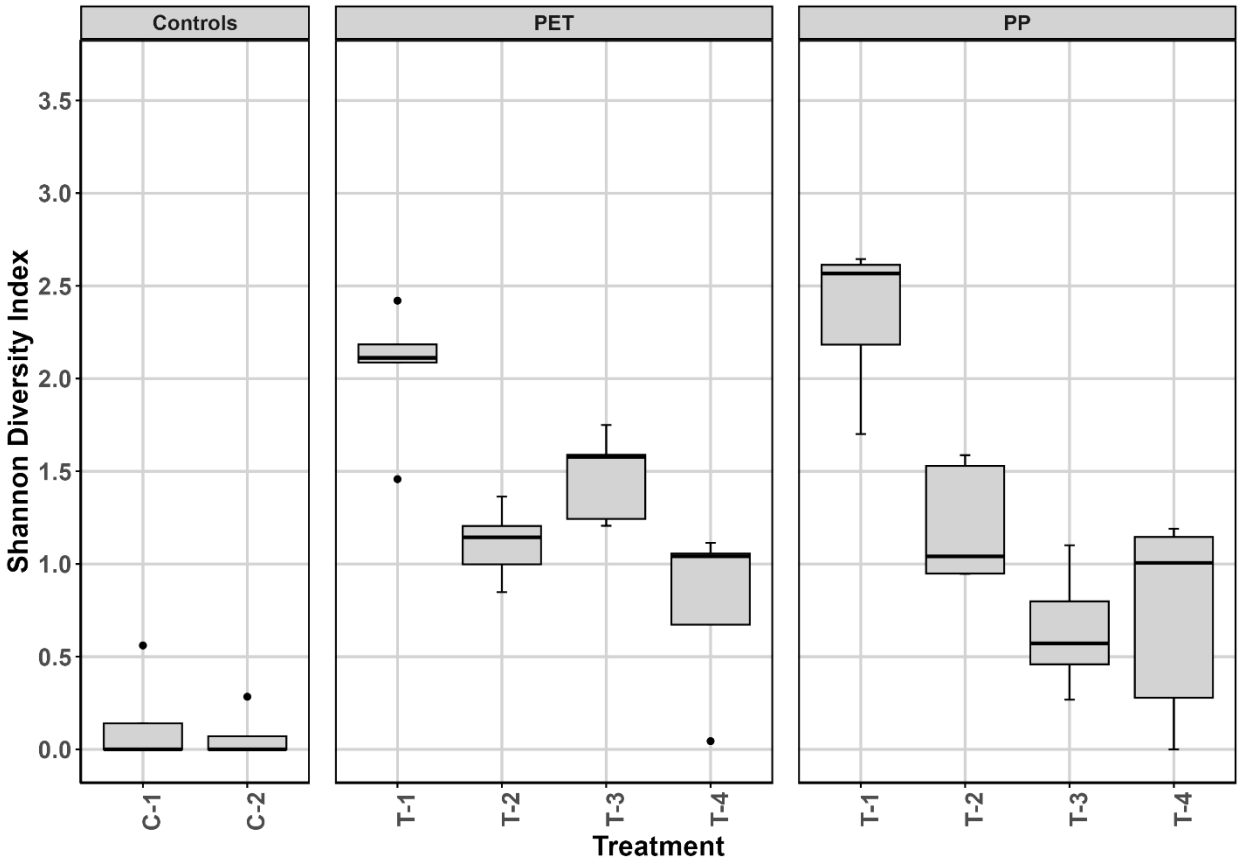
Controls
PET
PP
Shannon Diversity Index
3.5
3.0
2.5
2.0
1.5
1.0
0.5
0.0
C-1
C-2
T-1
T-2
T-3
T-4
T-1
T-2
T-3
T-4
Treatment

Figure 3.12.

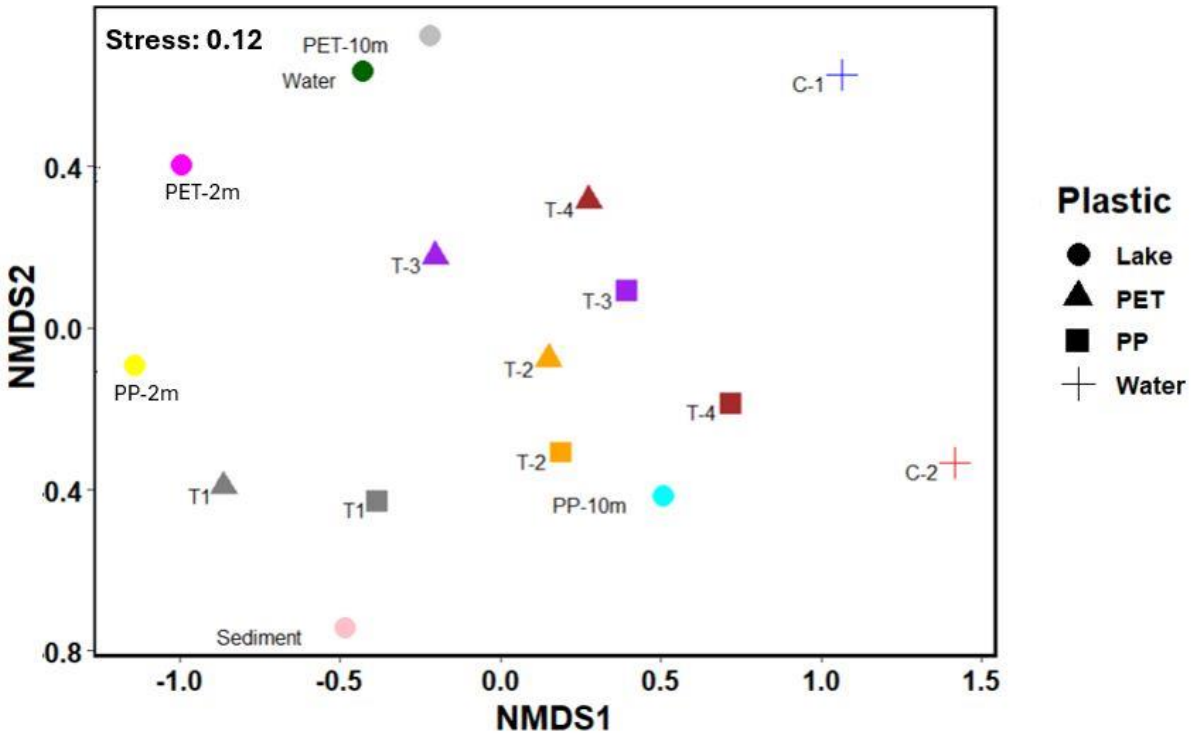
Stress: 0.12
PET-10m
Water
C-1
PET-2m
T-4
T-3
T-3
T-2
PP-2m
T-4
T-2
C-2
T1
T1
PP-10m
Sediment
0.4
0.0
0.4
0.8
-1.0
-0.5
0.0
0.5
1.0
1.5
NMDS2
NMDS1
Plastic
Lake
PET
PP
Water

Appendices

Appendix Table 3.1. DESeq results showed 186 ASVs that were differentially abundant. The following list of ASVs were identified to be more abundant in the epilimnion.

	log2FoldChange	padj	Phylum	Family	Genus
ASV89	1.71	0.0004	Bacteroidota	env.OPS 17	NA
ASV99	1.93	0.0010	Bacteroidota	Sphingobacteriaceae	Solitalea
ASV172	2.18	0.0028	Bdellovibrionota	Bacteriovoracaceae	Peredibacter
ASV39	2.47	0.0016	Proteobacteria	Comamonadaceae	Rhizobacter
ASV138	2.49	0.0017	Verrucomicrobiota	Rubritaleaceae	Luteolibacter
ASV268	2.50	0.0009	Proteobacteria	Caulobacteraceae	NA
ASV18	2.51	1.73E-05	Proteobacteria	Comamonadaceae	Hydrogenophaga
ASV265	2.54	0.0008	Proteobacteria	Sphingomonadaceae	Novosphingobium
ASV555	2.55	0.0041	Proteobacteria	Xanthomonadaceae	Arenimonas
ASV489	2.79	7.91E-06	Hydrogenedentes	Hydrogenedensaceae	NA
ASV414	2.84	0.002	Bacteroidota	LiUU-11-161	NA
ASV455	2.85	5.58E-05	Actinobacteriota	Mycobacteriaceae	Mycobacterium
ASV68	3.00	1.66E-08	Proteobacteria	Rhodobacteraceae	Gemmobacter
ASV25	3.12	1.68E-05	Proteobacteria	Rhodobacteraceae	Rhodobacter
ASV13	3.19	4.05E-09	Proteobacteria	Comamonadaceae	NA
ASV527	3.41	1.50E-07	Bacteroidota	Chitinophagaceae	Edaphobaculum
ASV546	3.47	0.0096	Proteobacteria	Comamonadaceae	Ottowia

ASV262	3.69	0.0001	Proteobacteria	Caulobacteraceae	Phenylobacterium
ASV359	3.70	0.0007	Proteobacteria	Methylophilaceae	Methylophilus
ASV433	3.70	3.24E-05	Proteobacteria	Methylophilaceae	NA
ASV201	3.74	7.35E-05	Proteobacteria	Xanthomonadaceae	Luteimonas
ASV235	3.75	7.06E-08	Proteobacteria	Rhodobacteraceae	NA
ASV1036	3.80	4.00E-06	Armatimonadota	Fimbriimonadaceae	NA
ASV123	3.82	2.55E-08	Verrucomicrobiota	Verrucomicrobiaceae	NA
ASV9	3.83	4.34E-11	Proteobacteria	Sphingomonadaceae	Sphingorhabdus
ASV657	3.89	0.0006	Dependentiae	Vermiphilaceae	NA
ASV361	3.93	0.0001	Bacteroidota	Cytophagaceae	Cytophaga
ASV51	3.94	8.95E-08	Proteobacteria	Beijerinckiaceae	Bosea
ASV62	4.09	5.32E-08	Gemmatimonadota	Gemmatimonadaceae	Gemmatimonas
ASV202	4.17	8.26E-10	Proteobacteria	Rhizobiales Incertae Sedis	NA
ASV820	4.19	0.0001	Bacteroidota	Cyclobacteriaceae	NA
ASV111	4.20	2.14E-11	Verrucomicrobiota	Verrucomicrobiaceae	Brevifollis
ASV363	4.21	7.06E-08	Proteobacteria	Micropepsaceae	NA
ASV660	4.28	2.61E-05	Proteobacteria	Sphingomonadaceae	Sandarakinorhabdus
ASV778	4.28	0.0002	Actinobacteriota	Microbacteriaceae	NA
ASV323	4.29	9.87E-12	Bacteroidota	37-13	NA
ASV948	4.40	4.00E-06	Bdellovibrionota	Bdellovibrionaceae	OM27 clade

ASV709	4.44	0.0003	Patescibacteria	LWQ8	NA
ASV583	4.45	1.38E-06	Bacteroidota	Spirosomaceae	NA
ASV290	4.60	0.0001	Proteobacteria	Comamonadaceae	Caenimonas
ASV933	4.71	1.27E-05	Proteobacteria	Dongiaceae	Dongia
ASV316	4.83	1.34E-11	Verrucomicrobiota	Opitutaceae	Opitutus
ASV21	4.87	1.79E-05	Proteobacteria	Comamonadaceae	Aquabacterium
ASV47	4.87	7.45E-11	Proteobacteria	Hyphomonadaceae	UKL13-1
ASV507	4.89	8.76E-08	Actinobacteriota	Microtrichaceae	IMCC26207
ASV835	4.93	4.87E-05	Proteobacteria	Unknown Family	Candidatus Endonucleariobacter
ASV747	4.95	7.42E-10	Cyanobacteria	Cyanobiaceae	Cyanobium PCC-6307
ASV598	4.98	3.31E-11	Acidobacteriota	Vicinamibacteraceae	Luteitalea
ASV1014	5.00	1.79E-05	Proteobacteria	Xanthobacteraceae	Afipia
ASV96	5.00	9.08E-18	Proteobacteria	Hyphomonadaceae	Hirschia
ASV1003	5.08	2.88E-05	Bdellovibrionota	Oligoflexaceae	NA
ASV335	5.10	1.70E-12	Verrucomicrobiota	DEV007	NA
ASV787	5.14	5.30E-05	Proteobacteria	Moraxellaceae	Cavicella
ASV695	5.14	8.20E-06	Proteobacteria	Comamonadaceae	Azohydromonas
ASV1143	5.18	6.87E-05	Actinobacteriota	Solirubrobacteraceae	NA
ASV764	5.19	4.25E-10	Proteobacteria	Nitrosomonadaceae	Ellin6067
ASV129	5.20	3.61E-15	Proteobacteria	Xanthomonadaceae	Silanimonas

ASV178	5.22	8.51E-17	Bacteroidota	Chitinophagaceae	Aurantisolimonas
ASV605	5.28	1.37E-06	Myxococcota	Haliangiaceae	Haliangium
ASV84	5.37	2.59E-18	Proteobacteria	Devosiaceae	Devosia
ASV362	5.38	5.40E-19	Proteobacteria	Acetobacteraceae	Roseomonas
ASV66	5.44	2.48E-26	Proteobacteria	Comamonadaceae	Leptothrix
ASV358	5.44	3.93E-10	Proteobacteria	Sphingomonadaceae	Sphingopyxis
ASV345	5.45	1.16E-07	Planctomycetota	Gemmataceae	Zavarzinella
ASV487	5.47	3.91E-18	Proteobacteria	Beijerinckiaceae	NA
ASV253	5.52	1.87E-07	Proteobacteria	Sphingomonadaceae	SD04E11
ASV594	5.60	1.13E-09	Bacteroidota	Saprospiraceae	Lewinella
ASV639	5.61	4.86E-12	Acidobacteriota	Blastocatellaceae	Stenotrophobacter
ASV586	5.68	7.53E-07	Proteobacteria	Pseudohongiellaceae	BIyi10
ASV738	5.70	6.41E-08	Myxococcota	BIrii41	NA
ASV15	5.70	1.24E-12	Proteobacteria	Sphingomonadaceae	Porphyrobacter
ASV75	5.72	7.42E-19	Bacteroidota	Chitinophagaceae	Dinghuibacter
ASV1085	5.75	1.74E-16	Proteobacteria	Legionellaceae	Legionella
ASV582	5.78	1.13E-09	Acidobacteriota	Blastocatellaceae	JGI 0001001-H03
ASV296	5.78	3.20E-14	Proteobacteria	Rhizobiales Incertae Sedis	Phreatobacter
ASV649	5.79	4.18E-09	Verrucomicrobiota	Pedosphaeraceae	DEV114
ASV567	5.83	1.34E-09	Deinococcota	Deinococcaceae	NA

ASV646	5.85	2.52E-06	Proteobacteria	Burkholderiaceae	Limnobacter
ASV608	5.89	9.15E-07	Proteobacteria	Micavibrionaceae	NA
ASV44	5.95	2.75E-19	Proteobacteria	Rhodanobacteraceae	Aquimonas
ASV12	6.00	7.56E-18	Bacteroidota	Saprospiraceae	NA
ASV786	6.07	3.63E-12	Proteobacteria	Rhodospirillaceae	NA
ASV539	6.08	1.88E-11	Proteobacteria	Sphingomonadaceae	Blastomonas
ASV139	6.11	2.71E-14	Proteobacteria	Rhodocyclaceae	Methyloversatilis
ASV458	6.14	4.45E-16	Proteobacteria	Rhizobiales Incertae Sedis	Alsobacter
ASV558	6.15	2.44E-13	Verrucomicrobiota	Opitutaceae	IMCC26134
ASV609	6.21	2.59E-16	Proteobacteria	TRA3-20	NA
ASV492	6.24	2.37E-08	Cyanobacteria	Leptolyngbyaceae	Chamaesiphon PCC-7430
ASV50	6.25	1.03E-12	Proteobacteria	Sphingomonadaceae	Parablastomonas
ASV266	6.26	9.42E-19	Proteobacteria	Halieaceae	OM60(NOR5) clade
ASV173	6.29	5.05E-30	Proteobacteria	Hyphomonadaceae	Hyphomonas
ASV152	6.31	1.63E-13	Proteobacteria	Sphingomonadaceae	NA
ASV297	6.32	4.78E-15	Proteobacteria	Caulobacteraceae	Asticcacaulis
ASV456	6.33	6.48E-12	Proteobacteria	Devosiaceae	NA
ASV91	6.37	3.55E-12	Proteobacteria	Solimonadaceae	Nevskia
ASV519	6.40	2.12E-09	Bacteroidota	Spirosomaceae	Runella
ASV449	6.40	4.81E-14	Proteobacteria	Comamonadaceae	Acidovorax

ASV351	6.48	1.51E-16	Verrucomicrobiota	Pedosphaeraceae	NA
ASV114	6.58	2.01E-05	Proteobacteria	Sphingomonadaceae	Sphingobium
ASV600	6.64	4.90E-08	Proteobacteria	Diplorickettsiaceae	Aquicella
ASV82	6.68	8.00E-23	Bacteroidota	NS9 marine group	NA
ASV397	6.69	7.09E-09	Proteobacteria	Nitrosomonadaceae	DSSD61
ASV404	6.69	1.86E-13	Planctomycetota	WD2101 soil group	NA
ASV87	6.75	6.78E-16	Verrucomicrobiota	Chthoniobacteraceae	Chthoniobacter
ASV384	6.77	2.11E-14	Proteobacteria	Sphingomonadaceae	Sandaracinobacter
ASV343	6.95	2.23E-11	Bacteroidota	Microscillaceae	Hassallia
ASV503	6.96	8.30E-24	Acidobacteriota	Bryobacteraceae	Bryobacter
ASV304	7.01	2.67E-09	Proteobacteria	Solimonadaceae	Hydrocarboniphaga
ASV734	7.08	8.34E-19	Proteobacteria	Steroidobacteraceae	NA
ASV441	7.22	4.35E-12	Proteobacteria	SM2D12	NA
ASV287	7.23	1.05E-13	Proteobacteria	Sutterellaceae	AAP99
ASV365	7.25	1.38E-28	Bacteroidota	Chitinophagaceae	NA
ASV488	7.27	1.46E-14	Myxococcota	Sandaracinaceae	NA
ASV474	7.28	1.04E-12	Verrucomicrobiota	Opitutaceae	Lacunisphaera
ASV186	7.32	5.11E-24	Proteobacteria	Rhizobiaceae	NA
ASV459	7.33	1.02E-08	Cyanobacteria	Cyanobacteriaceae	Geitlerinema LD9
ASV299	7.34	3.82E-34	Proteobacteria	Hyphomicrobiaceae	Hyphomicrobium

ASV73	7.37	6.04E-31	Proteobacteria	Comamonadaceae	Ideonella
ASV308	7.39	3.46E-11	Proteobacteria	Nitrosomonadaceae	966-1
ASV275	7.50	2.48E-12	Acidobacteriota	Blastocatellaceae	Blastocatella
ASV241	7.52	2.22E-23	Proteobacteria	KI89A clade	NA
ASV238	7.52	2.13E-10	Actinobacteriota	Microbacteriaceae	Cryobacterium
ASV385	7.54	6.98E-16	Myxococcota	Phaselicystidaceae	Phaselicystis
ASV246	7.55	4.12E-13	Proteobacteria	Sphingomonadaceae	Sphingomonas
ASV219	7.64	1.92E-13	Proteobacteria	Beijerinckiaceae	FukuN57
ASV30	7.68	6.78E-60	Proteobacteria	Rhodobacteraceae	Tabrizicola
ASV170	7.71	2.10E-33	Planctomycetota	Rubinisphaeraceae	NA
ASV236	7.77	3.80E-16	Myxococcota	Nannocystaceae	Nannocystis
ASV303	7.92	3.88E-22	Proteobacteria	Comamonadaceae	Rubrivivax
ASV270	7.98	1.04E-12	Proteobacteria	Hyphomicrobiaceae	Pedomicrobium
ASV240	7.99	1.74E-17	Bacteroidota	Chitinophagaceae	Lacibacter
ASV191	7.99	3.31E-11	Proteobacteria	Rhizobiaceae	Mesorhizobium
ASV130	8.00	1.03E-31	Planctomycetota	Pirellulaceae	NA
ASV23	8.00	3.61E-47	Bacteroidota	Saprospiraceae	Haliscomenobacter
ASV146	8.02	3.16E-25	Proteobacteria	Comamonadaceae	Piscinibacter
ASV183	8.09	1.02E-14	Bdellovibrionota	Oligoflexaceae	Oligoflexus
ASV228	8.24	1.60E-23	Proteobacteria	Reyranellaceae	Reyranella

ASV153	8.45	1.22E-10	Proteobacteria	Comamonadaceae	Pseudorhodoferax
ASV279	8.48	5.69E-27	Planctomycetota	Rubinisphaeraceae	SH-PL14
ASV258	8.49	5.77E-29	Verrucomicrobiota	Pedosphaeraceae	SH3-11
ASV381	8.55	1.95E-24	Bacteroidota	Chitinophagaceae	Terrimonas
ASV211	8.61	9.82E-24	Proteobacteria	A0839	NA
ASV179	8.69	2.95E-30	Bacteroidota	Saprospiraceae	Phaeodactylibacter
ASV56	8.75	1.40E-62	Bacteroidota	Microscillaceae	OLB12
ASV147	8.77	4.42E-26	Gemmatimonadota	Gemmatimonadaceae	NA
ASV196	8.82	3.28E-32	Proteobacteria	Unknown Family	Acidibacter
ASV150	8.82	4.56E-29	Cyanobacteria	Leptolyngbyaceae	Calothrix KVSF5
ASV4	8.97	3.54E-23	Cyanobacteria	Leptolyngbyaceae	Leptolyngbya SAG 2411
ASV159	8.98	7.64E-30	Verrucomicrobiota	Pedosphaeraceae	Oikopleura
ASV104	9.00	3.71E-12	Planctomycetota	Schlesneriaceae	Planctopirus
ASV276	9.16	5.05E-30	Proteobacteria	Hyphomonadaceae	SWB02
ASV76	9.27	4.48E-22	Proteobacteria	Unknown Family	Candidatus Berkiella
ASV74	9.29	2.66E-17	Proteobacteria	Nitrosomonadaceae	NA
ASV98	9.31	3.25E-30	Acidobacteriota	Vicinamibacteraceae	NA
ASV148	9.37	5.93E-18	Cyanobacteria	Chamaesiphonaceae	Chamaesiphon PCC-6605
ASV122	9.48	1.71E-28	Bdellovibrionota	Bdellovibrionaceae	Bdellovibrio
ASV102	9.61	2.47E-74	Planctomycetota	Pirellulaceae	Pirellula

ASV80	9.66	5.05E-30	Planctomycetota	Pirellulaceae	Rhodopirellula
ASV109	10.00	9.99E-40	Bacteroidota	Microscillaceae	NA
ASV72	10.06	4.31E-30	Proteobacteria	Nitrosomonadaceae	oc32
ASV36	10.36	5.98E-18	Proteobacteria	Comamonadaceae	Methylibium
ASV26	10.54	4.85E-15	Proteobacteria	Devosiaceae	Arsenicitalea
ASV20	10.55	3.21E-25	Proteobacteria	Rhodanobacteraceae	NA
ASV6	10.70	6.42E-33	Cyanobacteria	Pseudanabaenaceae	Pseudanabaena PCC-7429
ASV14	11.82	1.64E-32	Cyanobacteria	Leptolyngbyaceae	NA

Chapter 4: Phosphorus Net Flux by the Plastisphere in a Salinized Eutrophic Suburban Lake

Abstract

Stormwater runoff from homes and highways is a route for transferring excessive nutrients, deicing salt, and even microplastics from land-based sources to the aquatic environment. Microplastics (MPs) quickly become colonized by microbes during their transit; this microbial population is referred to as the plastisphere. However, the impacts of the plastisphere on biogeochemical cycles are poorly understood. My research examines the influence of the plastisphere on phosphorus (P) dynamics in Church Lake (MI), a salt-impacted lake with very different P concentrations in the epilimnion and hypolimnion. To achieve this, I incubated unweathered MPs in Church Lake in retrievable flow-through containers to promote biofilm formation on two common polymers: polypropylene (PP) and polyethylene terephthalate (PET). After incubation, MPs were brought back to the lab and were exposed to a set of controlled environmental conditions. The experimental design consisted of two treatments: 1) MPs incubated in the low P, low salinity, high light epilimnion of Church Lake, retrieved and then in the lab, grown in either its ambient water or placed in water from the hypolimnion, which is high P, high salinity, and low light; and 2) the reverse treatment using microplastics incubated in the hypolimnion of Church Lake, and placed in either ambient conditions or epilimnetic water in the lab. My goal was to test the role of lake salinity and P content on P uptake by the plastisphere, given the very high P concentrations in the bottom waters of Church Lake. The results showed no significant impact of polymer type on SRP or TP uptake rates, indicating that environmental conditions, biofilm community structure, and biofilm P uptake capacity were more influential. Microbial communities on MPs in the

hypolimnion exhibited a trend of SRP/TP uptake, while SRP/TP concentrations increased with MPs from epilimnetic lab conditions. Overall, P uptake by MPs in the lake was minimal, suggesting that MPs do not significantly affect P dynamics, even during lake turnover.

Introduction

In 2013, Zettler et al. (2013) first coined the term plastisphere to describe the community of microorganisms (i.e., biofilm) that colonize plastic debris in aquatic environments. Microplastics (MPs) are hydrophobic and persist in the environment for hundreds of years making them ideal substrates for microorganisms (Zettler et al., 2013). Biofilm communities play a key role in cycling materials and energy in aquatic ecosystems (Chen et al., 2020). Biofilms coating substrates are composed of bacteria, fungi, algae, and protozoans (He et al., 2021). Some of these microorganisms produce enzymes that break down polymers, while others consume mineralized nutrients, working in synergistic or commensalistic relationships within the biofilm community (Yuan et al., 2020). This cycle of organic matter mineralization and nutrient uptake allows for the efficient cycling of nutrients in aquatic ecosystems, especially when systems are nutrient limited (cf. Mulholland et al., 1991). Biofilm nutrient cycling can be important to help reduce nutrient pollution and improve water quality (Dodds 2003).

Biofilm communities produce a protective matrix of extracellular polymeric substances (EPS) (He et al., 2021). The matrix is composed of DNA, proteins, lipids, and lipopolysaccharides, creating a sticky adhesion of biofilm (He et al., 2021). The EPS acts as a buffer against potential environmental stressors (e.g., temperature, pH, nutrient availability) (He et al., 2021) and aids nutrient adsorption (Tan et al., 2023). Biofilm communities are influenced by flow, nutrients,

temperature, light, salts, herbivory, and pH (Chen et al., 2020). When stressors occur in the environment, they can disrupt the balance of microorganisms within the biofilm, leading to a potential decrease in nutrient cycling efficiency and biodiversity (Chen et al., 2020; Diaz et al., 2022; He et al., 2021).

Common and emerging stressors found in freshwater lakes are eutrophication and salinization, respectively. Excessive nutrient loading from anthropogenic sources (e.g., agricultural, urban, and industrial developments) has caused declines in the water quality of freshwater ecosystems (Lind et al., 2018). Phosphorus (P) and nitrogen (N) are the primary nutrients from anthropogenic sources that cause water quality impairments (Diaz et al., 2022). Excessive loading of nutrients in water bodies leads to eutrophication; elevated levels of P and N in water bodies also can stimulate algal blooms. In response, submerged aquatic vegetation in littoral zones can experience reduced growth and die-offs because the algal blooms decrease sunlight penetration in the water. Decreased light penetration also reduces the success rate of visual predators who need light to hunt prey. Eutrophication-related primary production can lead to photosynthetically induced decreases in dissolved inorganic carbon and increases in pH during the daytime (Turner, 2010). Microbial-mediated mineralization of organic matter and associated respiration reduces dissolved oxygen levels and produces carbon dioxide when the dense algal blooms start to die and settle to the lake bottom. This process can create hypoxic (< 2 mg/L DO) or anoxic (<0.1 mg/L) zones that have insufficient oxygen to support many organisms. Many lakes, including portions of the Laurentian Great Lakes, experience hypoxia or anoxia during summer from eutrophication (Arend et al., 2011; Biddanda et al., 2018), and can create conditions that lead to continued anoxia over time (Lewis et al. 2023).

Eutrophication can result in MPs becoming coated with biofilms at a faster rate than lower-nutrient systems, and also lead to a more diverse microbial community, including microbial taxa that can preferentially enhance human pathogens (Numberger et al., 2022). Furthermore, biofilm formation can alter the density of microplastics, causing those with densities greater than water to sink rather than to stay suspended in the water column (Qiang et al., 2021).

In the colder areas of the United States, deicing salts are commonly used on roads during winter to reduce traffic accidents. During snow melts, high concentrations of chloride (Cl^-) enter freshwater ecosystems that may exceed US EPA thresholds (chronic = 230 mg/L) (Lind et al., 2018). The combination of eutrophication and deicing salts in impaired lakes can profoundly influence the aquatic biota. Lind et al. (2018) studied the combined effects of eutrophication and deicing salts on freshwater communities. Their work showed that the combined impacts, though affecting aquatic ecosystems via different mechanisms, promote large phytoplankton and periphyton blooms while causing declines in invertebrates and macrophytes. In accordance with other studies, salinity is a key abiotic factor affecting species richness in freshwater lakes (Larson and Belovsky, 2013; Niu et al., 2022). Some organisms are physiologically unable to survive the osmotic stress caused by salt and are outcompeted by less sensitive species. Despite the ecological adaptations and metabolic trade-offs of complex biofilm formation, the influence of excess nutrients and salinity on the plastisphere, as well as the reciprocal influence of the plastisphere on these stressors, is unknown. Further studies are required to understand the influence of MPs and their attached communities in freshwater ecosystems.

My study addresses plastisphere-mediated P dynamics in Church Lake. This site is a salinized eutrophic lake, which has experienced years of exposure to highway deicing salts and fertilizers. I examined if microbial communities growing on MPs in Church Lake are removing P, and if so, is there a difference between 1) plastisphere communities growing on different polymers (i.e., PP vs. PET) and 2) plastisphere communities exposed to high phosphorus and salinity (as is found in Church Lake's hypolimnion) vs. those exposed to low phosphorus and salinity (as is found in Church Lake's epilimnion)? To do this, I placed MPs in retrievable flow-through containers in Church Lake to encourage biofilm production (Steinman et al. 2020), brought the MPs back to the lab, and subjected them to a series of treatments under controlled environmental conditions, measuring biofilm biomass and P dynamics. Specifically, the MP-attached biofilms were grown under either their ambient conditions (i.e., epilimnetic-grown biofilm exposed to epilimnetic water and hypolimnetic-grown biofilm exposed to hypolimnetic water), or a reversed scenario, where epilimnetic-grown biofilms were exposed to hypolimnetic water and hypolimnetic-grown biofilms were exposed to epilimnetic water, to mimic what might happen if Church Lake underwent a complete mixing event.

I hypothesized the following: 1) microbial communities growing on MPs in their native environment and then exposed to the same environment in the lab will have greater absolute P uptake in low-salinity (epilimnion) vs. high-salinity conditions (hypolimnion) due to greater abundance and greater P uptake per unit biomass because of less salinity stress; and 2) microbial communities transferred from hypolimnion to epilimnion and vice versa will decline in P uptake compared to control systems. However, the decline will be greater in communities

transferred from the epilimnion to the hypolimnion than the hypolimnion to the epilimnion because of the sudden shock to salinity in the hypolimnetic environment.

Methods

Study site

The sampling occurred in Church Lake, an urban lake located in Kent County, Grand Rapids, Michigan (Figure 4.1). The lake represents one of three lakes connected through marshy wetlands and groundwater in this area (Molloseau and Steinman, unpubl. data). Church Lake spans 7.7 hectares and has a maximum depth of ~ 16.5m. Runoff from a major highway (East Beltline) flows into an unnamed tributary that enters the east side of Church Lake. The deepest region of the lake, approximately 3-5% of total lake volume, does not seasonally mix due to a chemocline (~9m) that has formed from deicing salt runoff from the East Beltline highway (Foley and Steinman, 2023).

Microplastic Type

I used two polymers in this experiment: polypropylene (PP) and polyethylene terephthalate (PET). PP is found in auto parts and food containers while PET is found in textiles and water bottles. PP and PET are the most common polymers found in urban areas (Driedger et al., 2015; Lutz et al., 2021). I sourced PP and PET pellets from Plastic Pellets 4 Fun (High Point, NC). The bulk material was sieved, resulting in a size range of 2– 4 mm.

Incubation: Frame Deployment and Retrieval

I placed unweathered MPs in flow-through tubes based on a design by Steinman et al. (2020), allowing biofilms to grow on the MPs (Figure. 4.2). I placed ~46 g of MP pellets in each

incubation tube. The incubation tubes are made from Harvel Clear^{TM} Rigid PVC (outer diameter of 7.62 cm) cut into 15 cm-long sections. I drilled six evenly spaced holes (5 cm diameter) along the sides of the tubes to allow for the passage of lake water. The section holding the microplastics is made of a clear PVC pipelined with stainless steel wire cloth (mesh size 1 mm) forming a sleeve. The wire cloth prevented microplastics from leaving incubation tubes. I placed clear PVC slip caps on the ends of each incubation tube and then inserted a 0.64 cm threaded rod in the center of each tube and through holes drilled in the center of each slip cap. Washers and metal locknuts secured both the slip cap and an automotive brake line tab to both sides of each tube. The assembled incubation tube was attached via the brake line tab to double loop chains along each attachment frame with a metal quick link. The chains allow the incubation tubes to move with wave motion while still attached to the frame and for easy removal at the end of deployment (Steinman et al., 2020).

I deployed the frames in June of 2022 during the growing season and retrieved them two weeks after deployment. The deployment period was selected because microbial communities grow quickly (Wang et al., 2020), making it unnecessary to leave frames out longer than two weeks. Frames were attached to a buoy and deployed at ~2-m (oxic) and 10-m (hypoxic) depths at a site used in a prior study (Figures. 4.1, 4.2; Foley and Steinman, 2023). I chose the deployment depths to examine the effect of salinity and phosphorus on microbial community structure and function; MPs in tubes near the lake surface were exposed to lower salinity water, higher light, higher levels of dissolved oxygen, and lower mean conductivity and phosphorus concentrations (see below) compared to those deployed deeper (Table 4.2; see also Foley and Steinman, 2023).

I removed and filtered 72 L of lake water (36 L from each depth) to use in the laboratory experiment. Zooplankton and other floating organisms were removed from the epilimnion and the hypolimnion by a two-step sequential filtration process first using 1 µm filters, followed by 0.2 µm filters (Watertec QMC1-10NPCS and 0.2-10NPCS, respectively). After the two-week incubation period, lake water was collected from the 2-m and 10-m depths via Van Dorn samplers to measure microbial community structure, conductivity, total phosphorus (TP), and soluble reactive phosphorus (SRP).

Water Chemistry

I measured the following water quality parameters at each sampling event: water temperature, pH, dissolved oxygen (DO), specific conductivity (Sp Cond), total dissolved solids (TDS), and turbidity, using a Yellow Springs Instruments (YSI) EXO multi-sensor sonde. I estimated chloride concentrations from conductivity using the equation y=0.296x-184 (r^2= 0.92; n=51), established previously at this site (Foley and Steinman, 2023).

Laboratory Experiment

The laboratory (microcosm) experiment involved the collection of MPs incubated at the 2-m and 10-m depths in Church Lake, which were then placed in 1-L beakers in the lab under the environmental conditions present at either 1) the water and depth at which they were collected or 2) the water and conditions at the alternate depth. This design allowed us to examine the responsiveness of the biofilm to new environmental conditions should the lake fully turn over in the future. Environmental conditions from prior sampling efforts defined the conditions in the microcosms. Conditions at the deployment site in the epilimnion during summer included: average water temperature of 16 °C; mean irradiance of 190 µmol/m^2/s;

mean conductivity of 865 µS/cm; and mean SRP and TP concentrations of 5 µg/L and 13 µg/L, respectively. Light levels in the growth chamber were lower than ambient conditions because of bulb limitations, resulting in an irradiance of ~34.5 µmol/m^2/s. Conditions in the hypolimnion had mean water temperature of 5°C; mean irradiance of 0.03 µmol/m^2/s; mean conductivity: 1315 µS/cm; and mean SRP and TP concentrations of 500 and 450 µg/L, respectively. Iron in the water samples collected in Church Lake's hypolimnion interfered during TP analysis, resulting in lower TP than SRP values in treatments receiving hypolimnetic water. Following digestion, the samples showed obvious floc and an orange tint. Similar problems have previously affected TP and SRP sampling from prior Church Lake research (Brian Scull, pers. comm.). Given that TP cannot be less than SRP in nature, I replaced the 450 µg/L value with 500 µg/L, which is equivalent to the SRP concentration and the minimum possible value for TP and provides a conservative estimate for the starting concentration in the hypolimnion.

The experimental design consisted of six different treatments. One-L beakers served as the experimental units. Each beaker contained 750 mL of filtered water (two-step sequential filtration:1 µm filter-Watertec QMC1-10NPCS and 0.2 µm filter-0.2-10NPCS) from Church Lake. The six treatment groups included (Table 4.1): Treatment group 1 (T-1) had MPs incubated in the lake epilimnion under ambient conditions (mean temperature: 16 °C; mean irradiance: 190 µmol/m^2/s; mean conductivity: 865 µS/cm; mean SRP and TP: ~5 and ~13 µg/L) transferred to hypolimnetic water and maintained at summer hypolimnetic conditions (mean temperature: 5°C; mean irradiance: 0.03 µmol/m^2/s; mean conductivity: 1315 µS/cm; mean SRP ~500 and TP ~500 µg/L) in the growth chamber. Treatment group 2 (T-2) had MPs incubated in the lake hypolimnion and transferred to epilimnetic water in the growth chamber. Treatment group 3

(T-3) had MPs incubated in the lake epilimnion and transferred to epilimnetic water in the growth chamber. Treatment group 4 (T-4) had MPs incubated in the lake hypolimnion and transferred to hypolimnetic water in the growth chamber. Control group one (C-1) had no MPs added to epilimnetic water, put in low light conditions. Control group 2 (C-2) had no MPs added to hypolimnetic water, put in high light conditions. The four treatments with MPs had 5 replicates each and the 2 control treatments (no MPs) had 4 replicates each. This design was conducted for each of the two polymers being used in the experiment. Hence, a total of 48 beakers were used ([5 reps × 4 MP treatments] × 2 polymer types) + [4 reps × 2 controls]). Changes in the control treatments were subtracted from changes in the treatments to account for the possible influence of any non-biofilm related changes except for AFDM.

Beakers were placed in environmental growth chambers that coincided with each treatment's environmental factors. Photoperiod was set at a 15:9 light: dark cycle for treatments simulating epilimnetic conditions (i.e., treatment #'s 2, 3, C-2; Table 4.1) to reflect ambient conditions; treatments simulating hypolimnetic conditions (i.e., 1, 4, C-1; Table 4.1) were kept in the dark.

TP and SRP Analysis

Approximately 40 mL of water from each beaker was subsampled for TP and SRP analysis at the start (Day 0), halfway (Day 12), and at the end of the laboratory experiment (day 25), accounting for a total reduction in volume of 12%. I did not replace the subsampled water to minimize alteration of the salinity and phosphorus concentrations. Every beaker in each treatment and control group was covered with plastic wrap to minimize evaporation, DO was introduced to each beaker by pipetting a known volume of air every two days. A separate test

showed that this level of pipetting did not alter the anoxic environment in the hypolimnetic treatments. SRP (USEPA Method 365.1) and TP (USEPA Method 365. 1 Rev. 2.0 [1993]) were analyzed following standard methods protocols on a Seal Autoanalyzer (SEAL Analytical, Mequon, Wisconsin). These included a 20-ml unfiltered sample for TP analysis and a 20 ml acid-washed 0.45 µm membrane-filtered sample for SRP.

Flux, in the context of this study, refers to the movement or transfer of SRP or TP into or out of the plastisphere over a specified period. The absolute SRP/TP flux is measured by changes in SRP/TP concentration over time, indicating whether the biofilm is taking up or releasing phosphorus. Biomass-normalized SRP/TP flux accounts for the amount of biofilm biomass, providing a measure of SRP/TP uptake or release per unit of biofilm mass.

Net flux was based on the change in mean TP or SRP concentrations in the microcosms for each treatment using the following equation:

$$V= ([C_f - C_o] * L)/t$$

Where V is the net flux of SRP or TP in µg P/d; C_o is the initial SRP or TP concentration; C_f is the final SRP or TP concentration; L is the incubation volume in liters; and t is the time of incubation in days (Steinman and Duhamel, 2017).

A net positive flux indicates a P release-dominated scenario, while a net negative flux indicates a P uptake-dominated scenario. P net flux was calculated over three time periods: 0-25 days, 0-12 days, and 12–25 days. P net flux was normalized by biofilm biomass (mg/g of MP pellets) (Table 4.9; Figure 4.5, 4.6).

Lake-Wide Scenario Analysis

To estimate the potential overall effect of plastisphere P uptake in Church Lake, assuming the lake fully mixed, we compared mean SRP and TP net flux and from Treatments 1 and 2 to the overall abundance of SRP and TP in the lake. P abundance was estimated using the trapezoidal method to calculate water volume by stratum. This volume was then multiplied by SRP concentrations based on depth profiles taken from Foley and Steinman (2023). Mean uptake rates of the two polymers were used (SRP: 8.2 µg/L/d; TP: 7.9 µg/L/d), and the mass of MPs in the beakers (61.3 g/L) was compared to the mass of MPs in the lake (7.4 µg/L [J. Scott, unpubl. data]) to derive an uptake dilution factor of 8.248×10^6. This dilution factor was multiplied by the uptake rates for SRP and TP, and then by the lake's total volume, to calculate total uptake rates in the lake.

Biofilm Calculation

The pellets from each treatment were retrieved and pooled for total biofilm biomass (ash-free dry mass: AFDM) at the end of the 25-day experiment, and measured by gravimetric analysis (Steinman et al., 2017). MP pellets were subsampled for biofilm by placing 8g of MP pellets into a 50 ml centrifuge tubes with DI water. Plastic pellets were sonicated to remove biofilm attached to the surface of the pellets. Selected pellets were checked microscopically for remaining biofilm after sonication; if biofilm remained, pellets were sonicated again. If no biofilm was found on the surface of the pellets, sonication stopped, and the liquid was filtered. The biofilm retained on the filter was dried at 105 °C for 48 h and then placed in a muffle furnace at 550 °C for 1 h. AFDM was calculated as the difference between the dry weight and

the ashed weight. I first extrapolated the subsampled AFDM to the entire beaker based on the entire MP weight in each beaker, and then normalized P flux to AFDM (µg P/mg AFDM/d), as it was not possible to measure individual MP surface area to normalize by area. Control treatments were also analyzed for AFDM but were not included in AFDM tables (Table 4.3; 4.4; 4.5).

Statistical Analysis

All statistics and data visualization were conducted with R version 4.3.1 (2023-06-16 ucrt) using R studio (2022) version 4.2.2 (Integrated Development for R. RStudio, PBC, Boston, MA). A Shapiro-Wilk normality test package version 4.3.1 was used to assess normality of data. Biomass was log-transformed before application of analysis of variance (ANOVA) and followed by a Tukey HSD post hoc test. If transformation did not work, a non-parametric Kruskal-Wallis test package version 4.3.1 was used to compare the differences in mean P concentrations and between each treatment and polymer for TP, SRP, and biomass. When Kruskal-Wallis had a significant p-value, a multiple comparisons Dunn's test using the Benjamini-Hochberg method (Benjamini and Hochberg, 1995) for p-adjustment in R statistical package FSA v0.94 “dunn.test” (Dinno, 2017) was used (see chapter 3).

Results

Environmental Conditions

Church Lake conditions at the time of MP retrieval show distinct differences between the two deployment depths (Table 4.2). The 2-m depth water was relatively warm and supersaturated with DO, and characterized by relatively high conductivity, and relatively low turbidity (NTU: 1.52). The phosphorus concentrations at 2-m had mean SRP and TP

concentrations of ~ 5 and 13 μg/L, respectively (Table 4.2). In contrast, water at the 10-m depth was cold and severely hypoxic, with very high conductivity, a circumneutral pH, and turbidity that is more than double that at 2-m (NTU: 3.45). At 10-m, SRP and TP concentrations averaged 606 and 555 μg/L, respectively (Table 4.2). Turbidity conditions at 2 and 10m were not replicated for any of the beakers. Turbidity remained low in all treatment beakers throughout the experiment (data not reported). Phosphorus concentration was more than 100 times higher in the hypolimnion than in the epilimnion. TP values were lower than SRP values in treatments receiving hypolimnetic water, presumably because of the interference by iron in the water samples taken in the hypolimnion of Church Lake (Brian Scull, pers. comm.), and set to 500 μg/L as a conservative value.

The experimental conditions, clearly showing different water quality between the epilimnetic and hypolimnetic water, were appropriate for me to test my hypothesis regarding the impact of transferring MPs from one environment to another. In treatment #1, MPs biofilms were grown in the lake epilimnion and then incubated in hypolimnetic water under hypolimnetic conditions for 25 days, which included low DO (0.33 mg/L), high specific conductivity (1177 μS/cm), and high phosphorus (SRP: 504 μg/L; TP: 500 μg/L). In treatment #2, MPs biofilm was grown in the lake hypolimnion and then incubated in epilimnetic water under epilimnetic conditions for 25 days, which included high DO (11 mg/L), low specific conductivity (880 μS/cm), and low phosphorus (SRP: 5 μg/L; TP: 10 μg/L). Treatment #3 involved MPs biofilms was grown in the lake epilimnion and then incubated in epilimnion water under epilimnetic conditions for 25 days, which included high DO (11 mg/L), low specific conductivity (873 μS/cm), and low phosphorus (SRP: 5 μg/L; TP: 10 μg/L). In treatment #4, MPs biofilms

were grown in the lake hypolimnion and then incubated in hypolimnion water under hypolimnetic conditions for 25 days, which included low DO (0.33 mg/L), high specific conductivity (1199 µS/cm), and high phosphorus (SRP: 504 µg/L; TP: 500 µg/L). Treatment C-1 involved lake epilimnion water being exposed to hypolimnetic conditions (low temperature, low light) for 25 days, with no MPs. Treatment C-2 involved lake hypolimnetic water exposed to epilimnetic conditions (warmer temps, high light) for 25 days, but again without MPs (Table 4.2).

Biomass

The range of biomass on each polymer was from 0.23- 0.76 mg/g on PET and from 0.17 to 0.49 mg/g on PP (Table 4.3). There was no statistically significant difference in AFDM between PP and PET ($p = 0.20$; df = 1; F-value 1.62).

PP Biomass: Biofilm AFDM on PP was significantly different among the 4 treatment groups ($p < 0.01$; df = 3; F-value = 4.54). The two significant differences based on a Tukey post-hoc HSD test both involved treatment 2 (Hypo→Epi). In one case, treatment 2 AFDM was significantly lower than treatment 1 (Epi→Hypo), in contrast to my expectations associated with the first hypothesis; in the other case, treatment 3 biomass was significantly greater than treatment 2 (Epi→ Epi), which is consistent with hypothesis 1 expectations (Table 4.4).

PET Biomass: AFDM growing on PET was significantly different among treatments ($p < 0.0001$; df = 3; F-value = 28.29). A Tukey post hoc test showed that AFDM in Treatment 2 (Hypo→Epi) was significantly less than in treatment 1 (Epi→Hypo), again in contrast to my expectations associated with hypothesis 1. AFDM in treatment 3 (Epi→ Epi) was significantly less than in

treatment 1 but in treatment 3, AFDM was greater than in treatment 2 (Hypo→Epi). Treatment 4 (Hypo→Hypo) AFDM was less than in both treatment 1 (Epi→Hypo) and 3 (Epi→ Epi) (Table 4.5).

SRP Concentrations

SRP water concentrations in treatment 1 (Epi→Hypo; Table 4.6.A), where MPs incubated in low SRP water of the epilimnion were introduced to high SRP hypolimnetic water, decreased for both PP and PET over the 25-day experiment, indicating uptake and/or adsorption by the biofilm. The absolute decline was greater with biofilm growing on PET (348 µg/L) than on PP (166 µg/L; Table 4.6A; Figure. 4.4), which may be related to the greater biomass on PET (Table 4.3) and/or an inhibitory effect of PP. In treatment 2 (Hypo→Epi), where MPs incubated in high SRP water of the hypolimnion were introduced to low SRP epilimnetic water, SRP concentration increased slightly in the water column of the beakers in both the PET (0.5 µg/L) and PP (7.6 µg/L) treatments over the 25 days (Table 4.6A: Figure. 4.4), suggesting a slight net release of SRP from the biofilms. Similar results were observed in treatment 3 (Epi →Epi), with a doubling of SRP in the water column with the PET polymer and a tripling of SRP in the water column with the PP polymer, although the absolute SRP concentrations remained low (<16 µg/L) (Figure. 4.4; Table 4.6A). In Treatment 4 (Hypo →Hypo; Figure. 4.4; Figure. 4.6A), SRP was absorbed in both the PET and PP treatment over the first 12 days and increased a small amount in the last 13 days, for an overall net reduction of 62 and 71 µg/L, respectively.

SRP concentrations on PP: SRP concentrations in microcosms with PP were significantly different among the 4 treatment groups from day 12-25 (chi-squared = 35.191, df = 7, p-value = 1.03e-05). A pairwise comparison revealed significant differences in SRP concentration over

time between treatments 1 (Epi→Hypo) and 3 (Epi→Epi). Treatment 2 (Hypo→Epi) was significantly different than treatment 4 (Hypo→Hypo). Treatment 3 (Epi→Epi) was significantly different than treatment 4 (Hypo→Hypo). This suggests that the SRP levels in microcosms with PP were influenced by the treatment conditions and changed over time.

SRP concentrations on PET: SRP concentrations in microcosms with PET were significantly different among the 4 treatment groups from day 12-25 (chi-squared = 37.438, df = 7, p-value = 3.875e-06). Treatment 1 (Epi→Hypo) and 3 (Epi→Epi) were significantly different from one another. Both Treatment 2 (Hypo→Epi) and treatment 3 (Epi→Epi) were significantly different than treatment 4 (Hypo→Hypo). It is clear from these results that polymer type had little influence on SRP flux in this study. SRP concentrations on PET varied significantly among treatment groups from day 12 to 25, with significant differences observed between treatments 1 and 3, as well as between Treatments 2 and 4, indicating that polymer type had minimal to no impact on SRP flux.

SRP Net Flux

I calculated absolute SRP flux based on changes in concentration over time (Figure. 4.4), as well as biomass-normalized flux at the end of the experiment (Figure. 4.5). Absolute SRP flux was greatest in treatment 1, when biofilm grown in the low-P epilimnion was transferred to the high-P hypolimnetic water; uptake rates were greater by biofilm on PET than on PP in treatment 1 (Table 4.7). The next highest net uptake rate was in Treatment 4, although these rates were much lower than in Treatment 1, as the biofilm on both polymers was transferred from hypolimnetic lake water to hypolimnetic water in the lab. Transfers to epilimnetic water (Treatments 2 and 3) had very low flux, and all indicated a small net release of SRP. There was

no consistent trend with respect to time throughout the experiment; in some cases, flux was higher during the first 12 days and in other cases, it was higher in the latter 13 days (Table 4.7).

Biomass-normalized SRP flux from day 0-25 was similar to the measurements for absolute SRP flux (Tables 4.7 and 4.9), reflecting the relatively small differences in biomass among treatments (Table 4.3). Treatments 1 and 4 had the highest net flux with values of -11.11 µg P/L/mg and -5.79 µg P/L/mg, respectively (Table 4.9; Figure 4.5). SRP flux in treatments 2 and 3, with biofilm in epilimnetic water, released SRP at very low rates (0.31 µg P/L/mg and 0.62 µg P/L/mg, respectively). Control 1 had an overall SRP flux rate of 0 µg P/L per AFDM mg/g while control 2 had an uptake rate of -0.56 µg P/L per AFDM mg/g. This suggests that the controls had significantly lower, or no SRP flux compared to the treatments with biofilm.

TP Concentrations

Overall, absolute TP concentration results were very similar to SRP. In treatment 1 (Epi→Hypo), TP decreased substantially over the 25-day experiment with biofilm on PET taking up more TP (307 µg/L) than that on PP (203 µg/L; Figure. 4.4; Table 4.6.B). In treatments 2 (Hypo→Epi) and 3 (Epi →Epi), TP concentrations increased modestly over time in both polymer incubations (Figure. 4.4; Table 4.6.B). Unlike SRP, which declined in treatment 4 from day 0 to day 12 before increasing on day 25, TP concentration in treatment 4 (Hypo →Hypo) increased throughout the 25-day experiment with both polymers, albeit in relatively small amounts (Figure. 4.4; Table 4.6.B).

PP TP concentrations: TP concentrations in microcosms with PP were significantly different among the 4 treatment groups from day 12-25 (chi-squared = 36.615, df = 7, p-value = 5.547e-06). Results from the pairwise comparison showed a significant difference between treatment 1 and 3. Treatment 2 and 3 were both significantly different from treatment 4.

PET TP concentrations: TP concentrations in microcosms with PET were significantly different among the 4 treatment groups from day 12-25 (chi-squared = 37.332, df = 7, p-value = 4.058e-06). Results from the pairwise comparison showed a significant difference between treatment 1 and 3. Treatment 2 and 3 were both significantly different from treatment 4. PET and PP had similar differences among the same treatment as one another. These results were similar to those for SRP.

TP Net Flux

The only treatment that showed a net TP uptake was treatment 1, especially in the first 12 days of the experiment when flux was 13.23 µg TP/L/d for biofilm on PET and 11.30 µg TP/L/d for biofilm on PP (Table 4.8). Absolute TP flux in the other three treatments reflected a net release, with no consistent trend over time or with polymer type, although flux was very modest in all releases (Table 4.8; Figure 4.6).

When TP flux was normalized by biomass (Table 4.9), again the only treatment with a net uptake was treatment 1 (Epi→Hypo), with little difference among polymer types. Treatment 4 had higher biomass-normalized TP release rates than what I measured in treatments 2 and 3; interestingly, biomass-normalized SRP was taken up in treatment 4 but TP was released (Table 4.9; Figure 4.6). The unusual findings in Treatment 4 regarding TP flux are

likely due to iron interference and possibly influenced by differences in biomass activity and biofilm characteristics; as a consequence, TP results should be viewed with caution.

Discussion

My experimental design, to investigate the plastisphere-mediated P dynamics on two different microplastic polymers in a salinized eutrophic lake after simulated turnover, effectively mimicked the environmental conditions between the epilimnion and the hypolimnion. There were distinct environmental differences between the 2-m and 10-m depths, with the former being warm, supersaturated with DO, and having lower P concentrations, while the latter was cold, severely hypoxic, and had significantly higher P concentrations.

I observed very little effect of polymer type on plastisphere dynamics. Mean plastisphere biomass ranged from 0.23-0.76 mg/g on PET and 0.17-0.49 mg/g on PP. Marchant et al. (2023) also observed no effect of polymer type on biofilm productivity, although they used different polymers than those used in this study. Guasch et al. (2022) reviewed the direct impacts of microplastics on biofilms and found the studies provided conflicting results, with some reporting impacts on gene expression in biofilms (Lagarde et al. 2016), and others reporting either negative effects on growth (Besseling et al. 2014) or positive effects on growth (Canniff and Hoang 2018).

Although in my study I saw no overall effect of polymer type on biomass, treatment-specific variations were observed in biofilm AFDM on both PP and PET individually, with significant differences among treatment groups, particularly in the Hypo→Epi treatment for

both polymers. For example, biomass on PP and PET transferred from the hypolimnion to the epilimnion (T-2) accumulated less biomass than MPs transferred from the epilimnion to the hypolimnion (T-1). This result was somewhat surprising, as we hypothesized that moving to a high light, low salinity environment would stimulate growth, despite the lower P concentration, compared to moving to very low light and high salinity conditions. Apparently, the high P concentrations in the hypolimnetic water stimulated growth; molecular analyses indicated an abundance of Flavobacterium taxa on both PP and PET in this treatment (see Chapter 3). Additionally, PET left in the epilimnion (T-3) had greater biomass than MPs in treatment 2. This decrease in biomass after being transferred from high nutrients and high salinity to a lower nutrient and low salinity environment may be due to the sudden reduction in nutrients or it may be a lag effect in growth, whereby organisms must acclimate from the prior high salinity conditions to a lower salinity environment (Shetty et al. 2019). Biomass on PET in Treatment 2 (incubated in the hypolimnion and transferred to the epilimnion) was lower than in Treatment 3 (grown and kept in the epilimnion), likely due to the lower phosphorus concentrations in the epilimnion; similarly, biomass in Treatment 3 was lower than in Treatment 1 (grown in the epilimnion and transferred to the hypolimnion), and Treatment 4 (grown and kept in the hypolimnion) had the least biomass compared to both Treatment 1 and Treatment 3. These results indicated that MPs grown in the epilimnion adjusted well when transferred to a new environment or thrived on their own environment at 2-m depth. MP pellets grown in hypolimnetic environments had less biomass than MPs grown in the epilimnion, although the absolute differences were small. Overall, these results suggest that biomass on MPs grown in

the hypolimnion are limited by high salinity or low light, whereas MPs biofilm grown in the epilimnion were limited by P.

There was no obvious effect of polymer type on SRP uptake rate, as some treatments had greater uptake with PP and others with PET. It would appear that environmental conditions had greater influence than polymer on uptake; a similar conclusion was drawn by Li and Liu (2022), although they compared P dynamics in soils using polyethylene and polypropylene.

Nutrient uptake rates are influenced by many factors, including the absolute concentrations in the water column, N:P elemental ratios in the water column as well as in the cells, light levels, cell size, micronutrients, and many others (Reynolds, 2006). My focus on phosphorus uptake was predicated on the extremely high P concentrations (up to 5000 µg/L) in the high-salinity region of Church Lake (Foley and Steinman, 2023), and the potential ecological implications if this lake turned over and this phosphorus was to reach the photic zone. In addition to potential P uptake by planktonic organisms, would there be uptake by the plastisphere, and if so, would it be of ecological consequence?

The changes in SRP and TP over time and calculated fluxes were consistent, as one might expect. By far, the treatment with the greatest P uptake was treatment 1, regardless of polymer type. This treatment, which involved plastisphere incubation in the epilimnion and then growth in hypolimnetic water, exposed organisms to high P, high salinity, and low light conditions. At least over this 25-day lab experiment period, nutrient concentration played a greater role stimulating P uptake than the low light or high salinity in potentially inhibiting P

uptake. Sudden exposure to high nutrient environments has stimulated uptake in some studies (De Haan et al., 2016) but not all (Powers et al., 2009) However, it is important to note that even these highest uptake rates in T-1 are still 1-2 orders of magnitude lower than other studies examining P uptake by phytoplankton across a range of N:P ratios (Suttle and Harrison, 1988); we could find no equivalent studies for the plastisphere. The very low uptake rates in this study may reflect low biomass, physiological impairment due to stressful environmental conditions, or insufficient water movement in the beakers. Attempts to compare P uptake rates in Church Lake to other studies (besides Suttle and Harrison) were hampered by our use of volume in place of chlorophyll, which is the more common unit with which to normalize uptake, in studies of this type.

We estimated the potential overall effect of plastisphere P uptake in Church Lake assuming the lake fully mixed by comparing mean SRP uptake or release rates from Treatments 1 and 2 to the overall abundance of SRP and TP in the lake. P abundance was estimated using the trapezoidal method to estimate water volume by stratum (2.51 billion liters) multiplied by SRP concentrations based on depth profiles taken from Foley and Steinman (2023). Total SRP in Church Lake varied from 28.4 to 77.3 kg and TP varied from 82.5 to 153.4 kg, depending on time of year. We then used the mean uptake rates of the two polymers (SRP: 8.2 µg/L/d; TP: 7.9 µg/L/d) and factored in the mass of MPs in the beakers (61.3 g/L) vs. the mass of MPs in the lake (7.4 µg/L [J. Scott, unpubl. data]) to derive an uptake dilution factor of 8.248×10^6. Multiplying the dilution factor by the uptake rates for SRP and TP, and then multiplying by the lake's total volume allows us to calculate total uptake rates in the lake. Based on this approach, the plastisphere has the ability to process 2.51 mg/d of SRP and 2.26 mg/d of TP, or a tiny

fraction of the total SRP and TP in Church Lake. We recognize these values are crude estimates, and may actually be overestimates, as it does not account for the potential release of P as seen in Treatment 2. Regardless, it is clear from these first order estimates that if Church Lake was to turn over in the future, it is highly unlikely that the plastisphere would play a substantial role in alleviating the P mass currently situated in the hypolimnion. It is possible that the influence of the plastisphere may be greater at the sediment-water interface where MPs will settle, but given the very high concentrations measured at the near-bottom hypoxic zone of Church Lake, it is unlikely they are having a significant ecological impact.

I acknowledge that the study has several limitations. First, TP concentrations should be considered underestimates since iron in the water samples taken in Church Lake's hypolimnion interfered with TP analysis, causing lower TP than SRP results in treatments receiving hypolimnetic water. Hence, the TP results involving hypolimnetic water should be viewed with caution. Second, it is unlikely that the MPs and their associated plastisphere were evenly distributed throughout Church Lake. Indeed, given the increased density of plastisphere-coated MPs, most of the MPs are likely in the hypolimnion or sediment, and we did not calculate uptake rates from the sediment-bound plastisphere, which may behave very differently than the plastisphere in the water column.

Conclusion

The study investigated the impact of transferring MPs between different water layers (epilimnion and hypolimnion) in Church Lake. The conclusions partially align with the hypothesis. We reject hypothesis 1, as the microbial communities growing on MPs in the epilimnion and then exposed to epilimnetic conditions had lower P uptake than those grown

and exposed to hypolimnetic conditions. It appears the high P environment had a stronger influence on P uptake than the potential inhibiting effect of high salinity and low light. Hypothesis 2 was partially accepted, as microbial communities transferred from hypolimnion to epilimnion released P whereas there was no change in the control system; however, the communities transferred from epilimnion to hypolimnetic conditions had the highest uptake rates. Our lake-wide scenario suggests, even taking into account various assumptions, that the plastisphere has very limited potential to influence P dynamics in the lake should the lake ever turnover.

References

Arend, K. K., Beletsky, D., Depinto, J. V., Ludsin, S. A., Roberts, J. J., Rucinski, D. K., Scavia, D., Schwab, D. J., & T, H. O. (2011). Seasonal and interannual effects of hypoxia on fish habitat quality in central Lake Erie. Freshwater Biology, 56, 366–383. https://doi.org/10.1111/j.1365-2427.2010.02504.x

Benjamini, Y., Hochberg, Y., (1995). Controlling the false discovery rate: a practical and powerful approach to multiple testing. J. R. Stat. Soc. 57, 289–300.

Besseling, E., Wang, B., Lurling, M. and Koelmans, A.A., 2014. Nanoplastic affects growth of S. obliquus and reproduction of D. magna. Environmental science & technology, 48(20), pp.12336-12343.

Biddanda, B.A., Weinke, A.D., Kendall, S.T., Gereaux, L.C., Holcomb, T.M., Snider, M.J., Dila, D.K., Long, S.A., VandenBerg, C., Knapp, K., & Koopmans, D.J. (2018) Chronicles of hypoxia: Time-series buoy observations reveal annually recurring seasonal basin-wide hypoxia in Muskegon Lake–A Great Lakes estuary. Journal of Great Lakes Research, 44(2), 219-229.

Canniff, P.M. and Hoang, T.C., 2018. Microplastic ingestion by Daphnia magna and its enhancement on algal growth. Science of the Total Environment, 633, pp.500-507.

Chen, X., Chen, X., Zhao, Y., Zhou, H., Xiong, X., & Wu, C. (2020). Effects of microplastic biofilms on nutrient cycling in simulated freshwater systems. Science of the Total Environment, 719, 137276. https://doi.org/10.1016/j.scitotenv.2020.137276

Den Haan, J., Huisman, J., Brocke, H.J., Goehlich, H., Latijnhouwers, K.R., Van Heeringen, S., Honcoop, S.A., Bleyenberg, T.E., Schouten, S., Cerli, C. and Hoitinga, L., 2016. Nitrogen and phosphorus uptake rates of different species from a coral reef community after a nutrient pulse. Scientific reports, 6(1), p.28821.

Diaz, R., Mackey, B., Chadalavada, S., kainthola, J., Heck, P., & Goel, R. (2022). Enhanced Bio-P removal: Past, present, and future – A comprehensive review. Chemosphere, 309(P2), 136518. https://doi.org/10.1016/j.chemosphere.2022.136518

Dinno, A., (2017). dunn.test: Dunn's test of multiple comparisons using rank sums. https:// cran.r-project.org/package=dunn.test

Dodds, W.K., (2003). The role of periphyton in phosphorus retention in shallow freshwater aquatic systems. Journal of Phycology, 39(5), 840-849. https://doi.org/10.1046/j.1529-8817.2003.02081.x

Driedger, A. G. J., Dürr, H. H., Mitchell, K., & Van Cappellen, P. (2015). Plastic debris in the Laurentian Great Lakes: A review. Journal of Great Lakes Research, 41(1), 9–19. https://doi.org/10.1016/j.jglr.2014.12.020

Foley, E., & Steinman, A. D. (2023). Urban lake water quality responses to elevated road salt. Science of the Total Environment, 905, 167139. https://doi.org/10.1016/j.scitotenv.2023.167139

Guasch, H., Bernal, S., Bruno, D., Almroth, B.C., Cochero, J., Corcoll, N., Cornejo, D., Gacia, E., Kroll, A., Lavoie, I., Ledesma, J.L., et al. 2022. Interactions between microplastics and benthic biofilms in fluvial ecosystems: Knowledge gaps and future trends. Freshwater Science, 41(3), pp.442-458.

He, S., Jia, M., Xiang, Y., Song, B., Xiong, W., Cao, J., Peng, H., Yang, Y., Wang, W., Yang, Z., & Zeng, G. (2021). Biofilm on microplastics in aqueous environment: Physicochemical properties and environmental implications. Journal of Hazardous Materials, 127286. https://doi.org/10.1016/j.jhazmat.2021.127286

Lagarde, F., Olivier, O., Zanella, M., Daniel, P., Hiard, S. and Caruso, A., 2016. Microplastic interactions with freshwater microalgae: hetero-aggregation and changes in plastic density appear strongly dependent on polymer type. Environmental pollution, 215, pp.331-339.

Larson, C. A., & Belovsky, G. E. (2013). Salinity and nutrients influence species richness and evenness of phytoplankton communities in microcosm experiments from Great Salt Lake, Utah, USA. Journal of Plankton Research, 35(5), 1154–1166. https://doi.org/10.1093/plankt/fbt053

Lewis, A.S.L, Lau, M.P., Jane, S.F., Rose, K.C., Be'eri-Shlevin, Y., Burnet, S.H., Clayer, F., Feuchtmayr, H., Grossart, H.P., Howard, D.W., Mariash, H., et al. 2024. Anoxia begets anoxia: A positive feedback to the deoxygenation of temperate lakes. Global Change Biology, 30(1), e17046.

Li, H. and Liu, L., 2022. Short-term effects of polyethene and polypropylene microplastics on soil phosphorus and nitrogen availability. Chemosphere, 291, p.132984.

Lind, L., Schuler, M. S., Hintz, W. D., Stoler, A. B., Jones, D. K., Mattes, B. M., & Relyea, R. A. (2018). Salty fertile lakes: how salinization and eutrophication alter the structure of freshwater communities. Ecosphere, 9(9). https://doi.org/10.1002/ecs2.2383

Lutz, N., Fogarty, J., & Rate, A. (2021). Accumulation and potential for transport of microplastics in stormwater drains into marine environments, Perth region, Western Australia. Marine Pollution Bulletin, 168(April), 112362. https://doi.org/10.1016/j.marpolbul.2021.112362

Marchant, D.J., Rodríguez, A.M., Francelle, P., Jones, J.I. and Kratina, P., 2023. Contrasting the effects of microplastic types, concentrations and nutrient enrichment on freshwater communities and ecosystem functioning. Ecotoxicology and Environmental Safety, 255, p.114834.

Mulholland, P.J., Steinman, A.D., Palumbo, A.V., Elwood, J.W., & Kirschtel, D.B. (1991) Role of nutrient cycling and herbivory in regulating periphyton communities in laboratory streams. Ecology, 72(3), 966-982. https://doi.org/10.2307/1940597

Niu, L., Hu, J., Li, Y., Wang, C., Zhang, W., Hu, Q., Wang, L., & Zhang, H. (2022). Effects of long-term exposure to silver nanoparticles on the structure and function of microplastic

biofilms in eutrophic water. Environmental Research, 207(October 2021), 112182. https://doi.org/10.1016/j.envres.2021.112182

Numberger, D., Zoccarato, L., Woodhouse, J., Ganzert, L., & Sauer, S. (2022). Urbanization promotes specific bacteria in freshwater microbiomes including potential pathogens. Science of the Total Environment, 845(February), 157321. https://doi.org/10.1016/j.scitotenv.2022.157321

Powers, S.M., Stanley, E.H. and Lottig, N.R., 2009. Quantifying phosphorus uptake using pulse and steady-state approaches in streams. Limnology and Oceanography: Methods, 7(7), pp.498-508.

Qiang, L., Cheng, J., Mirzoyan, S., Kerkhof, L. J., & Häggblom, M. M. (2021). Characterization of microplastic-associated biofilm development along a freshwater-estuarine gradient. Environmental Science and Technology, 55(24), 16402–16412. https://doi.org/10.1021/acs.est.1c04108

Reynolds, C.S., 2006. The ecology of phytoplankton. Cambridge University Press.

Shetty, P., Gitau, M.M. and Maróti, G., 2019. Salinity stress responses and adaptation mechanisms in eukaryotic green microalgae. Cells, 8(12), p.1657.

Steinman, A. D., & Duhamel, S. (2017). Phosphorus limitation, uptake, and turnover in benthic stream algae. In F. R. Hauer & G. A. Lamberti (Eds.), Methods in Stream Ecology, Volume 2 (Third Edition), pp. 197-218. Academic Press.

Steinman, A. D., Lamberti, G. A., Leavitt, P. R., & Uzarski, D. G. (2017). Biomass and pigments of benthic algae. In F. R. Hauer & G. A. Lamberti (Eds.), Methods in Stream Ecology, Volume 1 (Third Edition), pp. 223–241). Academic Press. https://doi.org/https://doi.org/10.1016/B978-0-12-416558-8.00012-3

Steinman, A. D., Scott, J., Green, L., Partridge, C., Oudsema, M., Hassett, M., Kindervater, E., & Rediske, R. R. (2020). Persistent organic pollutants, metals, and the bacterial community composition associated with microplastics in Muskegon Lake (MI). Journal of Great Lakes Research, 46(5), 1444–1458. https://doi.org/10.1016/j.jglr.2020.07.012

Tan, X., Gao, W., Duan, Z., Zhu, N., Wu, X., Ali, I., & Ruan, Y. (2023). Synthesis of novel algal extracellular polymeric substances (EPS)-based hydrogels for the efficient removal and recovery of phosphorus from contaminated waters: Development, characterisation, and performance. Journal of Environmental Chemical Engineering, 11(1). https://doi.org/10.1016/j.jece.2022.109044

Turner, A. M. A. C. M. F. (2010). Blinded by the stink: Nutrient enrichment impairs the perception of predation risk by freshwater snails Communications. Ecological Society of America, 20(8), 2089–2095. https://doi.org/10.1890/10-0208.1

Wang, L., Luo, Z., Zhen, Z., Yan, Y., Yan, C., Ma, X., Sun, L., Wang, M., Zhou, X., & Hu, A. (2020). Bacterial community colonization on tire microplastics in typical urban water

environments and associated impacting factors. Environmental Pollution, 265, 114922. https://doi.org/10.1016/j.envpol.2020.114922

Yuan J, Ma J, Sun Y, Zhou T, Zhao Y, Yu F. Microbial degradation, and other environmental aspects of microplastics/plastics. Sci Total Environ. 2020 May 1; 715:136968. Doi: 10.1016/j.scitotenv.2020.136968. Epub 2020 Jan 27. PMID: 32014782.

Zettler, E. R., Mincer, T. J., & Amaral-zettler, L. A. (2013). Life in the “Plastisphere”: Microbial Communities on Plastic Marine Debris. Environmental Science & Technology, 47(13), 7137–7146. https://doi.org/DOI: 10.1021/es401288x

Tables

Table 4.1. Environmental conditions in Church Lake at 2m and 10m compared to treatment conditions the plastisphere was grown in and their ambient conditions. Treatment #1: MPs incubated in lake epilimnion transferred to hypolimnetic water. Treatment #2: MPs incubated in lake hypolimnion transferred to epilimnetic water. Treatment #3: MPs incubated in lake epilimnion and transferred to epilimnetic water. Treatment #4: MPs incubated in lake hypolimnion and transferred to hypolimnetic water. C-1: No MPs were added to epilimnetic water put in hypolimnetic conditions. C-2: No MPs were added to hypolimnetic water put in epilimnetic conditions. Spec. Cond: specific conductivity.

Treatment #	Initial Conditions				Treatment Conditions				
	Spec. Cond µS/cm	STDEV.P	Light	P	Spec. Cond µS/cm	STDEV.P	Light	P	MPs
#1-Epi→Hypo	865	4	High	Low	1178	11	Low	High	Present
#2-Hypo→Epi	1315	100	Low	High	880	5	High	Low	Present
#3-Epi→Epi	865	4	High	Low	873	2	High	Low	Present
#4Hypo→Hypo	1315	100	Low	High	1200	2	Low	High	Present
C-1-Epi→Hypo	865	4	High	Low	877	2	Low	High	Absent
C-2-Hypo→Epi	1315	100	Low	High	1187	4	High	Low	Absent

Table 4.2. Water quality data from the experiment. Samples labeled retrieval are measurements taken from the Church Lake water column at 2 and 10 meters after the 2-week frame incubation period. Remaining rows are water quality samples from the beakers taken on the final day of the experiment (excluding P values which are from first day of the microcosm experiment [see below]) after removing MP pellets (except Controls, where no pellets were present). SRP and TP values are means (± SD) from each treatment taken at the beginning of the experiment regardless of polymer (n = 10). SRP and TP values labeled "retrieval" were sampled from Church Lake after the 2-week frame incubation period and had no replicates. SRP values are higher than TP values in the hypolimnion because of interference from high iron concentrations in the hypolimnion. DO: dissolved oxygen, SPC: specific conductivity (T1= Epi→Hypo; T2= Hypo→Epi; T3= Epi→ Epi; T4=Hypo→Hypo; C-1= Epi→ Hypo; C-2= Hypo → Epi) (see Table 4.1)

Treatment	Temp (°C)	DO (%)	DO (mg/L)	pH	SPC (µS/cm)	SRP (µg/L)	TP (µg/L)
Retrieval-2m	24	134	11.24	8	865	5	13
Retrieval-10m	4	2.6	0.33	6	1315	606	555
#1-Epi→Hypo	5	2.6	0.33	8	1177.5	504±37	500±23*
#2-Hypo→Epi	16	134	11.24	8	880	5±0	10±1
#3-Epi→Epi	16	134	11.24	8	873	5±0	10±1
#4-Hypo→Hypo	5	2.6	0.33	8	1199.5	504±37	500±23*
C-1- Epi→Hypo	5	2.6	0.33	8	877	5±0	10±1
C-2- Hypo→Epi	16	134	11.24	8	1187	502±34	500±25*

*TP values set at 500 µg/L to match SRP values (see methods for explanation)

Table 4.3. Minimum, maximum and mean (± SD, n = 5) AFDM values in each treatment. The average was taken from replicates of biofilm biomass for each treatment measured on the 25th day. (T1= Epi→Hypo; T2= Hypo→Epi; T3= Epi→ Epi; T4=Hypo→Hypo) (see Table 4.1).

Treatment	Min	Max	Mean AFDM mg/g
T-1-PET-Epi→Hypo	0.40	0.76	0.59 ± 0.14
T-1-PP-Epi→Hypo	0.33	0.49	0.40 ± 0.07
T-2-PET-Hypo→Epi	0.23	0.31	0.26 ± 0.03
T-2-PP-Hypo→Epi	0.17	0.31	0.24 ± 0.05
T-3-PET-Epi→Epi	0.41	0.49	0.44 ± 0.03
T-3-PP-Epi→Epi	0.31	0.40	0.36 ± 0.03
T-4-PET-Hypo→Hypo	0.23	0.34	0.28 ± 0.04
T-4-PP-Hypo→Hypo	0.18	0.41	0.33 ± 0.09

Table 4.4. Tukey multiple comparisons for differences in the mean values of biofilm biomass on PP microplastics between 4 treatments. A negative value indicates the first treatment in the treatment pair was significantly lower than the second treatment in the pair. Asterisks indicate level of significance: *** $p < 0.0001$, ** $p < 0.01$, * $p < 0.05$. Diff stands for the differences in means between two groups being compared. lwr stands for lower confidence interval and describes the lower bound of the confidence interval for the differences in means. Upr stands for upper confidence interval and describes the upper bound of the confidence interval for the differences in means.

Treatment	diff	lwr	upr	p adj
T2PP-T1PP	-0.496	-0.905	-0.087	0.015**
T3PP-T1PP	-0.092	-0.501	0.317	0.917
T4PP-T1PP	-0.203	-0.612	0.206	0.505
T3PP-T2PP	0.404	-0.005	0.813	0.053*
T4PP-T2PP	0.293	-0.116	0.701	0.212
T4PP-T3PP	-0.111	-0.520	0.297	0.863

Table 4.5. Tukey multiple comparisons for differences in the mean values of biofilm biomass on PET microplastics between 4 treatments A negative value indicates the first treatment in the treatment pair was significantly lesser than the second treatment in the pair. Asterisks indicate level of significance: *** p < 0.0001, ** p < 0.01, * p < 0.05. Diff stands for the differences in means between two groups being compared. Lwr stands for lower confidence interval and describes the lower bound of the confidence interval for the differences in means. Upr stands for upper confidence interval and describes the upper bound of the confidence interval for the differences in means.

Treatment	diff	lwr	upr	p adj
T2PET-T1PET	-0.812	-1.105	-0.519	3.4E-06***
T3PET-T1PET	-0.287	-0.579	0.006	0.056*
T4PET-T1PET	-0.740	-1.033	-0.447	1.09E-05***
T3PET-T2PET	0.525	0.233	0.818	0.001***
T4PET-T2PET	0.072	-0.221	0.365	0.895
T4PET-T3PET	-0.453	-0.746	-0.161	0.002**

Table 4.6. A. Mean corrected water column SRP concentrations (± SD, n = 5) (changes in control treatment SRP concentrations were subtracted from each corresponding time period) taken on days 0,12, and 25 for each treatment, for the two different polymers. (T1 = Epi→Hypo; T2 = Hypo→Epi; T3 = Epi→ Epi; T4 = Hypo→Hypo; C-1 = Epi→ Hypo; C-2 = Hypo → Epi) (see Table 4.1).

Treatment	Corrected SRP Concentration (μg/L)		
	Day 0	Day 12	Day 25
T-1-PET- Epi→Hypo	513.6 ± 41.9	345.4 ± 37.1	165.7 ± 89.4
T-1-PP- Epi→Hypo	494.5 ± 39.1	365.6 ± 16.8	328.7 ± 144.5
T-2-PET- Hypo→Epi	5 ± 0	5 ± 0	5.5 ± 0.9
T-2-PP- Hypo→Epi	5 ± 0	7.6 ± 3.6	12.6 ± 5.3
T-3-PET- Epi→ Epi	5 ± 0	5 ± 0	11 ± 0
T-3-PP- Epi→ Epi	5 ± 0	5 ± 0	15.4 ± 0
T-4-PET- Hypo→Hypo	513.6 ± 41.9	423.8 ± 3	451 ± 3.5
T-4-PP- Hypo→Hypo	494.5 ± 41.7	400.4 ± 4.7	423.2 ± 12.5

Table 4.6. B. Mean corrected water column TP concentrations (± SD, n = 5) (changes in control treatment TP concentrations were subtracted from each corresponding time period) taken on days 0,12, and 25 for each treatment, for the two different polymers. (T1= Epi→Hypo; T2= Hypo→Epi; T3= Epi→ Epi; T4=Hypo→Hypo) (see Table 4.1). Starting TP concentration for hypolimnetic treatments is a conservative value (see text).

Treatment	TP Concentration (µg/L)		
	Day 0	Day 12	Day 25
T-1-PET- Epi→Hypo	500 ± 0	338.3 ± 30.4	193.6 ± 88.6
T-1-PP- Epi→Hypo	500 ± 0	367.3 ± 20.2	297.4 ± 14
T-2-PET- Hypo→Epi	9.6 ± 1.6	10.1 ± 6.2	19.9 ± 2.6
T-2-PP- Hypo→Epi	10.4 ± 1.9	18.2 ± 11.2	31.6 ± 5.5
T-3-PET- Epi→ Epi	10.2 ± 2	14 ± 1	25 ± 1.9
T-3-PP- Epi→ Epi	10.4 ± 1.9	19.3 ± 1.5	26 ± 3.4
T-4-PET- Hypo→Hypo	500 ± 0	505.3 ± 8.3	523.3 ± 11.6
T-4-PP- Hypo→Hypo	500 ± 0	514.2 ± 8.4	515.1 ± 11.9

Table 4.7. Absolute net SRP flux (µg P/L/d) calculated from mean SRP concentrations. Negative values indicate uptake; positive values indicate release.

Treatment	Day 0-25	Day 0 -12	Day 12-25
T-1-PET- Epi→Hypo	-11.11	-10.35	-11.02
T-1-PP- Epi→Hypo	-5.28	-7.93	-2.23
T-2-PET- Hypo→Epi	0.02	0	0.03
T-2-PP- Hypo→Epi	0.24	0.16	0.31
T-3-PET- Epi→ Epi	0.19	0	0.37
T-3-PP- Epi→ Epi	0.32	0	0.62
T-4-PET- Hypo→Hypo	-2.00	-5.52	1.67
T-4-PP- Hypo→Hypo	-2.28	-5.79	1.40
C-1-Epi→Hypo	0	0	0
C-2-Hypo→Epi	-0.56	-1.11	4.44

Table 4.8. Absolute net TP flux (net rate µg P/L/d) per day calculated from mean TP concentrations. Negative values indicate uptake; positive values indicate release.

Treatment	Day 0-25	Day 0-12	Day 12- 25
T-1-PET- Epi→Hypo	-9.58	-13.23	-6.64
T-1-PP- Epi→Hypo	-6.26	-11.30	-2.04
T-2-PET- Hypo→Epi	0.56	0.03	0.60
T-2-PP- Hypo→Epi	0.91	0.54	0.81
T-3-PET- Epi→ Epi	0.47	0.25	0.68
T-3-PP- Epi→ Epi	0.50	0.59	0.41
T-4-PET- Hypo→Hypo	0.74	0.35	1.11
T-4-PP- Hypo→Hypo	0.48	0.95	0.06
C-1-Epi→Hypo	0.03	0.54	-0.44
C-2-Hypo→Epi	3.01	6.73	-0.43

Table 4.9. Biomass-normalized TP and SRP flux measurements (µg P/L/mg AFDM) based on changes from days 0-25.

Treatment	SRP Flux/Biomass	TP Flux/Biomass
T-1-PET- Epi→Hypo	-18.68	-16.11
T-1-PP- Epi→Hypo	-13.38	-15.85
T-2-PET- Hypo→Epi	0.06	2.15
T-2-PP- Hypo→Epi	1.01	3.74
T-3-PET- Epi→ Epi	0.44	1.08
T-3-PP- Epi→ Epi	0.91	1.40
T-4-PET- Hypo→Hypo	-7.15	2.66
T-4-PP- Hypo→Hypo	-6.86	1.45
C-1-Epi→Hypo	0	0.12
C-2-Hypo→Epi	-2.15	11.59

Figures Captions

Figure 4.1. Maps of Church Lake, located in Grand Rapids, MI. Figure 1: location of lake in Kent County, Michigan. Figure 2: Church, Middleboro, and Westboro Lakes that are hydrologically connected. Surface and groundwater flow is from east to west. Figure 3: close map of Church Lake, the red arrows indicate the unnamed tributary that flows from the East Beltline west to Church Lake. Figure 4: Bathymetry of Church Lake retrieved from Progressive Ae Tri-Lakes water quality assessment report (2010), which has residential housing on its south and west shorelines and is adjacent to the East Beltline state highway on its east side. Depth is in ft.

Figure 4.2. PVC frame holding Incubation tubes before deployment (Steinman et al., 2020).

Figure 4.3. Urban lake water column. View through the water column and frame setup in portion of lake with established chemocline.

Figure 4.4. Change in SRP and TP concentration in water for each treatment, with two different polymers per treatments with MP: PET = Polyethylene terephthalate; PP = Polypropylene. Error bars indicate the standard deviation in each treatment. (T1= Epi→Hypo; T2= Hypo→Epi; T3= Epi→ Epi; T4=Hypo→Hypo; C-1= Epi→ Hypo; C-2= Hypo → Epi) (Table 4.1). Note break in y-axis scale.

Figure 4.5. Histogram comparison of absolute net SRP flux (net rate µg P/L/d) per day (A) and Biomass-normalized SRP flux measurements (µg P/L/mg AFDM) (B). Negative values indicate uptake; positive values indicate release.

Figure 4.6. Histogram comparison of Absolute net TP flux (net rate µg P/L/d) per day (A) and Biomass-normalized TP flux measurements (µg P/L/mg AFDM) (B). Negative values indicate uptake; positive values indicate release.

Figures

Figure 4.1

Figure 1. Church Lake is located in Kent County, Michigan.

Figure 2. Church, Middleboro, and Westboro Lakes are hydrologically connected.

Figure 3. Close up of Church Lake.

Figure 4. Bathymetry of Church Lake.

Figure 4.2

Figure 4.3

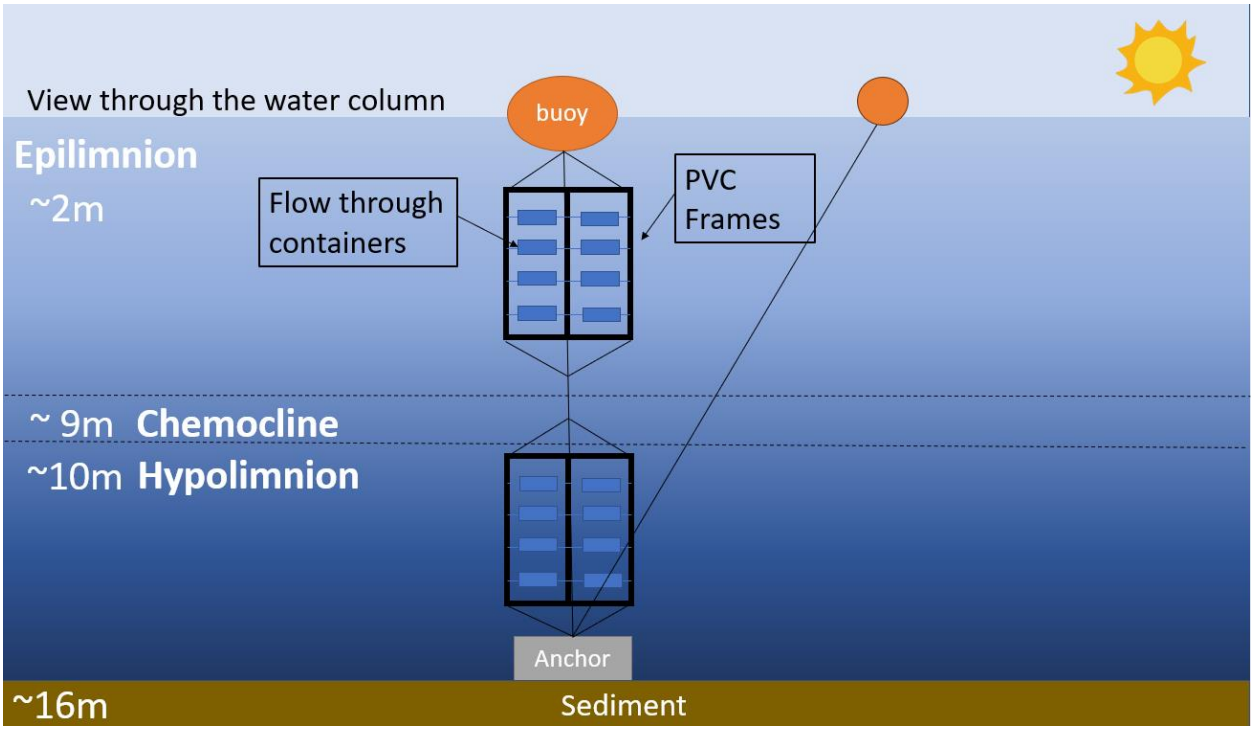
View through the water column
buoy
Epilimnion
~2m
Flow through containers
PVC Frames
~ 9m Chemocline
~10m Hypolimnion
Anchor
~16m
Sediment

Figure 4.4

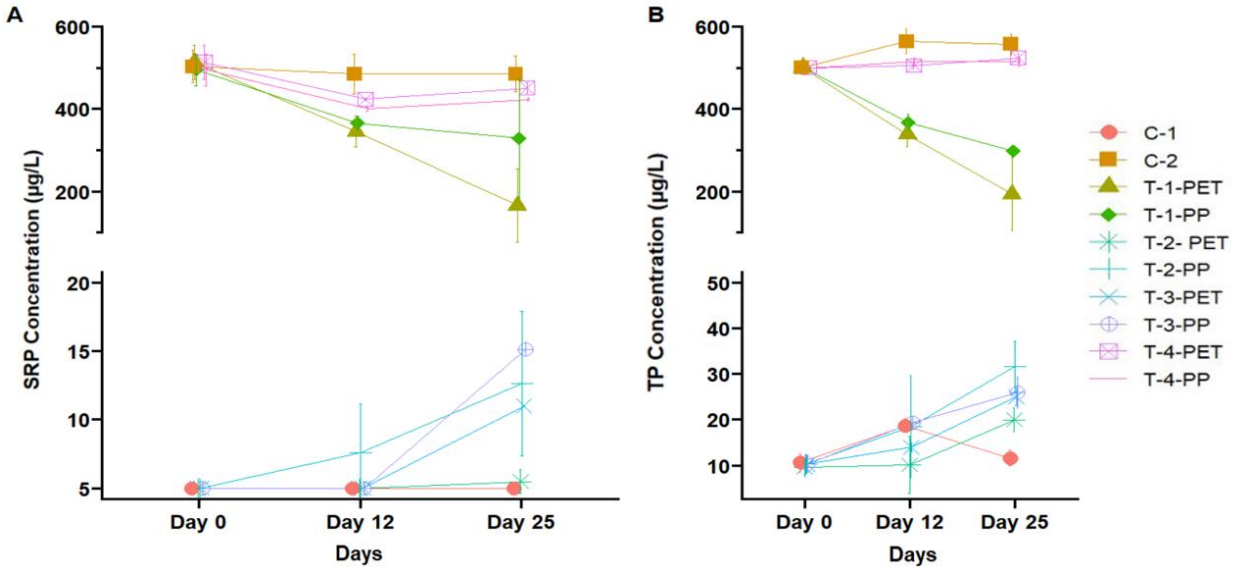
A
600
400
200
20
15
10
5
SRP Concentration (µg/L)
Day 0
Day 12
Day 25
Days
B
600
400
200
50
40
30
20
10
TP Concentration (µg/L)
Day 0
Day 12
Day 25
Days
C-1
C-2
T-1-PET
T-1-PP
T-2- PET
T-2-PP
T-3-PET
T-3-PP
T-4-PET
T-4-PP

Figure 4.5

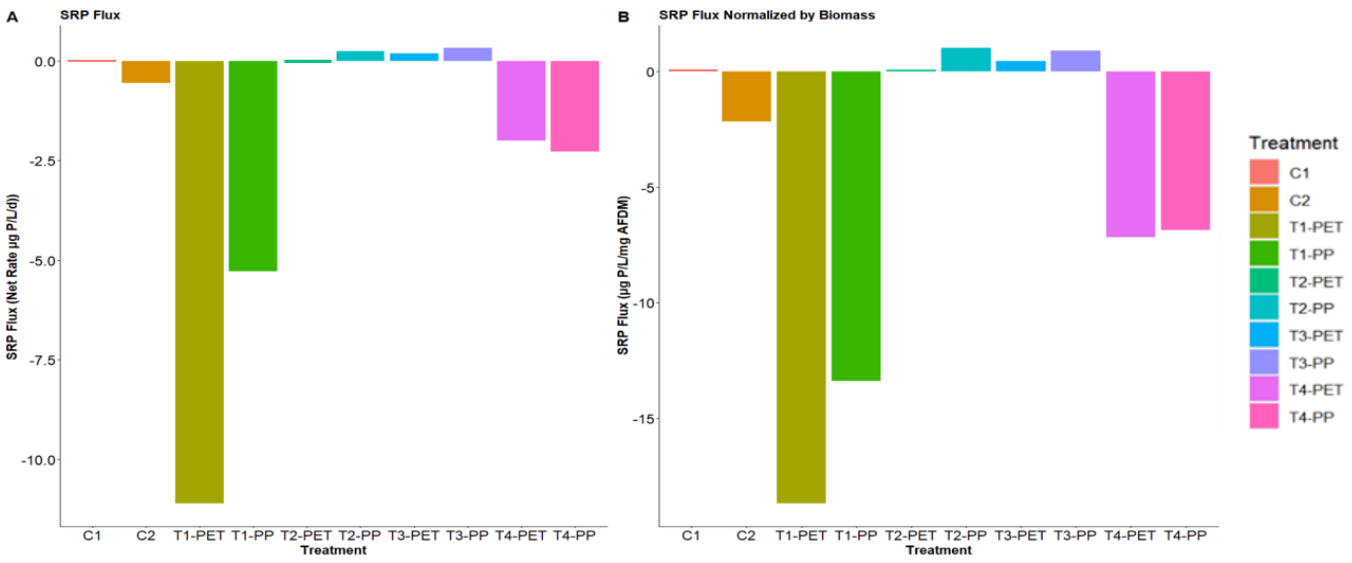
A
SRP Flux
SRP Flux (Net Rate µg P/L/d)
0.0
-2.5
-5.0
-7.5
-10.0
C1
C2
T1-PET
T1-PP
T2-PET
T2-PP
T3-PET
T3-PP
T4-PET
T4-PP
Treatment
B
SRP Flux Normalized by Biomass
SRP Flux (µg P/L/mg AFDM)
0
-5
-10
-15
Treatment
C1
C2
T1-PET
T1-PP
T2-PET
T2-PP
T3-PET
T3-PP
T4-PET
T4-PP

Figure 4.6

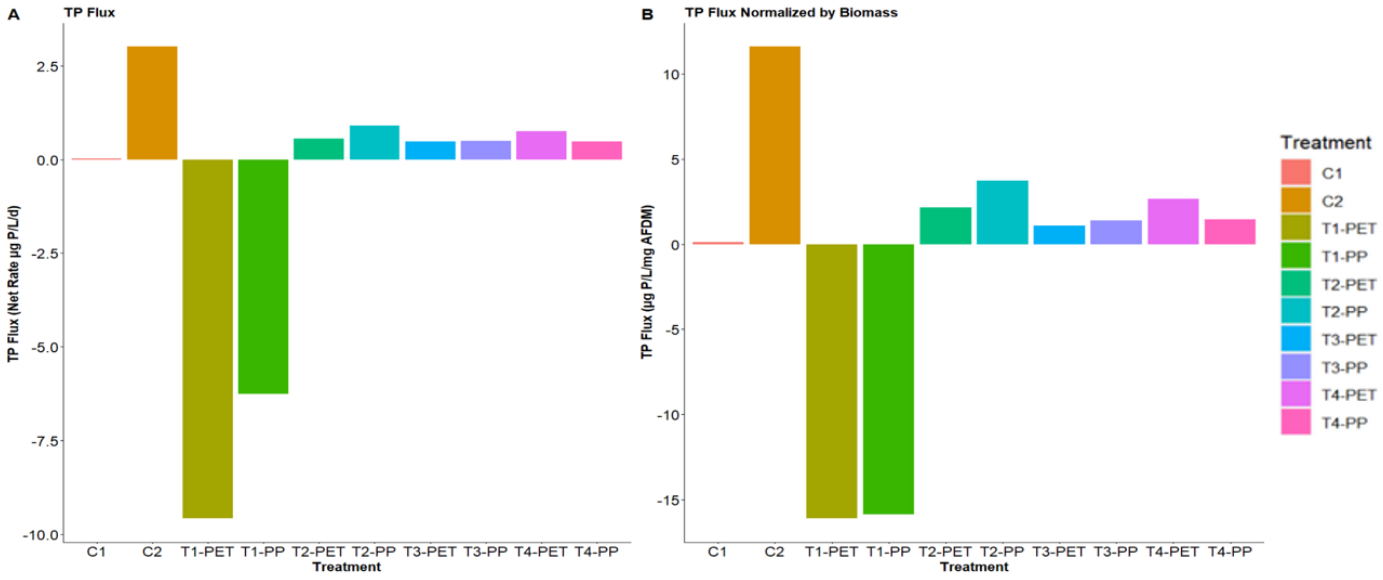
A
TP Flux
TP Flux (Net Rate µg P/L/d)
2.5
0.0
-2.5
-5.0
-7.5
-10.0
C1
C2
T1-PET
T1-PP
T2-PET
T2-PP
T3-PET
T3-PP
T4-PET
T4-PP
Treatment
B
TP Flux Normalized by Biomass
TP Flux (µg P/L/mg AFDM)
10
5
0
-5
-10
-15
C1
C2
T1-PET
T1-PP
T2-PET
T2-PP
T3-PET
T3-PP
T4-PET
T4-PP
Treatment
Treatment
C1
C2
T1-PET
T1-PP
T2-PET
T2-PP
T3-PET
T3-PP
T4-PET
T4-PP

Appendices

Appendix Table 4.1 A. After a Kruskal Wallis analysis, a Dunn Pos Hoc test for multiple comparisons was used on treatments (4 levels) with PP and SRP concentration over time (µg/L). Asterisks indicate level of significance: *** p < 0.0001, ** p < 0.01, * p < 0.05. Z: is a measure of how many standard deviations away from the mean, P. unadj: is the p-value associated with the Z-statistics before any adjustments for multiple comparisons, P. adj: is the adjusted p-value that accounts for type 1 errors using the Benjamini-Hochberg method.

Comparison	Z	P.unadj	P.adj	
T1-PP-12 vs T1-PP-25	0.194	8E-01	0.878	
T1-PP-12 vs T2-PP-12	2.253	2E-02	0.057	*
T1-PP-25 vs T2-PP-12	2.060	4E-02	0.079	
T1-PP-12 vs T2-PP-25	1.590	1E-01	0.209	
T1-PP-25 vs T2-PP-25	1.396	2E-01	0.268	
T2-PP-12 vs T2-PP-25	-0.664	5E-01	0.617	
T1-PP-12 vs T3-PP-12	2.751	6E-03	0.018	**
T1-PP-25 vs T3-PP-12	2.557	1E-02	0.027	*
T2-PP-12 vs T3-PP-12	0.498	6E-01	0.666	
T2-PP-25 vs T3-PP-12	1.161	2E-01	0.344	
T1-PP-12 vs T3-PP-25	2.751	6E-03	0.021	*
T1-PP-25 vs T3-PP-25	2.557	1E-02	0.030	*
T2-PP-12 vs T3-PP-25	0.498	6E-01	0.693	
T2-PP-25 vs T3-PP-25	1.161	2E-01	0.362	
T3-PP-12 vs T3-PP-25	0.000	1E+00	1.000	
T1-PP-12 vs T4-PP-12	-0.581	6E-01	0.655	
T1-PP-25 vs T4-PP-12	-0.774	4E-01	0.585	
T2-PP-12 vs T4-PP-12	-2.834	5E-03	0.018	**
T2-PP-25 vs T4-PP-12	-2.170	3E-02	0.065	
T3-PP-12 vs T4-PP-12	-3.331	9E-04	0.005	**
T3-PP-25 vs T4-PP-12	-3.331	9E-04	0.006	**
T1-PP-12 vs T4-PP-25	-1.327	2E-01	0.287	
T1-PP-25 vs T4-PP-25	-1.521	1E-01	0.225	
T2-PP-12 vs T4-PP-25	-3.580	3E-04	0.003	**
T2-PP-25 vs T4-PP-25	-2.917	4E-03	0.017	**
T3-PP-12 vs T4-PP-25	-4.078	5E-05	0.001	**
T3-PP-25 vs T4-PP-25	-4.078	5E-05	0.001	**
T4-PP-12 vs T4-PP-25	-0.746	5E-01	0.580	

Appendix Table 4.2 A. After a Kruskal Wallis analysis, a Dunn Pos Hoc test for multiple comparisons was used on treatments (4 levels) with PET and SRP concentration over time (µg/L). Asterisks indicate level of significance: *** p < 0.0001, ** p < 0.01, * p < 0.05. Z: is a measure of how many standard deviations away from the mean, P. unadj: is the p-value associated with the Z-statistics before any adjustments for multiple comparisons, P. adj: is the adjusted p-value that accounts for type 1 errors using the Benjamini-Hochberg method.

Comparison	Z	P.unadj	P.adj	
T1-PET-12 vs T1-PET-25	0.676	5E-01	0.559	
T1-PET-12 vs T2-PET-12	2.299	2E-02	0.055	*
T1-PET-25 vs T2-PET-12	1.623	1E-01	0.183	
T1-PET-12 vs T2-PET-25	1.353	2E-01	0.274	
T1-PET-25 vs T2-PET-25	0.676	5E-01	0.582	
T2-PET-12 vs T2-PET-25	-0.947	3E-01	0.458	
T1-PET-12 vs T3-PET-12	2.624	9E-03	0.027	*
T1-PET-25 vs T3-PET-12	1.948	5E-02	0.103	
T2-PET-12 vs T3-PET-12	0.325	7E-01	0.745	
T2-PET-25 vs T3-PET-12	1.271	2E-01	0.285	
T1-PET-12 vs T3-PET-25	3.192	1E-03	0.007	**
T1-PET-25 vs T3-PET-25	2.516	1E-02	0.033	*
T2-PET-12 vs T3-PET-25	0.893	4E-01	0.474	
T2-PET-25 vs T3-PET-25	1.839	7E-02	0.123	
T3-PET-12 vs T3-PET-25	0.568	6E-01	0.591	
T1-PET-12 vs T4-PET-12	-0.703	5E-01	0.587	
T1-PET-25 vs T4-PET-12	-1.380	2E-01	0.276	
T2-PET-12 vs T4-PET-12	-3.003	3E-03	0.011	**
T2-PET-25 vs T4-PET-12	-2.056	4E-02	0.093	
T3-PET-12 vs T4-PET-12	-3.327	9E-04	0.005	
T3-PET-25 vs T4-PET-12	-3.895	1E-04	0.001	**
T1-PET-12 vs T4-PET-25	-1.325	2E-01	0.273	
T1-PET-25 vs T4-PET-25	-2.002	5E-02	0.098	
T2-PET-12 vs T4-PET-25	-3.625	3E-04	0.002	**
T2-PET-25 vs T4-PET-25	-2.678	7E-03	0.026	*
T3-PET-12 vs T4-PET-25	-3.949	8E-05	0.001	**
T3-PET-25 vs T4-PET-25	-4.517	6E-06	0.0002	***
T4-PET-12 vs T4-PET-25	-0.622	5E-01	0.575	

Appendix Table 4.3 A. After a Kruskal Wallis analysis, a Dunn Pos Hoc test for multiple comparisons was used on treatments (4 levels) with PP and TP concentration (µg/L). Asterisks indicate level of significance: *** $p < 0.0001$, ** $p < 0.01$, * $p < 0.05$. Z: is a measure of how many standard deviations away from the mean, P. unadj: is the p-value associated with the Z-statistics before any adjustments for multiple comparisons, P. adj: is the adjusted p-value that accounts for type 1 errors using the Benjamini-Hochberg method.

Comparison	Z	P.unadj	P.adj	
T1-PP-12 vs T1-PP-25	0.676	5E-01	0.559	
T1-PP-12 vs T2-PP-12	2.218	3E-02	0.062	
T1-PP-25 vs T2-PP-12	1.542	1E-01	0.203	
T1-PP-12 vs T2-PP-25	1.434	2E-01	0.236	
T1-PP-25 vs T2-PP-25	0.757	4E-01	0.524	
T2-PP-12 vs T2-PP-25	-0.784	4E-01	0.527	
T1-PP-12 vs T3-PP-12	2.651	8E-03	0.028	*
T1-PP-25 vs T3-PP-12	1.975	5E-02	0.104	
T2-PP-12 vs T3-PP-12	0.433	7E-01	0.690	
T2-PP-25 vs T3-PP-12	1.217	2E-01	0.329	
T1-PP-12 vs T3-PP-25	3.165	2E-03	0.006	**
T1-PP-25 vs T3-PP-25	2.489	1E-02	0.036	*
T2-PP-12 vs T3-PP-25	0.947	3E-01	0.437	
T2-PP-25 vs T3-PP-25	1.731	8E-02	0.167	
T3-PP-12 vs T3-PP-25	0.514	6E-01	0.654	
T1-PP-12 vs T4-PP-12	-0.974	3E-01	0.440	
T1-PP-25 vs T4-PP-12	-1.650	1E-01	0.173	
T2-PP-12 vs T4-PP-12	-3.192	1E-03	0.007	**
T2-PP-25 vs T4-PP-12	-2.408	2E-02	0.041	*
T3-PP-12 vs T4-PP-12	-3.625	3E-04	0.002	**
T3-PP-25 vs T4-PP-12	-4.139	3E-05	0.0005	***
T1-PP-12 vs T4-PP-25	-1.055	3E-01	0.408	
T1-PP-25 vs T4-PP-25	-1.731	8E-02	0.156	
T2-PP-12 vs T4-PP-25	-3.273	1E-03	0.006	**
T2-PP-25 vs T4-PP-25	-2.489	1E-02	0.040	*
T3-PP-12 vs T4-PP-25	-3.706	2E-04	0.002	**
T3-PP-25 vs T4-PP-25	-4.220	2E-05	0.001	**
T4-PP-12 vs T4-PP-25	-0.081	9E-01	0.935	

Appendix Table 4.4 A. After a Kruskal Wallis analysis, a Dunn Pos Hoc test for multiple comparisons was used on treatments (4 levels) with PET and TP concentration over time (µg/L). Asterisks indicate level of significance: *** $p < 0.0001$, ** $p < 0.01$, * $p < 0.05$. Z: is a measure of how many standard deviations away from the mean, P. unadj: is the p-value associated with the Z-statistics before any adjustments for multiple comparisons, P. adj: is the adjusted p-value that accounts for type 1 errors using the Benjamini-Hochberg method.

Comparison	Z	P.unadj	P.adj	
T1-PP-12 vs T1-PP-25	0.676	5E-01	0.559	
T1-PP-12 vs T2-PP-12	2.218	3E-02	0.062	
T1-PP-25 vs T2-PP-12	1.542	1E-01	0.203	
T1-PP-12 vs T2-PP-25	1.434	2E-01	0.236	
T1-PP-25 vs T2-PP-25	0.757	4E-01	0.524	
T2-PP-12 vs T2-PP-25	-0.784	4E-01	0.527	
T1-PP-12 vs T3-PP-12	2.651	8E-03	0.028	*
T1-PP-25 vs T3-PP-12	1.975	5E-02	0.104	
T2-PP-12 vs T3-PP-12	0.433	7E-01	0.690	
T2-PP-25 vs T3-PP-12	1.217	2E-01	0.329	
T1-PP-12 vs T3-PP-25	3.165	2E-03	0.006	**
T1-PP-25 vs T3-PP-25	2.489	1E-02	0.036	*
T2-PP-12 vs T3-PP-25	0.947	3E-01	0.437	
T2-PP-25 vs T3-PP-25	1.731	8E-02	0.167	
T3-PP-12 vs T3-PP-25	0.514	6E-01	0.654	
T1-PP-12 vs T4-PP-12	-0.974	3E-01	0.440	
T1-PP-25 vs T4-PP-12	-1.650	1E-01	0.173	
T2-PP-12 vs T4-PP-12	-3.192	1E-03	0.007	**
T2-PP-25 vs T4-PP-12	-2.408	2E-02	0.041	*
T3-PP-12 vs T4-PP-12	-3.625	3E-04	0.002	**
T3-PP-25 vs T4-PP-12	-4.139	3E-05	0.0005	***
T1-PP-12 vs T4-PP-25	-1.055	3E-01	0.408	
T1-PP-25 vs T4-PP-25	-1.731	8E-02	0.156	
T2-PP-12 vs T4-PP-25	-3.273	1E-03	0.006	**
T2-PP-25 vs T4-PP-25	-2.489	1E-02	0.040	*
T3-PP-12 vs T4-PP-25	-3.706	2E-04	0.002	**
T3-PP-25 vs T4-PP-25	-4.220	2E-05	0.001	**
T4-PP-12 vs T4-PP-25	-0.081	9E-01	0.935	

Chapter 5: Synthesis and Conclusion

Plastic materials have become indispensable in our daily lives due to their insulating properties, durability, and lightweight nature. These characteristics make plastics highly versatile but also notoriously persistent. The 20th century is now known as the "plasticene" or "age of plastic" due to the persistence and prevalence of plastic pollution caused by their durability and low cost of manufacturing (Arpia et al., 2021). Over time, however, plastics can become brittle and fragment into tiny particles termed microplastics (MP) (1µm to 5 mm) or nanoplastics through mechanical, thermal, and biological processes (Chamas et al., 2020). Beyond being unsightly, plastic waste poses serious environmental hazards: it can obstruct the flow of rivers and streams, entangle marine and freshwater animals, cause starvation from ingestion, and block sunlight essential for photosynthetic organisms in aquatic ecosystems. The most common sources of MPs are urban runoff, wastewater treatment plant inputs, sewage system overflows, and industrial inputs (Hitchcock, 2020). Urban lakes, including Church Lake, which is the focus of my thesis, have been impacted by poor management of non-point source pollutants. Numerous non-point source pollutants, including nutrients, pathogens, road salt, sediment, and MPs, are transported by rain and storm events (Eadie et al., 2002; Hitchcock, 2020; Johnson et al., 2011; Kaushal et al., 2022).

In aquatic environments, MPs quickly become colonized by microbial communities. This biofilm, termed the "plastisphere," is composed of a diverse array of microorganisms including bacteria, algae, fungi, and protozoa (He et al., 2021; Zettler et al., 2013). Biofilm development on MPs is influenced by various environmental factors such as pH, salinity, nutrients, flow, temperature, and light (Chen et al., 2020). Biofilm communities play a key role in cycling

materials and energy in aquatic ecosystems (Chen et al., 2020). Biofilms secrete an extracellular polymeric substance (EPS), which provides protection and facilitates the adhesion of particles from the surrounding environment (He et al., 2021; Zafar et al., 2023). The presence of such biofilms not only protects MPs from degradation but also increases the longevity of MPs, potentially heightening exposure to harmful microorganisms and contributing to their bioaccumulation in aquatic biota.

Currently, limited information exists regarding the characterization of MPs entering urban lakes via runoff from major highways. This study aims to establish the presence of plastic pollution at the study site by analyzing the MPs transported by a tributary connected to a nearby highway. Additionally, there is a need for more comprehensive research on how environmental conditions affect microbial colonization on MPs and influence nutrient dynamics within the plastisphere, which has implications for ecosystem health and water quality. By placing MPs in flow-through containers in Church Lake to promote biofilm formation, and then subjecting them to controlled environmental treatments in the lab, this study examines the potential responses of biofilms to environmental changes, such as a full lake turnover. The insights gained will enhance understanding of the adaptability and ecological roles of microorganisms on MPs in impacted urban lakes. The findings will have potential value for local governments, road and water resource commissioners, and homeowners by highlighting the significance of controlling plastic pollution and its broader environmental implications.

Characteristics of MPs Entering Church Lake

My objectives of this study were to discover whether MPs are entering Church Lake and to categorize them. The study on Church Lake and its tributary highlights the significant

seasonal and spatial variability in MP pollution. Water samples taken from the lake showed considerable variations in MP counts throughout time. This suggested that seasonal variations, storms, and human activity were probably responsible for the temporal variability in MP pollution inside the Lake. There was also significant variation in the MP counts in water samples obtained from the tributary during baseflow. Without storm-induced changes, baseflow conditions represent baseline MP contamination levels. MP counts during storms showed high spikes of MPs in the tributary, which is consistent with other studies that have shown storm events can wash large quantities of MPs from surrounding areas into tributaries and subsequently into lakes (Treilles et al., 2021; Werbowski et al., 2021). In my study, MP counts taken from the sediment in the tributary were the highest overall, suggesting that sediments act as a sink for MPs, accumulating particles over time. Similar patterns were observed for MP surface area and estimated mass. The highest MP density was observed in winter, with a significant presence of black particles across all habitats, likely from road runoff. The predominant MP shape found in my study were fragments; MP fragments were found in both water and sediment, with the highest counts in the tributary sediment, likely due to its proximity to highway runoff. Altogether, the highest MP concentrations occurred during storm events and winter months.

6-PPD-Q concentrations, associated with tires, in the lake were consistently below 1 ng/L, indicating dilution or perhaps efficient degradation/removal processes. 6-PPD-Q concentrations in the baseflow vary, with a notable peak of 24 ng/L in October. This variation suggests periodic inputs of 6-PPD-Q influenced by seasonal events, potentially linked to vehicular runoff or other urban sources. Storm events show significantly higher concentrations

of 6-PPD-Q, such as 201 ng/L (October), underscoring the role of stormwater as a major vector for runoff pollutants into aquatic systems.

6-PPD-QMP counts can vary greatly among studies due to differences in collection methods, size limitations, and density salts used for analysis. The lack of standardized methods for sampling, identifying, and quantifying MPs complicates comparisons across studies, leading to inconsistencies in reported MP concentrations. Thus, the findings from this study should be interpreted with caution.

MP characteristics varied significantly across seasons and flow conditions, highlighting the impact of environmental changes. The findings demonstrate the complex dynamics of MP distribution, influenced by land use and hydrological factors. Hence, there is a need for individual diagnoses for impacted lakes to identify the most appropriate management strategies (cf. Tammeorg et al. 2024).

Future studies in this location should prioritize measuring discharge during storm events and investigating the tributaries and groundwater pathways connecting Church Lake to downstream urban lakes such as Middleboro and Westboro. To mitigate plastic pollution, management actions must focus on controlling stormwater inflows into streams and lakes, thereby preventing contaminants like deicing salts and MPs from entering these aquatic systems. It is crucial to identify and address the primary sources of MPs and implement effective management strategies to protect water quality and ecosystem health. Continued research and monitoring are essential for better understanding the sources, fate, and impacts of MPs on freshwater ecosystems and for developing informed, evidence-based mitigation

strategies. Additionally, understanding the interactions between MPs and aquatic biota will require detailed monitoring of these pathways and their ecosystems.

Biodiversity Found in the Plastisphere

This investigation identified the microbial communities growing on MPs to examine the responsiveness of the biofilm to new environmental conditions should Church Lake fully turn over in the future. Microbial communities were significantly influenced by environmental conditions. The 2-meter depth during summer was warm, oxygen-rich, and had low phosphorus (P) concentrations, while the 10-meter depth was cold, hypoxic, and had high P concentrations. P concentration was more than 100 times higher in the hypolimnion compared to the epilimnion. The biomass of the plastisphere was generally greater on pellets incubated in the epilimnion (2-meter depth) compared to those in the hypolimnion (10-meter depth). The polymer type did not have an overall influence on the plastisphere. Additionally, Diversity was relatively the same for all of the treatments that started in the epilimnion (T-1 and T-3). This suggests that the high P concentration, despite also having the high chloride content, positively influenced biofilm formation.

I accept the hypothesis that algal communities growing on MPs in the hypolimnion exhibit lower species richness and abundance compared to those in the epilimnion. This is likely due to the harsher conditions in the hypolimnion, including lower light availability and higher salinity, which limit algal growth. However, I reject the hypothesis that bacterial communities in the hypolimnion show greater species richness and abundance. Contrary to this prediction, the results revealed that bacterial diversity was higher in the epilimnion. While higher salinity in the hypolimnion can stress many freshwater organisms, it may favor salt-tolerant or halophilic

bacteria. DESeq analysis identified notable differences in bacterial genera abundance between the two depths. Families such as Sulfurimonadaceae, Oxalobacteraceae, and Pseudomonadaceae were significantly more abundant in the hypolimnion. Sulfurimonadaceae are known for their ability to oxidize sulfur compounds, which is advantageous in environments with low oxygen levels and high sulfur concentrations, conditions typical of the hypolimnion. Oxalobacteraceae are capable of metabolizing oxalate, which can be a significant carbon source in certain environments. Pseudomonadaceae are a diverse family with members that exhibit a range of metabolic capabilities, including the degradation of organic compounds and adaptation to various environmental stresses. Overall, the results demonstrate that the initial environmental conditions in which bacteria colonized the plastisphere had a substantial influence on their community structure, with certain families adapting to the more extreme conditions of the hypolimnion.

The quantity of algae on MPs in the photic zone will grow due to the increase in phosphorus and salinity from hypolimnetic water, which could lead to higher settling rates if lake mixing does take place (Semcesen & Wells, 2021). By linking the microbial activities to the broader nutrient cycling processes, we can develop a more comprehensive understanding of how MPs contribute to the overall biogeochemical balance within these systems.

Phosphorus Net Flux by the Plastisphere

The P dynamics on the plastisphere are governed by several factors, including the microbial community composition, the physicochemical conditions of the surrounding water, and the availability of P itself (Amaneesh et al., 2022; Chen et al., 2020; Cunillera-Montcusí et al., 2022;

Kansman, 2015). The activities of these microbial communities, such as P uptake, storage, and release, directly influence the concentration and form of P in the environment (Chen et al., 2020; He et al., 2021). This interaction can lead to either the retention or release of P within the water column mediated by microorganisms, significantly affecting water quality.

My study aimed to explore the impact of plastisphere-mediated P dynamics growing on two different polymer pellets (PET and PP) in a partially meromictic lake, specifically after simulated turnover events between the epilimnion and hypolimnion. By examining the P dynamics of the plastisphere, we can better understand how these microbial processes contribute to overall ecosystem health and nutrient fluxes in the aquatic environment. Key observations and findings include:

My study found that the type of polymer (PET or PP) had minimal effect on plastisphere P dynamics, with mean plastisphere biomass being slightly higher on PET than on PP. However, microplastics transferred from the epilimnion to the hypolimnion exhibited increased biomass due to higher P concentrations; similar increases in biomass due to higher P have been observed in other studies (Chen et al., 2020; Miao et al., 2021). Conversely, MP pellets moved from the hypolimnion to the epilimnion experienced reduced biomass, likely due to nutrient scarcity and acclimatization challenges. When plastisphere remained within either the epilimnion or hypolimnion, biomass was lower, highlighting the significant role of nutrient availability and environmental stability.

There was no significant effect of polymer type on soluble reactive phosphorus (SRP) or total phosphorus (TP) uptake rates, suggesting that factors such as environmental conditions,

biofilm community structure, and biofilm P uptake capacity influenced uptake more than plastic type. The highest P uptake rates observed in this study were still comparatively low, indicating a limited ecological impact of the plastisphere on P dynamics in Church Lake. Lake-wide implications suggested that P uptake by the plastisphere was insignificant relative to total P content, thus unlikely to mitigate P levels during lake turnover, and despite potential influences at the sediment-water interface, these were deemed minimal given the high P concentrations. The conclusions partially align with the hypothesis. We reject Hypothesis 1, as microbial communities growing on MPs in the epilimnion and then exposed to epilimnetic conditions had lower P uptake than those grown and exposed to hypolimnetic conditions. It appears the high P environment had a stronger influence on P uptake than the potential inhibitory effects of high salinity and low light. Hypothesis 2 was partially accepted, as microbial communities transferred from the hypolimnion to the epilimnion released P, whereas there was no change in the control system. However, the communities transferred from the epilimnion to hypolimnetic conditions had the highest uptake rates.

In conclusion, the study found that plastisphere on microplastics had minimal impact on P dynamics in the lake, especially under simulated turnover conditions. Environmental factors such as nutrient concentration and light levels, and perhaps also community structure, were more influential than polymer type on plastisphere growth and nutrient uptake. The study did have limitations. First, TP concentrations were likely underestimated in the water column due to interference from iron in hypolimnion samples; second, the uneven distribution of microplastics in the lake was not well documented; and the sediment-bound plastisphere dynamics were not examined. Further research should utilize remote sensing technologies to

monitor plastic distribution and nutrient dynamics in real-time and develop biotechnological applications to harness plastisphere microorganisms for effective bioremediation and nutrient management.

Conclusion

This study aimed to establish the presence of MPs in Church Lake and assess the plastisphere impact on P dynamics and microbial biodiversity. We confirmed that runoff from nearby highways is a significant source of MP pollution, with the highest concentrations observed during storm events and winter months. The MPs, predominantly black fragments, were largely of unknown polymer composition and settled in the tributary sediments, before reaching Church Lake.

My research demonstrated that environmental conditions, such as nutrient concentration and light levels influenced community structure. The environmental condition also had a more substantial impact on plastisphere growth and nutrient uptake than the type of MP polymer. The high P concentrations in the hypolimnion stimulated microbial growth and P uptake, while the epilimnion supported lower P uptake despite favorable conditions. These findings suggest that the plastisphere's influence on P dynamics in the lake is minimal, indicating that MPs are unlikely to significantly affect P levels even if the lake undergoes turnover.

However, the study had limitations, including potential underestimation of TP concentrations due to interference from iron, uneven distribution of MPs in the lake, the loss of genomic data due to limited sample size, and the lack of examination of sediment-bound

plastisphere dynamics. Overall, the study underscores the importance of controlling plastic pollution and highlights the need for continued research to better understand the interactions between MPs and aquatic ecosystems.

References

Amaneesh, C., Anna Balan, S., Silpa, P. S., Kim, J. W., Greeshma, K., Aswathi Mohan, A., Robert Antony, A., Grossart, H. P., Kim, H. S., & Ramanan, R. (2022). Gross negligence: Impacts of microplastics and plastic leachates on phytoplankton community and ecosystem dynamics. Environmental Science and Technology. https://doi.org/10.1021/acs.est.2c05817

Arpia, A. A., Chen, W. H., Ubando, A. T., Naqvi, S. R., & Culaba, A. B. (2021). Microplastic degradation as a sustainable concurrent approach for producing biofuel and obliterating hazardous environmental effects: A state-of-the-art review. Journal of Hazardous Materials, 418(March), 126381. https://doi.org/10.1016/j.jhazmat.2021.126381

Chamas, A., Moon, H., Zheng, J., Qiu, Y., Tabassum, T., Jang, J. H., Abu-omar, M., Scott, S. L., & Suh, S. (2020). Degradation Rates of Plastics in the Environment. ACS Sustainable Chemistry & Engineering 2020 8 (9), 3494-3511. https://doi.org/10.1021/acssuschemeng.9b06635

Chen, X., Chen, X., Zhao, Y., Zhou, H., Xiong, X., & Wu, C. (2020). Effects of microplastic biofilms on nutrient cycling in simulated freshwater systems. Science of the Total Environment, 719, 137276. https://doi.org/10.1016/j.scitotenv.2020.137276

Cunillera-Montcusí, D., Beklioğlu, M., Cañedo-Argüelles, M., Jeppesen, E., Ptacnik, R., Amorim, C. A., Arnott, S. E., Berger, S. A., Brucet, S., Dugan, H. A., Gerhard, M., Horváth, Z., Langenheder, S., Nejstgaard, J. C., Reinikainen, M., Striebel, M., Urrutia-Cordero, P., Vad, C. F., Zadereev, E., & Matias, M. (2022). Freshwater salinisation: a research agenda for a saltier world. Trends in Ecology & Evolution, xx(xx), 1–14. https://doi.org/10.1016/j.tree.2021.12.005

Eadie, B. J., Schwab, D. J., Johengen, T. H., Lavrentyev, P. J., Miller, G. S., Holland, R. E., Leshkevich, G. A., Lansing, M. B., Morehead, N. R., Robbins, J. A., Hawley, N., Edgington, D. N., & Van Hoof, P. L. (2002). Particle transport, nutrient cycling, and algal community structure associated with a major winter-spring sediment resuspension event in Southern Lake Michigan. Journal of Great Lakes Research, 28(3), 324–337. https://doi.org/10.1016/S0380-1330(02)70588-1

He, S., Jia, M., Xiang, Y., Song, B., Xiong, W., Cao, J., Peng, H., Yang, Y., Wang, W., Yang, Z., & Zeng, G. (2021). Biofilm on microplastics in aqueous environment: Physicochemical properties and environmental implications. Journal of Hazardous Materials, 127286. https://doi.org/10.1016/j.jhazmat.2021.127286

Hitchcock, J. N. (2020). Storm events as key moments of microplastic contamination in aquatic ecosystems. Science of the Total Environment, 734, 139436. https://doi.org/10.1016/j.scitotenv.2020.139436

Johnson, K. A., Steinman, A. D., Keiper, W. D., & Ruetz, C. R. (2011). Biotic responses to low-concentration urban road runoff. Journal of the North American Benthological Society, 30(3), 710–727. https://doi.org/10.1899/10-157.1

Kansman, H. The effects of salinity on the stratification and nutrient dynamics of inland lakes in southeast Michigan (2015). Senior Honors Theses & Projects. 457. https://commons.emich.edu/honors/457

Kaushal, S. S., Reimer, J. E., Mayer, P. M., Shatkay, R. R., Maas, C. M., Nguyen, W. D., Boger, W. L., Yaculak, A. M., Doody, T. R., Pennino, M. J., Bailey, N. W., Galella, J. G., Weingrad, A., Collison, D. C., Wood, K. L., Haq, S., Newcomer-Johnson, T. A., Duan, S., & Belt, K. T. (2022). Freshwater salinization syndrome alters retention and release of chemical cocktails along flowpaths: From stormwater management to urban streams. Freshwater Science, 41(3). https://doi.org/10.1086/721469

Semcesen, P. O., & Wells, M. G. (2021). Biofilm growth on buoyant microplastics leads to changes in settling rates: Implications for microplastic retention in the Great Lakes. Marine Pollution Bulletin, 170(April), 112573. https://doi.org/10.1016/j.marpolbul.2021.112573

Tammeorg, O., Chorus, I., Spears, B., Nõges, P., Nürnberg, G.K., Tammeorg, P., Søndergaard, M., Jeppesen, E., Paerl, H., Huser, B., et al. 2024. Sustainable lake restoration: From challenges to solutions. Wiley Interdisciplinary Reviews: Water 11(2), p.e1689.

Treilles, R., Gasperi, J., Gallard, A., Saad, M., Dris, R., Partibane, C., Breton, J., & Tassin, B. (2021). Microplastics and microfibers in urban runoff from a suburban catchment of Greater Paris. Environmental Pollution, 287(May). https://doi.org/10.1016/j.envpol.2021.117352

Werbowski, L. M., Gilbreath, A. N., Munno, K., Zhu, X., Grbic, J., Wu, T., Sutton, R., Sedlak, M. D., Deshpande, A. D., & Rochman, C. M. (2021). Urban stormwater runoff: A major pathway for anthropogenic particles, black Rubbery fragments, and other types of microplastics to urban receiving waters. ACS ES and T Water, 1(6), 1420–1428. https://doi.org/10.1021/acsestwater.1c00017

Zettler, E. R., Mincer, T. J., & Amaral-zettler, L. A. (2013). Life in the “ plastisphere ” : microbial communities on plastic marine debris. Environmental Science & Technology, 47(13), 7137–7146. https://doi.org/DOI: 10.1021/es401288x